Università
Ca'Foscari
Venezia

Master's Degree

in Conservation Science and Technology
for Cultural Heritage

Final Thesis

Evaluation of COVID– 19 sanitisation impacts on historic silks

Supervisor

Prof. Elizabetta Zendri

Assistant supervisor

Dr Eleonora Balliana

Graduand

Benedetta Favaro

854786

Academic Year

2019 / 2020

TABLE OF CONTENTS

AIM OF THE THESYS

Phase 2 of Covid-19 emergency brought about new challenges in museums' management and in cultural heritage conservation. Balancing the need for sanitising and preventing virus spread in cultural sites and the need for preserving the artefacts there conserved results then to be of paramount importance. Therefore, the present project aims at evaluating possible impacts of sanitising products and procedures on cultural heritage artefacts. The study focuses on historic and traditional textiles, this type of material is quite diffused in cultural sites (museum, churches, …) and yet extremely fragile.

Specifically, due to the high and spread presence of tapestry in many historical buildings in Venice, the present study focuses on evaluating the effects of sanitisations on silk. Among the different types of textile, the attention was given to silk as this material has been widely used in the furnishing of historical houses and there is still an on-going tradition on silk production among important local factories as Bevilacqua La Masa, Rubelli and Fortuny.

Given this premise, the main objectives of this study are the evaluation of the physical and chemical effects of sanitising solutions proposed by MIBACT on silk and the evaluation of the morphological impact of sanitising solutions on such textile.

Tests to simulate possible interactions between silks and sanitising products were performed (vapour exposure, immersion). Chemical, physical and morphological variations have been evaluated both with traditional bench (XRD, FTIR, MicroRaman) and portable-non-invasive instruments (portable contact microscope, colorimeter, Raman, ES-FTIR, ATR), in order to develop a procedure for following in situ evaluations. All analyses have been performed in a non-destructive way, considering the need of cultural heritage field to study artefacts with minimum impacts on them.

1. INTRODUCTION

Between the end of 2019 and the beginning of 2020, the world has been involved in a pandemic due to the rapid spread of a new virus of the coronavirus family, also known as Covid-19.
To radically reduce the virus diffusion, many countries (Italy as one of the first) imposed a complete lockdown to the population, banning any type of unnecessary activity.
Starting from March 2020, all social activities and the access to places where many people could potentially crowd (such as stadiums, theatres, schools) were temporarily forbidden in order to reduce social contacts and, therefore, virus spread. Museums, churches and archaeological areas were, as well, shut down.

Having successfully limited the effects of the pandemic, Italy authorized the reopening of museums and other historical and religious buildings at the end of May 2020. Consequently, this reopening highlighted new problematics to the cultural heritage field, such as health risk management for visitors and sanitisation standards against Covid-19. Cultural institutions, both national and international, in order to be able to reopen, were requested to provide protocols and guidelines to maintain the required safety standards for Covid-19. The first aim of these acts was to protect visitors from virus contamination, but there is a general concern for estimating and understanding possible risks related to these sanitizing protocols for artworks and objects present in the collections. The employing of aggressive sanitising products and methods might, in fact, negatively affect artefacts' conservation. The *Ministero per i beni e le attività culturali e per il turismo (MIBACT)* recommended therefore a list of products and methodologies for the sanitisation of historical, cultural and ecclesiastical environments [1-3]. Guidelines have been sent to all national institutions, in order to safeguard the vast Italian cultural heritage.

The necessity to conciliate, at the same time, the safety of visitors and the protection of artworks represents a challenging task. So far, no specific systematic studies have been conducted on possible effects and impacts of frequent sanitisations on cultural heritage environments and materials such as papers, fabrics, wood, etc.

Among these materials, textiles, as mentioned before, are highly diffused in museums, places of worship and historic houses (tapestries, upholsteries, etc.) and can represent significant evidence of historical, cultural and industrial advancement.

Several types of textile fibres are used to produce fabrics and among them silk, with its properties, diffusion and history was extensively used for interior decorations, typically in Venetian historical buildings. Silk, therefore, is of great interest for evaluating the possible effects and impacts of cleaning and sanitising products due to its diffusion, historical relevance, and extreme fragility.

1.1 MUSEUM REOPENING AFTER COVID LOCKDOWN: ITALIAN SANITIZING GUIDELINES

Museums are alive places, meant to be locations where people can meet, reflect, and learn, especially during their free time. ICOM definition of a museum, indeed, bears an intrinsic reference to museum role on people and social gathering:

"A museum is a non-profit, permanent institution in the service of society and its development, open to the public, which acquires, conserves, researches, communicates and exhibits the tangible and intangible heritage of humanity and its environment for the purposes of education, study and enjoyment." [4]

The physical presence of people and their role in cultural sites are crucial aspects to chase museums' purpose; this aspect, however, can turn into a strong criticality during the Covid-19 emergency. Unfortunately, archaeological areas and museums, just like theatres and stadiums, where many people are present and gathering is difficult to control, are considered at high risk of virus spread, and particular care should be taken both in controlling flows of people and in performing cleaning and sanitising.

However, museums are also fragile places where artefacts and historical witnesses are conserved. These objects, clearly, cannot undergo standard sanitising procedures (such as solutions spreading for disinfecting enclosed spaces and common surfaces) in order to inactivate pathogenic microorganisms [1-5].

Taking into consideration the above-mentioned conditions and constrictions, the MIBAC suggested a distinct cleaning protocol for museums, aiming at safeguarding from one side the public from virus spread and, on the other side, the conservation of the artworks.

Consequently, MIBACT guidelines and recommendations state that sanitisation of historical buildings should not be carried out directly on cultural heritage artefacts, but only on spaces of common use, employing solutions of ethyl alcohol (70%), water, and quaternary ammonium salts (e.g. benzalkonium chloride) and, if needed, mild soaps, avoiding direct sprays on artistic materials. Disinfectants based on odourless quaternary ammonium salt solutions are suggested for the sanitisation of sensitive materials (e.g. wooden decors). Besides, upholsteries and other fragile materials should either be temporarily removed from the cleaning area or covered with a polyethylene (PE) or a non-woven fabric cloth. Frequent aeration of all enclosed spaces is recommended, especially during cleaning procedures.

The use of chlorine-based products, oxidising solutions (e.g. hydrogen peroxide and ozone) and UV light must be avoided particularly in the presence of metallic and organic-based artefacts. These agents are, in fact, highly reactive and can promote degradation processes on cultural heritage materials. No sanitisation interventions are required for spaces that have been kept close for more than 15 days since it appears that Covid-19 cannot persist on the surface for longer periods of time [1,5-6]. This prescription prevents from performing intense sanitisations before the reopening of museums that have been closed for a long time, but several cleaning procedures remain valid when the museum or institution reopens.

Museums and places of worship are not the only cultural sites to be involved in this sanitising procedure-making. Specific indications have been provided also for sanitisation and management of libraries since books' consultation is considered as a potential risk for virus spread [3,7] Free consultation of books is prohibited and new rules have been developed: after the use, books need to undergo a ten-day quarantine in order to make sure that the virus has naturally inactivated; frequent sanitisation of common surfaces and hand cleaning is also recommended since libraries are, by definition, places where objects (books) are shared among different people.

Scientific evidence shows that COVID-19 virus is transmitted through close contact and respiratory droplets, while its transmission via surface contact is still under study [8]. Considering the uncertainty regarding how the virus can be spread, increasing attention has been put on preventing possible infections related to contaminated surfaces' contact, based also on previously acquired information regarding SARS virus behaviour [9].

Different studies have reported the evaluation of virus' persistence on different types of surfaces, such as fabric and wood (1 day), glass (2 days), plastic (4 days) [8]. Cleaning and disinfection of surfaces and common areas is considered thus crucial to prevent the spreading of COVID-19 virus.

Several products have been reported to successfully inactivate COVID-19 virus, such as ethanol (70-90%), chlorine-based products and hydrogen peroxide. Moreover, the action of ozone and of UV rays results effective for the disinfection process [8], but not compatible with artworks [1].

Starting from the MIBACT official memo, several national and local authorities have released additional guidelines providing clear indications for all the involved institutions (museums, dioceses) [7, 10-16]. This was done in order to adapt the general MIBACT protocols to local and specific realities, supporting also small museums or institutions while defining sanitising procedures.

Among the various products available for cleaning and virus inactivating, MIBACT recommended specific sanitising solutions, mainly composed of ethanol and water blend. In particular, the sanitising solution indicated by MIBACT – Soprintendenza di Roma is composed by water (20%), ethanol (75%) and a quaternary ammonium salt (5%), benzalkonium chloride. This component is a quaternary ammonium compound with three main functions: surfactant, biocide and phase transfer agent [17]. Thanks to its antimicrobial action, it is present in many consumer products, such as pharmaceuticals, detergents with disinfectant function, personal care products, and several others.

Benzalkonium chloride is also employed in restoration as a cleaning agent for various surfaces (marble, stone, wall paintings, pottery, metals, gums, textiles and paper) [18]. It is recommended to use very low concentrations (0,3-0,6%), and particular attention must be paid during the application, as the compound is also known for the dangerousness of its concentrated form (hazard statements H302 – H314 – H400 [19]).

Benzalkonium chloride is strongly soluble in ethanol, and the combination of these two compounds might improve biocidal action; however, the blend must be carefully applied on artefacts since ethanol can cause the removal of some organic and photosynthetic pigments.

Based on preliminary researches, benzalkonium chloride results to effectively inactivate SARS virus on surfaces [9], together with certain enveloped and non-enveloped viruses [20]. Nevertheless, a recent study on the inactivation of coronavirus reports that benzalkonium chloride effects are sometimes contrasting: no clear results on its absolute efficacy have been observed [6].

Despite the fact that these sanitising procedures have been defined specifically for cultural heritage areas, frequent sanitisations may lead water and ethanol vapours to concentrate in the museum environment; besides, benzalkonium chloride might deposit on the different surfaces, interacting with delicate materials and consequently modifying their chemical and physical characteristics.

Risks associated with sanitizing operations in historical buildings may also derive from accidental contact of the sanitising solution with the artefacts, together with the accumulation of vapours in the environment. Airing rooms and historical buildings, as recommended by MIBACT for reducing the virus concentration in the air and removing sanitising vapours, is not always possible. Many artworks do need specific conservation requirements and fluctuations in temperature (T) and Relative Humidity (RH) can negatively impact very fragile materials [21].

This aspect is thus quite delicate, and the need to properly and fully understand the impact of these sanitizing methodologies on the patrimony is, therefore, mandatory.

As mentioned before, no specific systematic studies on compatibility between cultural heritage materials and sanitizing products are reported in the literature.

Only the Library of Congress (US) reported the results of a quick test on effects of hand sanitizer on books, assessing that frequent interaction between sanitizers (transferred by the users and readers) and paper can cause several alterations (e.g. colour variation) on books [22].

Furthermore, studies on other fields (e.g. aircraft cleaning) demonstrated that frequent use of aggressive cleaning and sanitizing agents can affect greatly the conservation of properties and characteristics of various materials [5-23].

1.3 SILK COMPOSITION

Silk is a widely used textile, largely present in museums all over the world [24]; it can be found on upholsteries, clothes and other objects.

Silk has been known in China since the 3rd millennium BCE, but started reaching other territories only after the 2nd century AD [25].

Raw silk threads are generated by several insect larvae and spiders, but the domesticated silkworm *Bombyx mori* is for sure the one responsible for most of the silk production. *Bombyx mori* silk is originated by organisms (worms) that synthesize silk fibres in order to create a protective envelope (*cocoon*) [26]; this type of silk is usually referred to as mulberry silk, for the silkworms that produce it

are fed with mulberry leaves. Other types of silkworm species exist, such as Chinese and Indian Tussah moth, and the African caterpillar [26].

Despite its remarkable characteristics such as strength and lustre, silk loses its properties with time, becoming extremely brittle and fragile. Its conservation is, therefore, considered quite challenging and preventive conservation is preferred in order to avoid drastic interventions.

Raw silk is composed of two proteinaceous structures: two fibroin filaments (around 66%wt) coated with sericin (around 26wt%) [24,27]; sericin, however, gets removed during industrial processes (degumming), leaving fibroin as the main component of silk threads. Figure 1 reports a scheme of silk structure [24].

Fibroin's primary structure consists of a series of 18 amino acids, whose distribution can vary from region to region: glycine (44.6%), alanine (29.4%), serine (12.1%), tyrosine (5.1%), valine (2.2%), aspartic acid (1.3%), leucine (1.2%), glutamic acid (1.0%), threonine (0.9%), arginine (0.5%), proline (0.4%), phenylalanine (0.4%), lysine (0.3%), cysteine (0.2%), histidine (0.1%) and tryptophan (0.1%) [24].

Secondary structure, instead, is characterized by the so-called β-sheet conformation which is surrounded by amorphous regions [27]. Silk is, in fact, a semi crystalline biopolymer constituted by crystalline areas surrounded by amorphous portions. In *Bombyx mori* silk the crystallinity degree appears to be between 62% and 65%, while wild silks usually present levels between 50% and 63%. The crystalline structure is constituted by ordered protein chains made up of small fibroin amino acids that fold together into anti-parallel-β-sheets, the components of silk crystallites [26,28]; small functional groups such as methyl- or hydroxyl- allow chains of amino acids to be closed together making possible the ordering into the secondary structure of β -sheets [24].

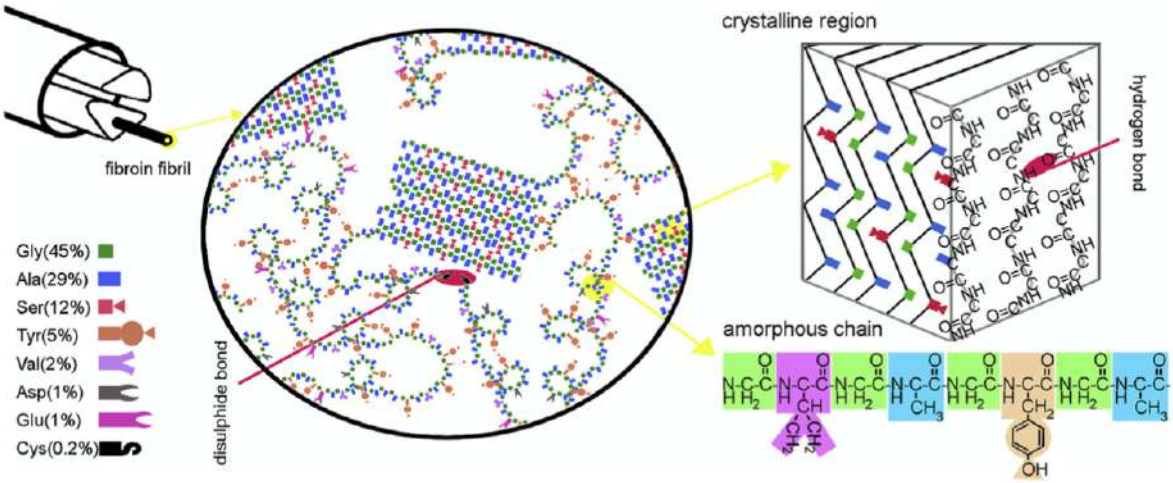

Figure 1: Scheme of silk's fibroin primary and secondary structure - Koperska, 2014

Fibroin amorphous matrix, instead, appears to be composed mainly by tyrosine residues [27]. Crystalline regions are responsible for the silk characteristic strength, while disordered amorphous regions give the fiber resilience [24]. Unlike most natural fibres, silk is characterized by high strength and high breaking extension [26] and presents the key property to be dyed in a wide range of shades.

Silk possesses many unique characteristics that made it an appealing material since early times. To make silk threads usable for textile production, however, some processing is needed. The most well-known processing procedure is for sure the "weighting" of silk, where the fabric gets treated with inorganic salts to increase its weight. Originally, this process was performed to increase silk value as it was sold by weight, and, later, also to obtain specific properties (improved drape and handle) [25,29]. Inorganic materials (but also organic ones, such as tannins) were employed both as weighting agents and as mordants for the dyeing process [26]. With time, however, it appeared clear that the weighting process greatly affects silk durability [26].

1.3.1 SILK DEGRADATION

Differing from the majority of textiles, silk results to be subject to chemical degradation, showing no particular sensibility to biological attacks [26]. Chemical degradation, instead, can be promoted by various agents, such as light and temperature or by water and other chemicals interacting with the fiber.

The two main **chemical** reactions that typically lead to silk degradation result in hydrolysis and oxidation.

Hydrolysis is mainly related to high humidity levels that can negatively affect silk conservation. High levels of Relative Humidity percentage (RH%) make it possible for water to reach the peptide bond in silk amorphous areas leading to carbonyl and amine groups formation. Hydrolysis of peptide bonds between amino acids, in fact, leads to polypeptide chain scission decreasing silk molecular weight [26]. Hydrolysis rate appears to be affected by pH and temperature levels and both strong and weak acids contribute to the process: the former attacking the main chain, the latter only end groups [26].

Hydrolysis of peptide bond:

$H_2N – (C=O) – (C-R) – (NH) – (C=O) – (CR) – NH_2 + H_2O \rightarrow$

$H_2N – (C=O) – (CR) – NH_2$ (amine gr. formation) + (Carbonyl gr. formation) $OH – (C=O) – (CR) – NH_2$

An intermediate level of humidity (around 40%) is, therefore, mandatory to prevent or at least retard the hydrolysis reactions [30] which, however, is strongly dependent both on temperature and on acidity [31-32]. Low humidity levels, on the other hand, may lead to desiccation and physical damages in fibres [33]. Both acids and alkali promote hydrolysis in silk fibres, affecting also (in the case of acids) secondary and tertiary silk structure attacking H and SS bonds [30].

Oxidation is caused by radical reaction, promoted by light (UV) and heat. Aromatic groups such as tryptophan, tyrosine and phenylalanine are reported to be the first molecules to be attacked, for degradation starts in easy-to-access amorphous regions. As a result, under light exposure, yellow chromophores are formed resulting in a colour variation [30]. Moreover, these chromophores can be considered responsible for silk embrittlement, for they tend to form cross likings, thus affecting the flexibility of silk. Radicals contribute also to the cleavage of peptide bonds resulting in silk weakening [30], as reported in the following scheme [34].

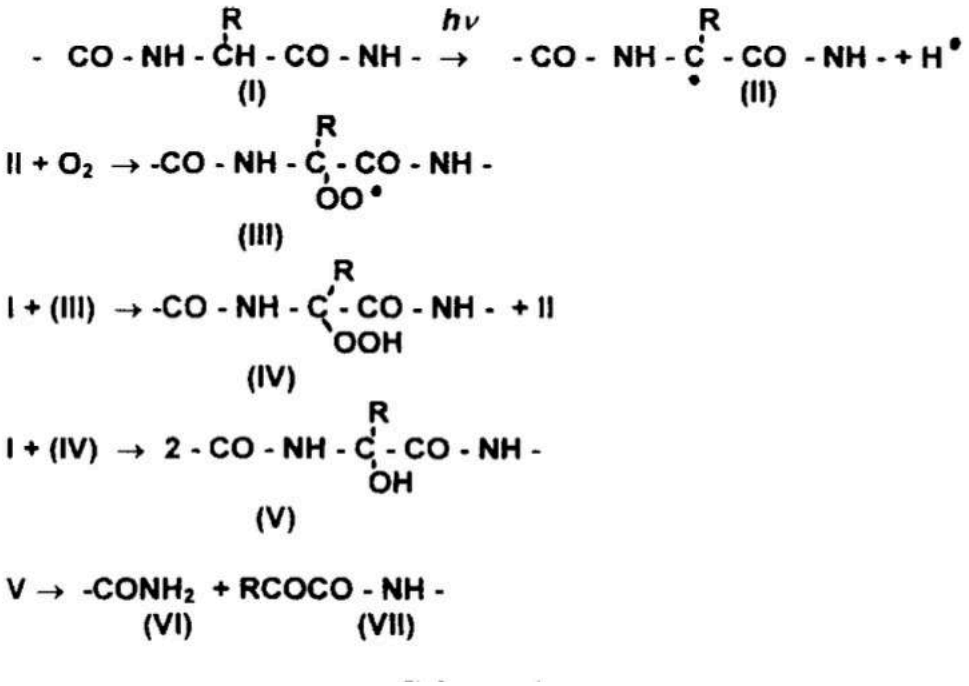

Ozone was reported to increase yellowing and loss of tensile strength thanks to its ability to promote radical oxidation [26]. Studies on uses of ozone for silk processing have reported that such treatment leads not only to yellowing of the textile but also to mechanical properties variation, such as decrease in breaking strength and elongation [35].

Physical degradation of silk objects is also a conservation issue that needs to be considered. Wear and tear can be considered cause of silk textiles degradation, since fabrics can be employed in upholstery that are (or were) meant to be in contact with bodies, resulting in abrasion of the material [33].

Together with abrasion, the other main physical degradation agent is, for sure, light, and UV in particular, that causes a rapid decrease in tensile strength [26]. It was reported that silk shows decrease in fracture strength and toughness and in extensibility, most likely related to bond rupture within the peptide chains [36].

Light irradiation affects crystalline regions, for the UV light energy is able to break polypeptide chain bonds, thus increasing the amorphous content in proportion [26], more accessible to chemical degrading agents attack. As reported above, mechanical properties of silk are affected by chemical modifications.

All these things considered, it appears clearly how silk is a highly complex material with remarkable properties and yet several weaknesses. Therefore, it is paramount to verify whether sanitising products may somehow affect silk properties and its conservation activating or accelerating one or more of the abovementioned processes.

1.3.2 ALCOHOL INTERACTIONS WITH PROTEINS

Alcohols are weak acids of the order of water, and they appear to be good hydrogen bond donors. They can, however, also act as H bond acceptors, which leads to alcohol self-association (evidently demonstrated also by the elevated boiling points) [37]. Nevertheless, water boiling point results to lay above those of methanol, ethanol and propanol, resulting in the conclusion that water is a stronger bond acceptor if compared to alcohols [37]. Moreover, evidences show that in water, two types of H bond are present, one stronger and the other weaker (differing of approximately 8,3 kJ/mol) [38]. Given these premises, it can be stated that the solubility of alcohol in water depends on hydroxyl group, which results to be involved in the formation of intermolecular H bonds. Hydrogen bonds are therefore formed between alcohol and water molecules, making alcohol soluble in water [37]. When diluted in water, alcohol gets positioned into a weak chain, making the adjacent H bond strong. As a consequence, this process results to be exothermic [38].

Alcohols are known for affecting structure and function of several proteins. Alcohols, as mentioned before, appear to act mainly as hydrogen bond donor, binding to the polypeptide chain, thus altering local protein structure. In fact, alcohols can directly affect protein folding. It is reported that this may be due to the fact that alcohol in aqueous system desolvates peptide amide groups, thus destabilizing planar peptide bonds by substituting to water molecules bonding [39]. Therefore, the type of interaction described does not lead to a chemical modification and new products creation but rather to a structural modification through a reorientation of peptide backbone. It is worth noticing, however, that such interaction is observed mainly when ethanol is in concentrations above 50% but below 100%. It is demonstrated, in fact, that too high concentrations of alcohol lead to a quick interaction which is, however, limited in area of action. The presence of water enables the process to take slightly more time and the alcohol to diffuse to several linking sites [40-41].

Based on these considerations, it clearly appears that alcohol treatments for sanitisation may have negative consequences on silk conservation, especially considering the frequency these treatments require to be effective on museums visited by hundreds of visitors a day.

2. EXPERIMENTAL PART

The aim of the present work is to study possible interactions between sanitising products employed in cultural sites and delicate materials such as silk.

To do so, several types of silk samples underwent laboratory tests to simulate the effects of this interaction. Specimens were characterized before and after treatments also with non-invasive techniques to assess the variation of specific parameters.

2.1.1 MATERIALS

2.1.1.2 SILK SAMPLES

Aiming at understanding the effects of the abovementioned solutions on different types of silk, several kinds of samples have been selected: silk produced according to traditional techniques, provided by artisan shops in Venice, historic silk (Fondazione Querini Stampalia in Venezia) and industrial silks. Samples were either directly purchased (contemporary white industrial silk) or donated expressly for the project by Venetian patrons and institutions (Ms Sonia Guetta Finzi, Fondazione Querini Stampalia, Bevilacqua La Masa, Rubelli).

In particular, 5 types of samples (Figure 2) employed for the present study are identified as follows:

- White contemporary plane industrial silk (“seta bianca”)
- Red contemporary industrial silk with flower motives (courtesy of Ms Sonia Guetta Finzi)
- Yellow contemporary silk produced with traditional methods (Bevilacqua La Masa - Venice)
- Red contemporary velvet produced with traditional methods (Bevilacqua La Masa - Venice)
- Greenish silk produced most likely in the past century, used as tapestry in the Fondazione Querini Stampalia Museum – Venice

These samples were chosen to be representative of different techniques (industrial, traditional production), different colours (white, yellow, red and greenish) and different conservation conditions.

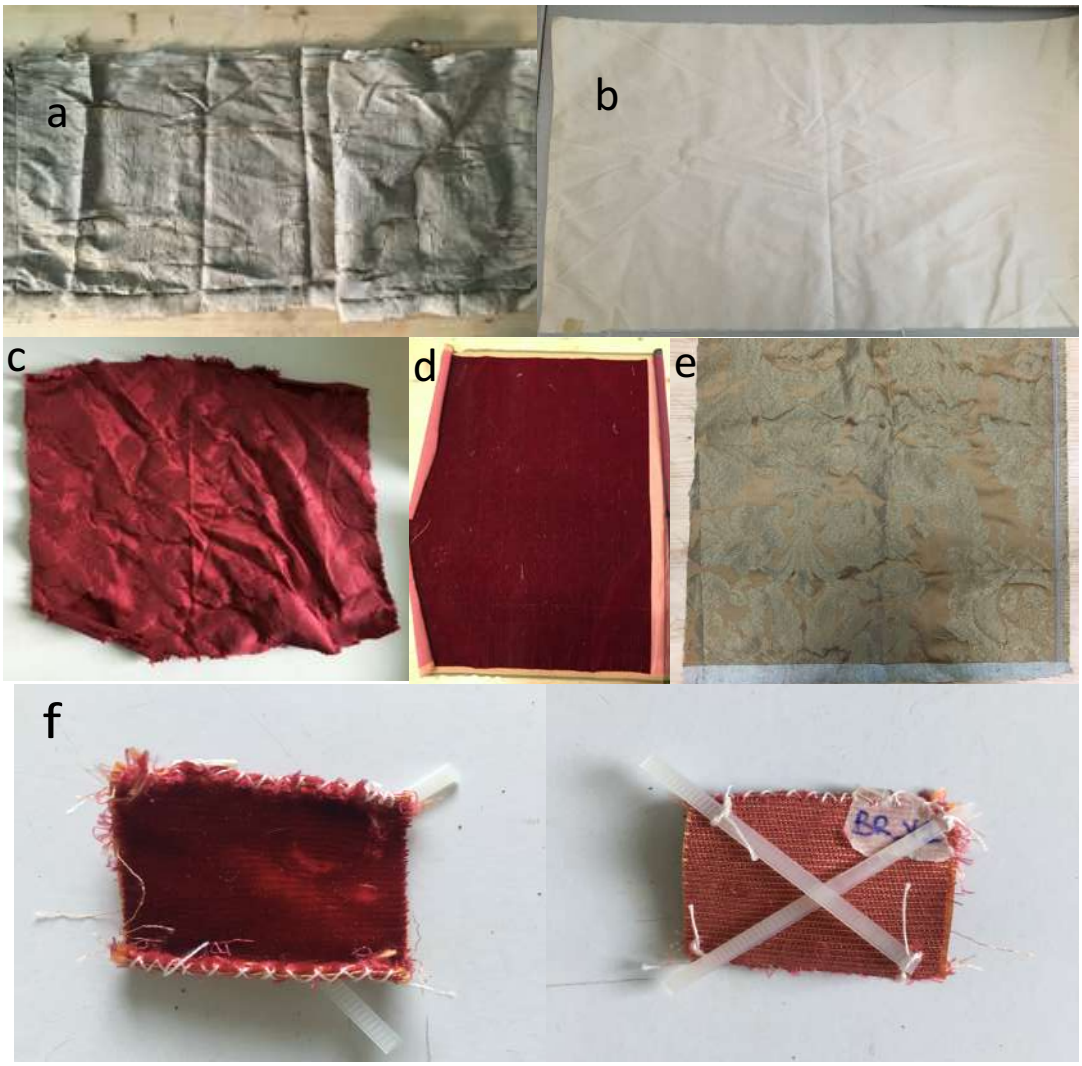

Figure 2: silk samples under analyses. a) Querini silk b) white industrial silk c) red Finzi silk d) red velvet e) yellow silk f) plastic portions sewed at the back of a red velvet sample to prevent it from rolling up

Silk samples did not undergo any preparation to make the analyses as realistic as possible. Fabrics were cut in rectangular pieces of area between 5 and 8 cm^2. Red velvet samples, due to the particular fabric weaving, were sewed at sides, in order to prevent defibering. Moreover, since the textile has been rolled up for a long time, two plastic portions were sewed at the back of each sample in order to make it straight, as shown in Figure 2 f.

2.1.1.3 SANITISING AGENTS

Even though many commercial products for cleaning, disinfecting and sanitising are available, in the present study only laboratory-prepared solutions were employed in order to control the concentration, compositions and to accurately follow the MIBACT indications [1].

In particular, the sanitising solution employed in this research has been prepared mixing 5ml benzalkonium chloride with 200 ml deionized water and 750 ml ethanol.

Since this study aims also at evaluating the effects caused by the single blend components, the following solutions were also chosen to perform the tests:

- Ethanol absolute (purchased from VWR Chemicals)
- Deionized water
- Ethanol/Water blend in different concentrations (50%, 70%, 75% and 79%).
- Benzalkonium Chloride 50% in water (purchased from Antares s.r.l. Bologna)

2.1.2 METHODS

Bearing in mind such objectives, it was decided to analyse different possible scenarios, identifying the situations (ordinary and accidental) in which heritage artefacts (and silk in particular) might get in contact with sanitising agents.

These situations were then simulated to understand the possible consequences on laboratory samples. Two main categories of interaction have been identified:

- Prolonged exposure to sanitising solution vapours (e.g. repeated sanitisation of a closed room)
- Accidental and prolonged contact with sanitising solution (e.g. accidental spill of sanitising solution)

For simulating these two possible scenarios, tests of vapour exposure and immersion were performed on silk samples, as described below (Table 1)

After treatments, samples were conserved into non-sealed desiccators at room conditions (25^{o}C). To study the behaviour of treated samples under moderately high-humidity conditions (typical, for instance, of Venice climate), 4 sets of samples (representative of the different treatments) were kept for 15 days into a closed controlled environment, as reported later in detail.

2.1.2.1 VAPOUR EXPOSURE

Museums, historical churches and, in general, enclosed historical and cultural sites are often wide spaces with little or no aeration. Therefore, the persistence in the enclosed environment of vapours deriving from the employing of sanitising solutions is a plausible scenario.

Thus, in order to verify possible consequences of the interaction between silk samples and sanitising solution vapours, laboratory tests have been performed, as described below.

A set of samples (4 specimens for each type of silk) have been hanged in a sealed desiccator (Figure 3) in which a known amount of sanitising solution had been put (dessicator A – 12 samples = 100 g solution; dessicator B – 8 samples = 70g solution). Samples were kept under these conditions for 10 days, at room temperature (24^{o} C).

Figure 3: silk samples hanged in the desiccator before exposure to sanitising solution's vapours

Samples were then characterized, as described in paragraph 2.1.2.3.

2.1.2.2 IMMERSION

While cleaning or sanitising, both drops and consistent quantities of solution can accidentally flow on delicate materials; therefore, tests to simulate this condition and analyse its consequences were performed.

Samples were immersed in the sanitising solutions for 30 min and for 24h, they were then let dry at room temperature (24^{o} C) and characterized soon after, as described in paragraph 2.1.2.3.

Moreover, in order to verify the the effects of the single solution's components, 24h immersion tests were performed also with pure ethanol, deionized water, ethanol/water blends in different concentrations (50%, 70%, 75% and 79%) and with benzalkonium chloride 50% in water.
After the immersion, samples were let dry before being characterized.

2.1.2.3 EXPOSURE TO CONTROLLED CONSTANT HUMIDITY

With the aim of understanding the possible different behaviours of treated samples in an environment with elevated relative humidity (such as the typical venetian environment), four selected sets of samples (untreated silks, silks after immersion in sanitising solution, in ethanol and in benzalkonium chloride) were exposed to RH 80% for two weeks.
In order to maintain stable humidity levels around 80%RH, an ammonium sulphate saturated solution was prepared and put at the bottom of a desiccator, inside which samples were hanged soon after [42].
Samples were then weighed every 48 hours in order to control their weight variation. After the treatment, samples were then characterized as described in paragraph 2.1.2.3.

Table 1 synthesises the different treatments performed on silk samples.

Table 1: treatments performed on silk samples

TREATMENT	TYPE OF TREATMENT	SOLUTION USED	TREATMENT DURATION
t1	Vapour exposure	MIBACT sanitising solution	10 days
t2	Immersion	MIBACT sanitising solution	30 minutes
t3	Immersion	MIBACT sanitising solution	24 hours
t4	Immersion	Deionized Water	24 hours
t5	Immersion	Ethanol Absolute	24 hours
t6	Immersion	Ethanol 50%	24 hours
t7	Immersion	Ethanol 70%	24 hours
t8	Immersion	Ethanol 75%	24 hours
t9	Immersion	Ethanol 79%	24 hours

TREATMENT	TYPE OF TREATMENT	SOLUTION USED	TREATMENT DURATION
t10	Immersion	Benzalkonium Chloride 50%	24 hours
t11	Vapour exposure	80% RH	15 days

2.1.2.3 SAMPLE CHARACTERIZATION BEFORE AND AFTER TREATMENT

All samples have been characterized before and after tests, analysing different characteristics, such as weight variation, morphological and colorimetric variations, and chemical transformations by FTIR and Raman spectroscopy.

In particular, together with bench instruments, non-invasive portable techniques have been employed. This choice was made with the aim of defining standards and reference parameters to be compared in following in situ analyses, in order to monitor the actual state of conservation of real cases.

2.1.2.3.1 Weight Variation

Every sample has been weighed before and after each treatment with AND HR-120 multifunctional top-loading analytical balance AND HR-120 (e=1mg; d=0,1mg).

After each immersion treatment, wet samples were left dripping for 5 minutes before weighting, in order to avoid weighting unabsorbed solution. Samples were then weighted after 24 hours and after one month to monitor weight variations.

2.1.2.3.2 Morphological characteristics

Morphological characteristics of samples were investigated via portable contact microscope Dino Lite Premier AM4113/AD4112 series. All samples were analysed both under VIS and UV light at two different magnifications (50x and 220x).

Optical microscope (ZEISS SteREO Discovery.V8 coupled with Zeiss Axiocom 208 color camera) was also employed for observation at different magnifications, with the aim of comparing the results obtained with portable tools.

Scanning Electron Microscopy observations were also performed. Samples were cut round and applied with a double sided adhesive tape on metallic disks (1 cm diameter), in order to be available

also for Atomic Force Microscope (AFM) analyses. Au sputtering was performed for 30 seconds with a portion of sample covered, in order to allow further investigations via atomic force microscopy on un-sputtered areas.

Instrument xxx was employed, with xxx magnifications

Instrument Carl Zeiss Sigma VP Field Emission Scanning Electron Microscope (FE-SEM) equipped with EDS Bruker Quantax 200 probe. Imaging was performed in high vacuum (pressure around 10^{-6} - 10^{-5} mbar) with different magnifications (100x -250x – 500x – 1.000x and 25.000x) at 5keV.

Further morphological characterization of the silk surface was carried out by using a Bruker Dimension ICON AFM in tapping mode with a RTESPA-300 silicon cantilever (nominal spring constant ~40 N/m, nominal tip radius ~8 nm, measured resonance frequency 325,3 kHz).

The aim of this investigation was to observe the 3D nanometric structure of silk before and after treatment. The final goal was to understand if and which variations occurred at micrometric level, which may provide an interesting and explicative insight of the macroscopic phenomena observed. Different areas of a single thread were investigated, ranging from 5 μm^2 to 1000 nm^2. The samples employed were the same specimens investigated via scanning electron microscopy.

2.1.2.3.3 Colour variations

Colorimetric analyses are largely performed in the cultural heritage field. This technique enables precise evaluation of colour indicators variation and can be performed in a totally non invasive way. Colour is a crucial aspect in visual perception of objects, and its variation can therefore affect significantly artefacts' appearance. Thus, considering the great importance of visual appearance for cultural heritage, colour parameters represent a fundamental aspect to be taken into consideration.

For the present study KONIKA MINOLTA CM-700 spectrofotometer equipped with CM-S100w (SpectraMagicTM NX, Tokyo, Japan) software was employed. Measurement conditions: Illuminant D65, observer 8 degree viewing angle geometry and a 3 mm diameter target area.

Measurements were performed on the basis of "Colourimetric space" CIELAB 1976, which describes colours by the combination of three parameters: L* indicating lightness (0 black – 100 white), and a* (+red/-green) and b* (+yellow/-blue) representing colour coordinates. Data were collected both in SCI

(Specular Component Included) and SCE (Specular Component Excluded) modes only SCI component is reported here.

Data collected were elaborated by Spectra Magic NX 6 software. The total colour difference, ΔE, was calculated by the formula: $\Delta E = \sqrt{(\Delta L *^2 + \Delta a *^2 + \Delta b *^2)}$ where ΔL*, Δa* and Δb* are the differences between values obtained on the same sample, after and before the treatment. According to literature, ΔE was considered detectable by human eye when higher than 1, and the tolerance threshold was fixed around 5 [43-44]

2.1.2.3.4 Infrared Analyses

Infrared spectroscopy is a technique widely used in the cultural heritage field: it enables detection and characterization both of artefacts components and of degradation products, thus providing paramount information for heritage study and conservation.

Fourier Transformed Infrared Spectroscopy (ESR-FTIR)

IR spectroscopy is reported to be one of the most exploited techniques for silk chemical analyses, for it does not provide paramount information for material characterization.

Table 2reports FTIR band assignments for silk in Attenuated Total reflectance (ATR) mode anlaysis [24,27,45-46].

Table 2: literature FTIR band assignments for silk

ATR	
cm^-1	**peak attribution**
3275	stretching C=O
1699	Amide I (stretching C=O, C-N, N-H)
1665	Amide I in antiparallel β sheet conformation
1656	Amide I in random coil and α helical conformation
1620	Amide I in parallel β sheet conformation
1595	C-C-C tryptophan stretching
1511-1524	Amide II (peptide bond N-H bending and C-N bending)
1442	CH_2 e CH_3 Alanine bending
1405	CH_2 Aspargine bending
1367	CH bending
1334	CH bending; phenylalanine

ATR	
cm^-1	**peak attribution**
1261-1277	Amide III in β sheet conformation
1230-1236	Amide III in random coil conformation
1160-1164	CN Tyrosine stretching
1083	CN Alanine stretching
1065	CH_3 rocking + CN stretching
1035	CN Phenylalanine stretching
997	CH_3 rocking
977	CC skeletal stretching in Glycine-Glycine and Glycine-Alanine
800	CC skeletal stretching + CH out of plane deformation in aromatic rings of tryptophan
605	Amide III mode
540	Deformation CCN mode
442	Deformation CCN mode

Furthermore, IR spectroscopy is also reported to be a useful tool for assessing degradation degree of silk [24,27,30,45]. Typical modifications to silk structure, in fact, result in variations on IR spectra bands (e.g. variation of intensity of specific absorption peaks).

In particular, three main processes (crystallinity degree, oxidation ratio and depolymerization degree) can be evaluated by specific indicators defined by the ratio between characteristic infrared peaks. Indeed, characteristic absorbance FTIR peaks for crystallinity evaluation are located at 1620 and 1656 cm^{-1} or at 1620 and 1699 cm^{-1} [24]. Crystallinity can also be defined as the ratio of areas under fitted curves at 1261 and 1230 cm^{-1}. Oxidation processes, instead, find their indicator in the ratio of absorbances FTIR peaks at 1620 and 1514 cm^{-1}, while depolymerisation is detectable by comparing the ratio of areas at 1318 and 1442 cm^{-1} [24,29] These indicators have been defined experimentally through thermal and chemical degradation (e.g. presence of VOCs) [24,30]. Since literature lacks of studies on silk degradation related to water and alcohol, these indicators are here reported with the aim of comparing them to the results observed in the present study.

Beside the potential of ATR for analysis of silk and its degradation reported in literature, some drawbacks are also present. In particular, as reported by Badillo-Sanchez [47] the pressure applied during the analysis may alter the structure of the fiber, thus providing similar results for aged and unaged samples.

External Spectroscopy Reflectance- ESR

Traditionally, FTIR spectroscopy is a non-portable invasive technique, for it requires sampling and preparation of specimens. Nowadays, however, portable non-invasive IR instruments are available, thus enabling the exploitation of IR spectroscopy also on a broader number of artefacts. This is possible thanks to spectra collection in External Reflection (ER) mode, a technique introduced several years ago but not yet integrated in the routine of artworks analyses, mostly due to distortions of band shape, position and intensity if compared to spectra acquired in transmittance or ATR mode [45,48-50].

Therefore, portable ESR-FTIR was employed here with the aim of both comparing the response of portable external reflectance spectrometer and bench FTIR instruments, and developing a reference library for silk in situ analyses. ER analysis, moreover, is performed in contact mode without applying additional pressure to the sample, thus avoiding the problem reported by Badillo-Sanchez [47].

In order to completely analyse silk samples before and after treatments, measures were performed both in ATR and ER modes.

Infrared spectroscopy analyses were performed with a portable Bruker ALPHA spectrometer equipped with an Attenuated Total Reflection (ATR) modulus based on a single-bounce diamond ATR crystal and an External reflection modulus. The acquisition involved 32 scans acquired in the spectral range 4000-400 cm^{-1} . Data have been acquired and processed by Opus 8.2.28 by Bruker Optics software.

Moreover, in order to validate the results acquired by portable instrument, ATR analyses with bench instrument have been conducted on reference samples. Spectrofotometer FITR Thermo Nicolet Nexus 670 FTIR spectrophotometer combined with a Smart Orbit Single Reflection Diamond ATR accessory (FT-IR-ATR, Thermo Fisher Scientific Spa, Rodano, Italy) was employed. Measures were collected from 4000 to 400 cm 1 for 128 scans with 4 cm 1 resolution was employed.

2.1.2.3.5 Raman Analyses

Together with IR analyses, Raman spectroscopy is considered a paramount technique for cultural heritage analyses, for it provides information complementary to FTIR and, if used in portable mode, can perform analyses without the need for sampling.

Raman spectra were here collected with Bravo portable Raman spectrometer by Bruker Optics. Spectra were collected in the wavenumber spectral range between 3200-300 cm-1 (resolution of 3

cm-1, scan time from 1s to 60s). Acquisition of spectra was here performed with two lasers working simultaneously. Each laser works on a different region of Raman spectrum (the first one, 758 nm on the 1500-300cm^{-1} range; the second, 852 nm, on the 3200-1500 cm^{-1} range). instrument is equipped with two lasers (at 758 and 852 nm) working simultaneously. Spectral acquisition has been performed by the proprietary software, OPUS (8.2.28 version).

Moreover, in order to validate the results acquired by portable instrument, Raman analyses were performed using a micro Raman DXR3 Thermo Fisher bench instrument have been conducted on reference samples. Micro Raman parameters for analyses were selected as follows:

- Laser wavelength 785nm
- Exposure time 0.5 s
- Laser power between 5mW and 7mW
- Aperture 25 μm
- Magnification 50x
-

Table 3 reports Raman band assignments for silk [26,39].

Table 3: literature characteristic Raman signals for silk

Raman	
cm^-1	**peak attribution**
622	Phenylalanine
645-54	Tyrosine ring-breathing mode
760	Tryptophan
830	Tyrosine (bending of ring)
855	Tyrosine (bending of ring)
885	CC skeletal stretch, Tryptophan
900-960	skeletal mode
979	CC skeletal stretch
1004	COC stretching vibration of tryptophan ring and phenyl ring of phenylalanine
1087	CN stretch
1159	CN stretch
1232	Amide III in β sheet conformation (bending)
1269	Amide III in β sheet conformation and disordered (bending)

Raman	
cm^-1	**peak attribution**
1308	CH bend
1337	CH bend, Phenylalanine
1449	CH_2, CH_3 bending modes
1585	Phenylalanine
1605	Phenylalanine
1616	Tryosine, Tryptophane
1668	Amide I in β sheet conformation (stretching)
1675	Amide I
2875	CH_3 symmetrical stretch
2934	CH_3 stretch asymmetrical
3063	CNH bend overtone
3286	NH stretch

As mentioned for FTIR spectroscopy, Raman analyses on silk can support identification both of materials and degradation processes.

Among the examples reported in literature, Shao (2004) focuses the attention to the tyrosine signals at 855 and 830 cm^{-1} as indicators of UV and Ozone induced degradation [45]. As mentioned before, silk photo-yellowing is related to the oxidation of tyrosine and tryptophan residues. The double peak at 855 and 830 cm^{-1} is therefore quite significant; the comparison of the relative intensity of the two peaks can, in fact, provide information about the hydrogen bonding and state of ionization of the phenolic hydroxyl group [45]. If the peak at 855 cm^{-1} is more intense than the other, then tyrosine residues result to be only moderately H-bonded or exposed in hydrophilic areas. On the contrary, having 830 cm^{-1} peak higher in intensity means that tyrosine is strongly H-bonded or buried in hydrophobic regions [45].

However, this is not the only indication for degradation: decreasing intensity of the 1232 cm^{-1} peak leads to the conclusion that UV/ozone irradiation causes peptide chain scission [45]. As reported before for FTIR degradation indicators, since literature does not provide specific studies on silk degradation related to water and alcohol, these indicators will be taken as reference to evaluate possible variations in silk structures, even though not related to UV or O_3 reactions.

2.1.2.3.6 Crystallinity evaluation

As mentioned before, crystallinity degree is a characteristic of great importance for evaluating the silk state of conservation. Therefore, X-Ray Diffraction analyses have been performed on two significant samples in order to assess crystallinity variation before and after treatments.

White silk and red Velvet have been analysed before and after treatment 3 (immersion in sanitising solution). The choice of these two types of silk was made to verify the crystallinity structure and crystallinity variation in one unaged, recently produced and uncoloured sample and on a coloured sample produced with traditional techniques.

X-ray diffraction (XRD) analysis was performed by means of a Phylips (Panalytical) Powder Difractometer (generator r-x PW1850, equipped with monocromator, proportional counter PW 1711, Tubo rx Philips PW2273/20 Cu LFF, Ni filter, 40kW, 30mA).

The patterns were collected in the 2θ range of 5-40 with step size of 0.05.

According to Koperska (2014) and Mei Ying Li (2013), silk presents diffraction peaks characteristic for the amorphous and crystalline regions, as reported in Table 4 [24, 51].

Table 4: literature XRD peaks for silk structure

REGION	PEAK (2θ)
amorphous	19,7°
	24,7°
	28,2°
crystalline	8,8°
	18,9°
	20,7°

Other studies, however, report contrasting results regarding crystalline characteristic peaks. In particular, while Koperska (2014) refers 24,7° peak to the amorphous component, Um (2004) and (2020) attribute it to the crystalline region [52,53]. These two latter studies, however, refer to unaged raw silk compared with regenerated fibroin. Therefore, despite the contrasting attribution of the peak at 24,7°, Koperska assignation was preferred here since the studies presented in his papers referred to historic silks, thus presenting closer similarities to the fabrics here investigated.

Data acquired in XRD analysis have been here compared with the results obtained with spectroscopic investigations, in order to perform a complete interpretation of data.

2.1.2.3.7 Wettability

The evaluation of wettability by measuring the contact angle before and after sample treatments gives an indication of possible modification occurred on the material. In fact, value of the contact angle strongly depends on the chemical and morphological (e.g. roughness) characteristics of the sample.

Therefore, the detection of a contact angle variation after sample treatments represents an immediate indicator of the fact that possible modifications may have occurred on the surface.

Wettability measures were here performed depositing a drop of deionised water on each sample and capturing a picture with a portable microscope fixed on a support that made it standing perpendicularly to the sample. The evaluation of the contact angle was performed calculating the angle between the surface of the sample and the upper side of the drop. The measuring was performed according to EN15802:2010 and documented with the software DinoCapture version 2.0.

3. RESULTS AND DISCUSSION

3. 1 SILK CHARACTERIZATION BEFORE TREATMENT

3.1.1. MORPHOLOGICAL CHARACTERIZATION

Figure 4 reports the photographs of untreated samples taken with portable microscope at two different magnifications both under UV and visible light.

Figure 4: untreated silk samples observed via portable contact microscope

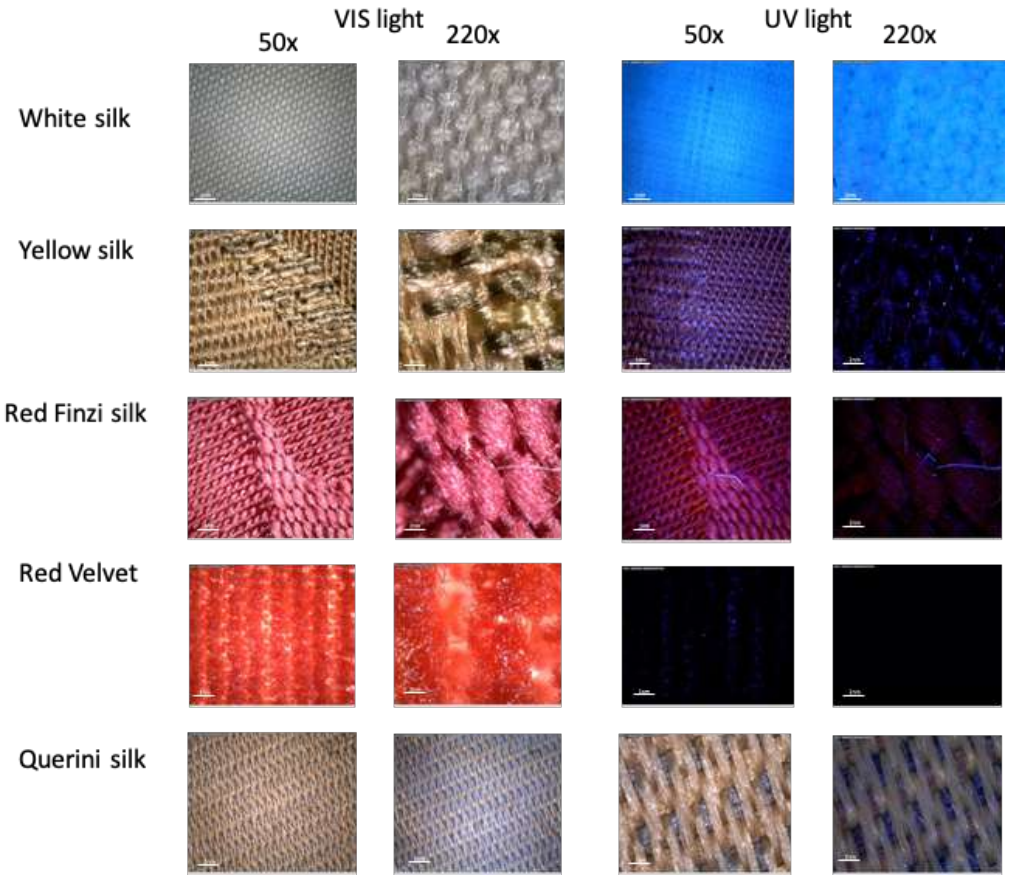

The five structures presented are quite different from many points of view: thread diameter, colour and weaving.

White silk, Finzi silk and Querini silk present a homogeneous structure, probably due to the industrial process of production and weaving. On the other hand, yellow silk and red velvet show an ordered but not so even fabric; this characteristic is probably due to the handcrafted traditional production methods.

No specific signs of fluorescence could be identified during observations under UV light.

3.1.2. CHEMICAL CHARACTERISATION

3.1.2.1 FOURIER TRANSFORMED INFRARED ANALYSES

3.1.2.1.1 PORTABLE ATR

In order to study the chemical structure of the different types of silk under analyses, Fourier Transformed Infrared Analyses (FTIR) in Attenuated Total Reflectance (ATR) spectra were collected on samples before treatments. As reported before, white, Finzi and Querini silk can be considered representative of three types of silk (new industrial silk, recent industrial silk and tapestry with strong signs of degradation), and will be therefore reported as reference also in following results' discussion.

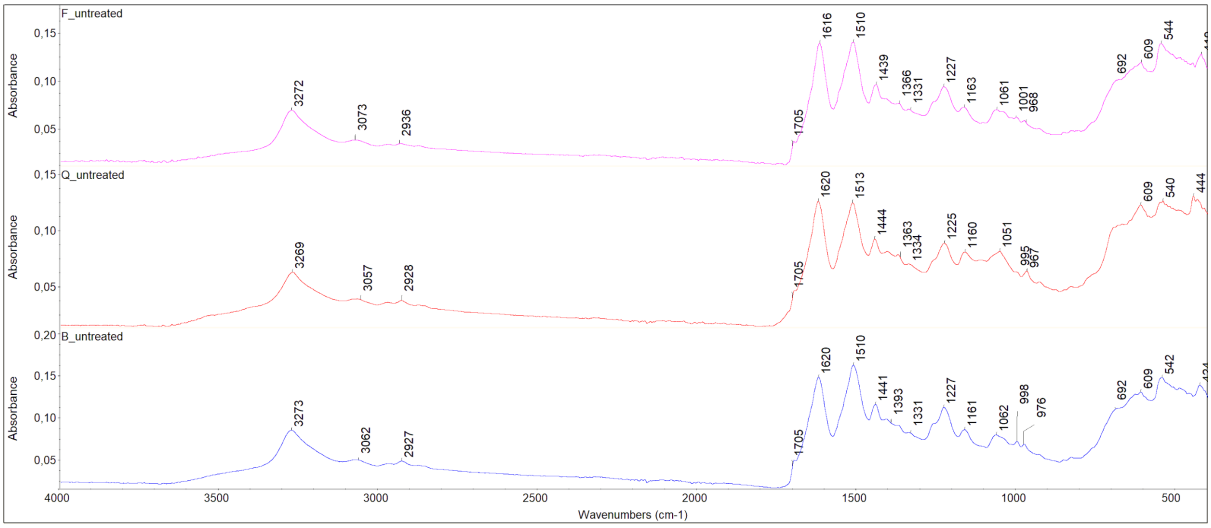

Figure 5: ATR spectra of white, Finzi and Querini untreated silks

Figure 5 reports a comparison between ATR spectra collected with the portable instrument. Despite the different production processes and the different colours, all the spectra show a strong resemblance, and it appears quite easy to identify silk characteristic peaks.

As reported in Table 2, the characteristic Amide I peaks can be identified at 1700 and at 1620 cm^{1}, as well as those attributable to Amide II at 1520cm^{-1}. Peaks around 1441 and 1408 cm^{-1} are referred to characteristic CH_2 and CH_3 Alanine bending and to CH_2 Aspargine bending, respectively. Weak peaks in the 1400-1300cm^{-1} region are probably ascribable to CH bending (1360-1370 cm^{-1}) and to CH Phenylalanine bending (1338 cm^{-1}). Amide III at 1260 cm^{-1} shows a weak signal, while Amide III at 1230 cm^{-1} has definitely a stronger absorption. Tyrosine CN stretching around 1160 cm^{-1} can be

spotted in all spectra. Signals around 1065 cm^{-1} (CH_3 rocking and CN stretching) and 1035 cm^{-1} are weak but well detectable in all spectra. Weaker signals in the 1000-900 cm^{-1} region can be spotted and attributed to CH_3 rocking (around 997 cm^{-1}) and CC skeletal stretching (977 cm^{-1}). 605 cm^{-1} Amide II mode and 540 cm^{-1} deformation CCN mode peaks are instead detectable but very weak.

Literature reports several FTIR studies on silk with a limited wavenumber range, therefore not including the whole region to 4000 cm^{-1}. The present study, however, presents a complete FTIR ATR analysis on silk collecting IR signals also for this expanded region.

As shown in Figure 5, a few characteristic peaks can be identified in the 4000-2000 cm^{-1} region such as: 2847, 2931, 2966, 3070 and 3270 cm^{-1}, probably attributable to OH stretching. Literature confirms the presence of these peaks as characteristic of silk [32].

3.2.2.1.2 FTIR ANALYSES BY BENCH INSTRUMENT

With the aim of comparing the response of portable ATR with a traditional laboratory ATR analyses, further investigations with bench ATR were conducted on untreated silk.

As shown in Figure 6, two main differences can be observed in the compared spectra. First, that portable spectrum is slightly shifted towards lower wavenumbers; second, that spectrum collected with bench tool presents an absorption around 2000 cm^{-1}, most likely ascribable to CO_2.

All these things considered, it might be concluded that ATR investigation with portable instruments are quite reliable and can therefore provide a powerful tool for in situ investigations.

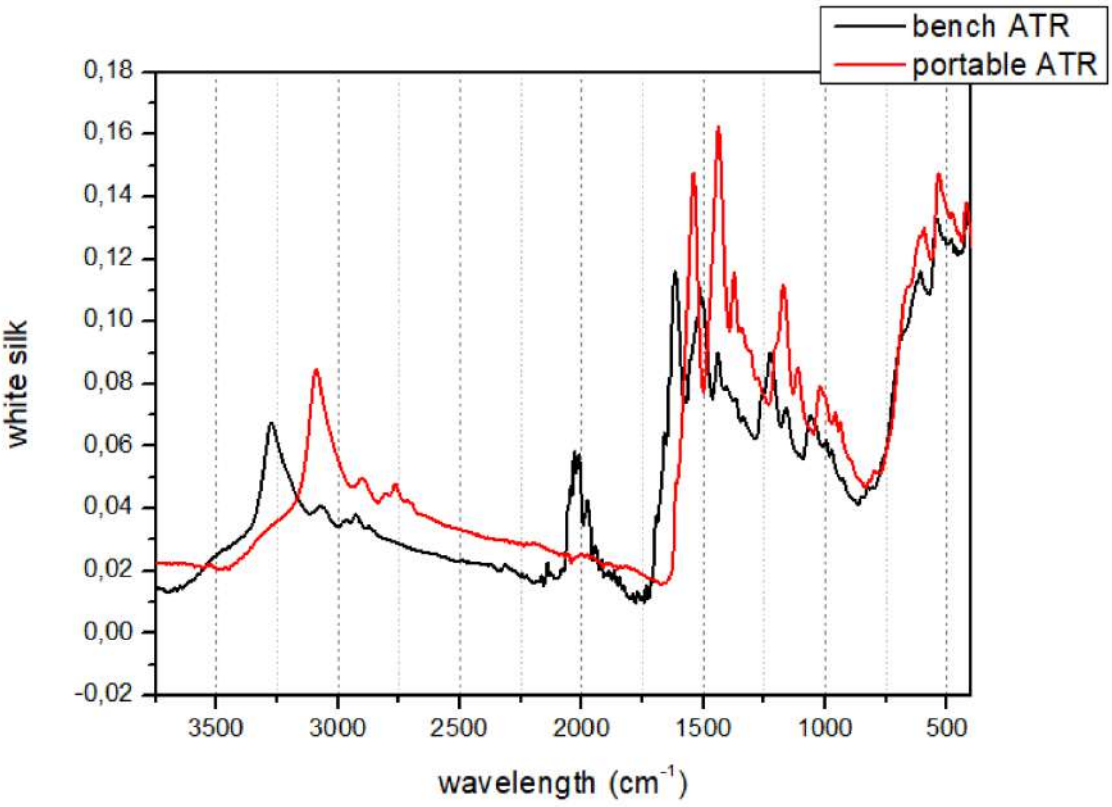

Figure 6: comparison between ATR spectra of untreated white silk acquired with portable and bench tool

3.2.2.1.3 EXTERNAL REFLECTANCE ANALYSES

Silk samples were investigated with ER technique, with the aim of characterizing and studying silk also with a non-invasive, portable technique more suitable to cultural heritage. ATR in fact, despite its remarkable characteristics, requires the sample to be thin enough to be inserted between the diamond and the pressure applicator and, as mentioned before, a significant pressure is applied to samples during the analyses [47].

Besides its potentialities, however, ER spectra lack of complete reference libraries and are thus quite challenging to interpret.

The present study, therefore, provided the possibility of collecting several spectra and comparing them to the correspondent ATR one.

References on ER analyses of silk report that some characteristic FTIR band tend to shift towards higher wavenumbers for external reference spectra; in particular, stretching of N-H amide band from 3275 cm^{-1} to 3325 cm^{-1}, stretching of C=O of amide I band from 1615 cm^{-1} to 1720 cm^{-1}, bending of N-H in amide II from 1515 cm^{-1} to 1541 cm^{-1} and stretching of C-N in amide III from 1235 cm^{-1} to 1248 cm^{-1} [46].

As it can be seen in Figure 7, literature ER spectra of silk report shifted characteristic peaks [46,50].

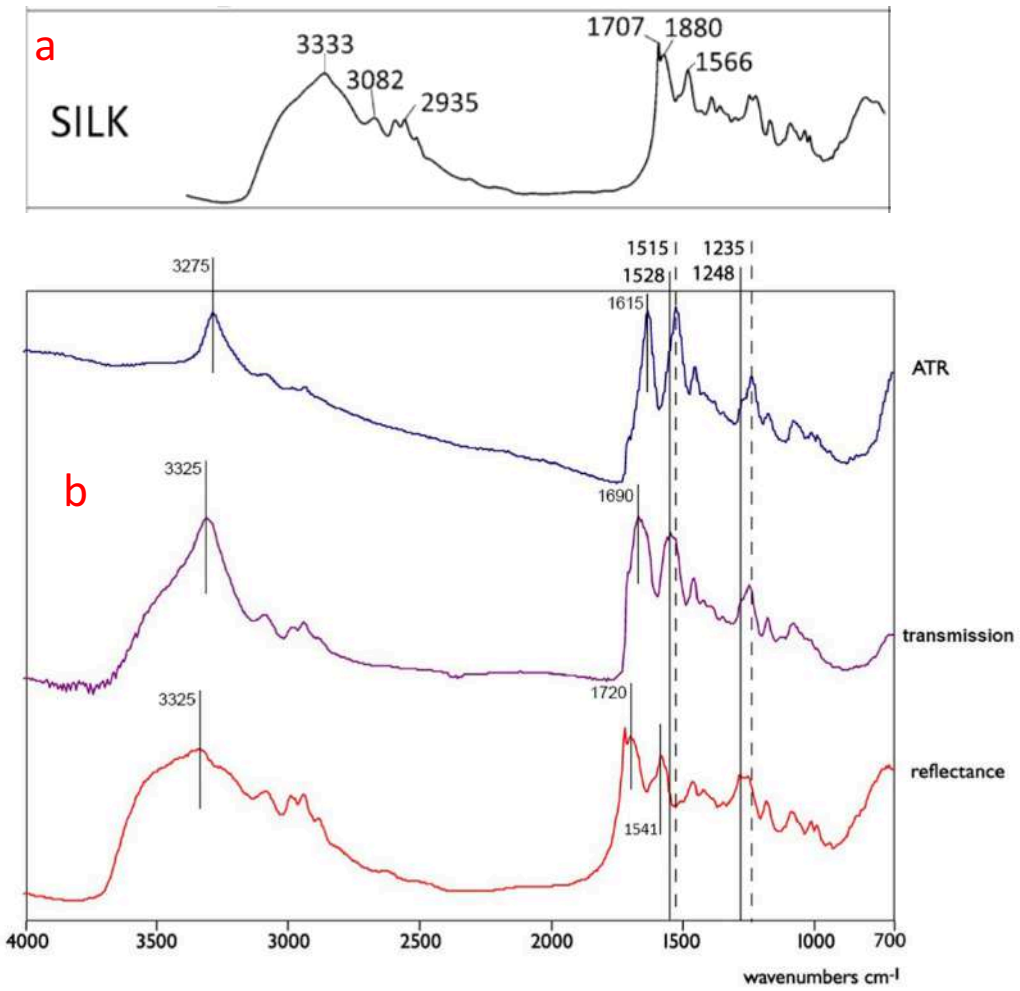

Figure 7: literature ATR spectra of silk: a)Peets (2019) b)Margariti (2019)

This phenomenon was indeed observed also in the present study, as reported in Figure 8. Finzi silk is here taken as representative of the different types of silks studied; its spectrum clearly shows the above-mentioned shift for amide characteristic peaks.

Finzi untreated silk

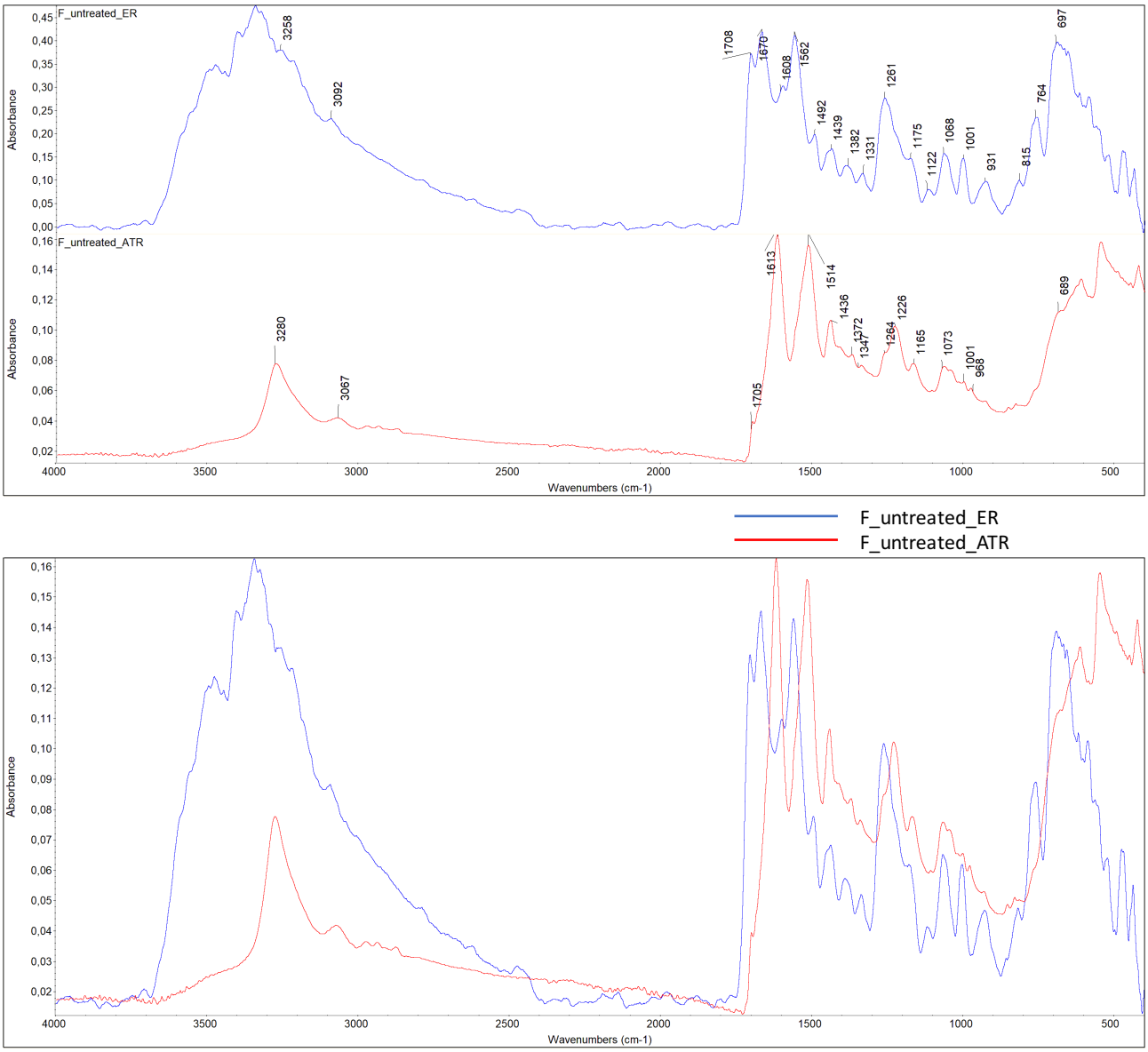

Figure 8: comparison of ATR and ER spectra of Finzi silk acquired with portable instruments

3.2.2.2 RAMAN

With the aim of performing the investigation more in detail, Raman spectra were collected both with portable and with micro Raman bench instruments.

3.2.2.2.1 PORTABLE RAMAN

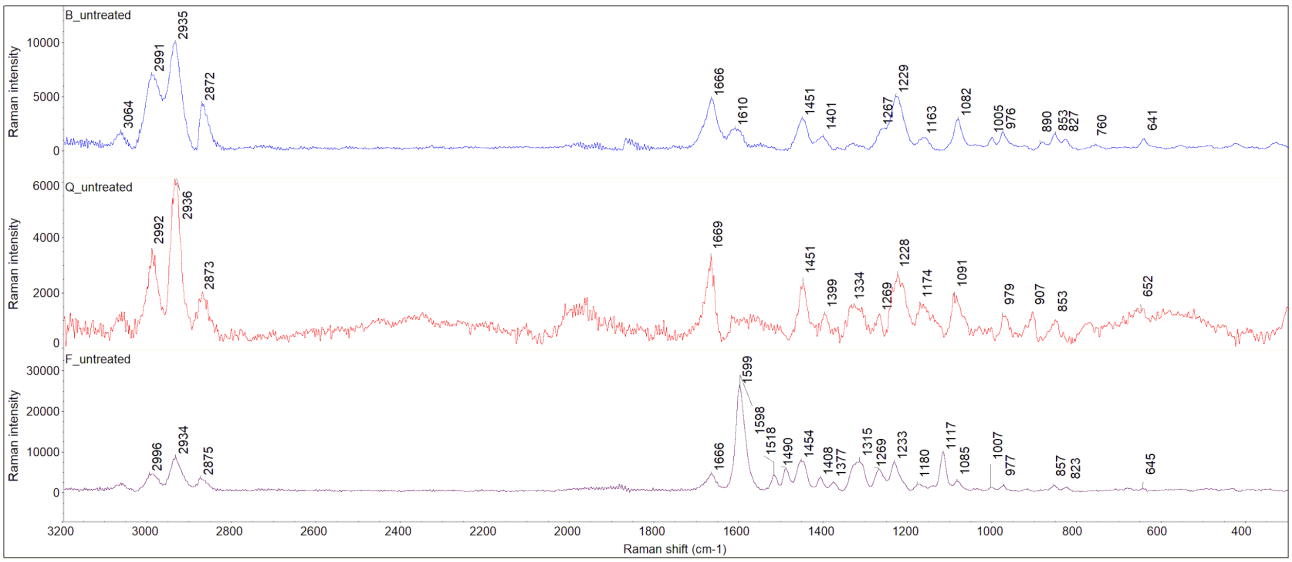

Figure 9 shows the comparison between silk spectra collected for each of the three reference-samples: white (B), Finzi (F) and Querini (Q) silk.

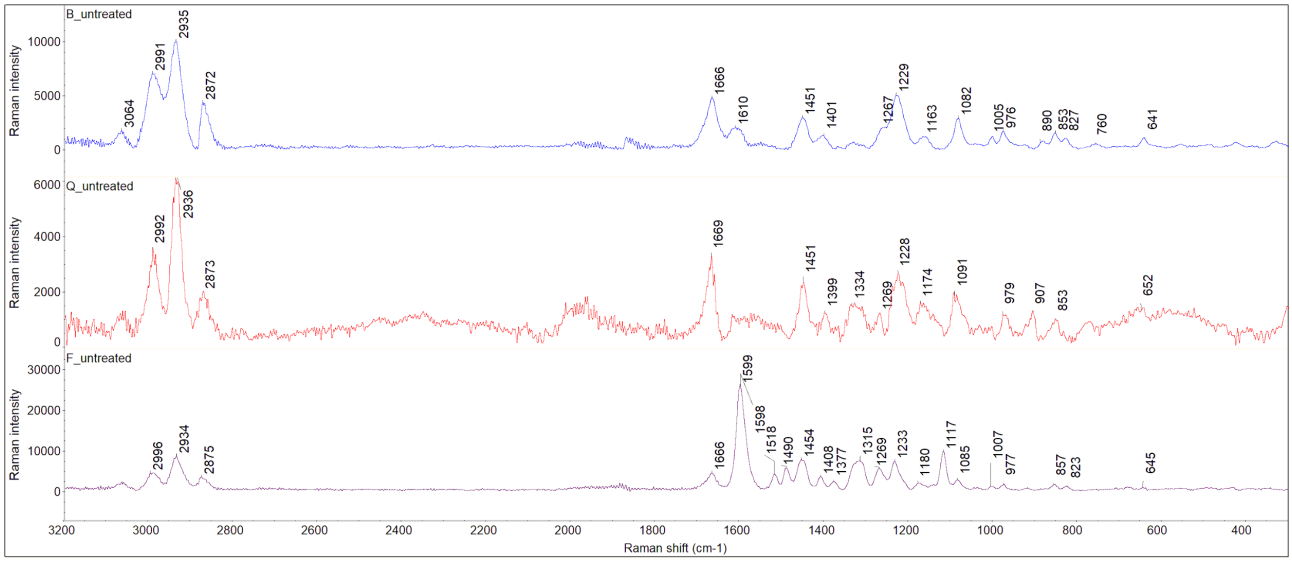

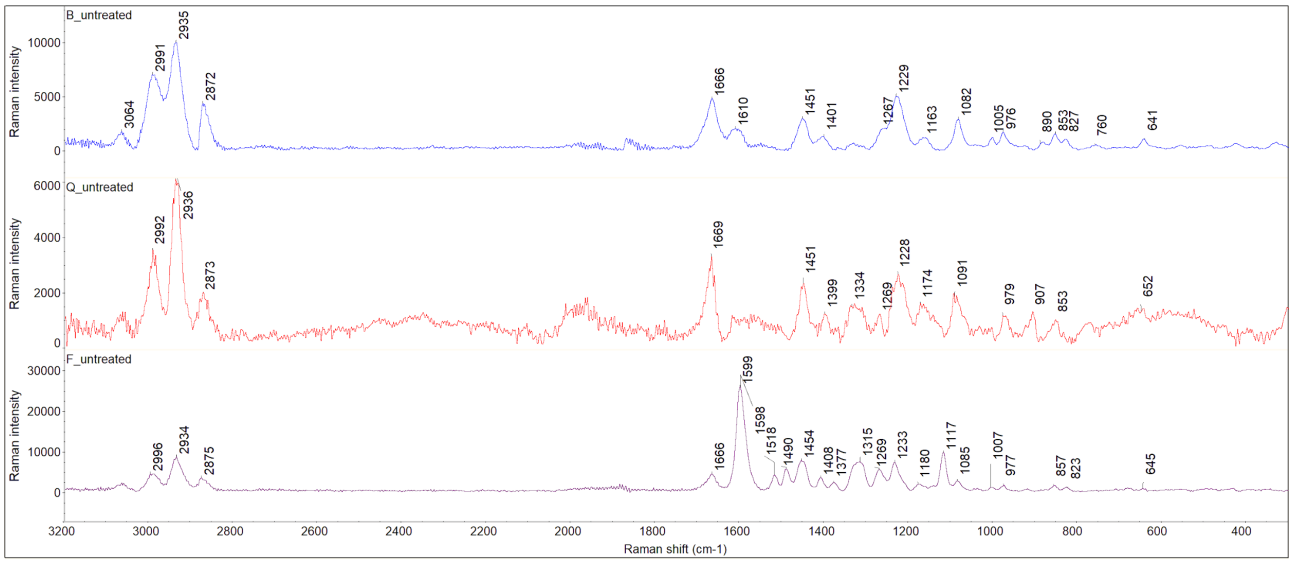

Figure 9: Raman spectra of white, Finzi and Querini silk

Even though characteristic silk peaks can still be identified, we can spot here a number of differences, for each spectrum, together with specific intensities, presents peaks probably related to colourants, processing components or (as in the case of Querini silk) dust.

As shown in

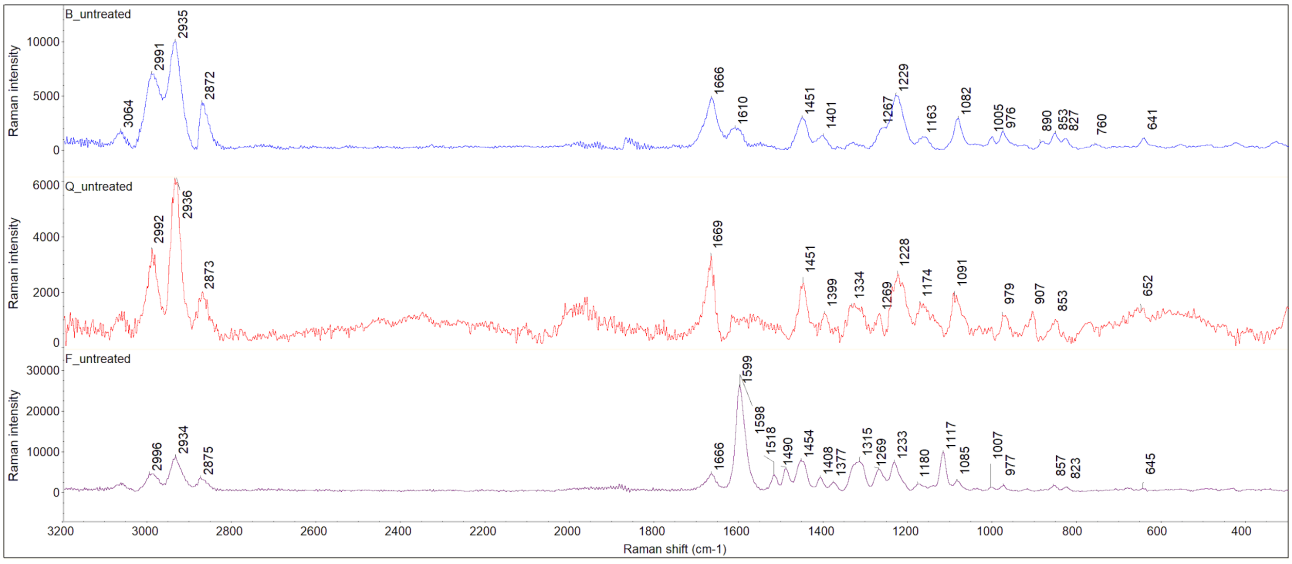

Figure 9, all silk samples characteristic tyrosine and tryptophan peaks can be spotted at 643 cm^{-1} (tyrosine) and 760 cm^{-1} (tryptophan), despite the weak or noisy signal. The characteristic doublet of tyrosine can be found at 830-855 cm^{-1}, together with another tryptophan signal at 880 cm^{-1}. Peaks at 930-975 cm^{-1} can be attributable to CC skeletal stretch, while peaks at 1001 and 1045 cm^{-1} are attributable to phenylalanine. CN stretch gives origin to peaks at 1086 and 1167 cm^{-1}, while Amide III is responsible for the signals at 1225 and 1260 cm^{-1}.

Peaks in the 1300-1400 cm^{-1} region are ascribable to CH bending; in particular, the peak at 1336 cm^{-1} appears to be due to phenylalanine, while peak at 1408 cm^{-1} relates to asparagine. Phenylalanine is also responsible for signals at 1602 and 1619 cm^{-1}, while peak at 1665 cm^{-1} refers to tyrosine and tryptophan. Signals between 2800 and 3100 cm^{-1} find here a correspondence in literature; 2800 and 2935 cm^{-1} peaks refer to CH_3 stretching, the former symmetric and the latter asymmetric, while the peak at 3065 cm^{-1} results in a CNH bend overtone.

Querini silk, together with the noisy signal, presents a strong absorption band at 1334 cm^{-1}, which could be attributed either to phenylalanine or to a signal related to silk colouring. However, the band might also be ascribed to the incoherent materials deposited on Querini silk over time.

Finzi silk, instead, besides silk characteristic peaks, shows a strong signal at 1599 cm^{-1}, together with two peaks at 1518 cm^{-1}, 1490 cm^{-1} and 1315 cm^{-1}. These signals can be probably assigned to colourant component of the sample; similar peaks can be detected, in fact, in red colourants such as permanent carmin [54-55].

3.2 SILK CHARACTERIZATION AFTER TREATMENTS

3.2.1 WEIGHT VARIATION

Weight was measured for each sample before and at least two times after every treatment to evaluate possible different behaviours towards liquids and environmental humidity absorption.

Silk samples did not undergo any drying treatment before performing tests. Therefore it can be presumed that before being treatment samples contained a defined amount of humidity they had absorbed along time. This condition can, therefore, have influenced samples' behaviour with regards to weight variation.

3.2.1.1 VAPOUR EXPOSURE (treatment 1)

Weight variation after exposure to sanitising solution's vapours in a closed environment presents a differing tendency for each type of sample, as shown in Table 5.

While all the samples showed a weight increase between 1 and 8% after the 10 days exposure to sanitising solution vapours, most probably due to absorption of humidity, the behaviours appear quite different for the dry treated samples. Querini silk and Finzi silk, the two industrial silks with an unknown conservation history, show a slight weight increase (between 1 and 5%), 24 hours after the

treatment, while they almost regained their original weight 1 month after the treatment, being conserved in a unsealed desiccator (weight increase between 0 and 2%).

The white wet silks, instead, shows a consistent increase of weight (between 2 and 8%), which, however, rapidly decreased after drying showing a general drop in weight (between -1 and -2%). This decrease might be ascribable to ethanol action, which, during the exposure time, might have displaced water bonding to the peptide chain. After the evaporation of the alcohol, however, some binding sites may have reorganized their structure, preventing water from completely hydrating the structure back. This loss of internal water can possibly explain the weight decrease observed [39].

Table 5: weight variation for samples exposed to sanitising solutions' vapours for 10 days

		before treatment	wet 10 days			dry (10 days wet + 24h drying)			dry (10 days wet + 1 month drying)		
		weight (g)	weight (g)	Δw (g)	Δw%	weight (g)	Δw (g)	Δw%	weight (g)	Δw (g)	Δw%
WHITE SILK	B1_t1	0,2443	0,2484	0,0041	2%	0,243	-0,0013	-1%	0,2398	-0,0045	-2%
	B2_t1	0,2448	0,2559	0,0111	5%	0,2411	-0,0037	-2%	0,2377	-0,0071	-3%
	B3_t1	0,2531	0,2457	-0,0074	-3%	0,2505	-0,0026	-1%	0,2463	-0,0068	-3%
	B4_t1	0,2362	0,2553	0,0191	8%	0,2475	0,0113	5%	0,2444	0,0082	3%
FINZI SILK	F1_t1	0,5132	0,5516	0,0384	7%	0,5289	0,0157	3%	0,5223	0,0091	2%
	F2_t1	0,4262	0,4495	0,0233	5%	0,4328	0,0066	2%	0,4261	-0,0001	0%
	F3_t1	0,5119	0,5441	0,0322	6%	0,5226	0,0107	2%	0,5157	0,0038	1%
	F4_t1	0,4172	0,4378	0,0206	5%	0,423	0,0058	1%	0,4172	0	0%
QUERINI SILK	Q1_t1	0,3457	0,3698	0,0241	7%	0,3561	0,0104	3%	0,3487	0,003	1%
	Q2_t1	0,3403	0,3613	0,021	6%	0,35	0,0097	3%	0,342	0,0017	0%
	Q3_t1	0,3296	0,3559	0,0263	8%	0,3455	0,0159	5%	0,337	0,0074	2%
	Q4_t1	0,3248	0,3417	0,0169	5%	0,3315	0,0067	2%	0,3214	-0,0034	-1%

3.2.1.2 IMMERSION IN SANITISING SOLUTION

30 minutes (treatment 2)

Table 6 reports the weight variations for the samples which undertook the immersion treatment in sanitising solution for 30 minutes. As it can be noticed by observing the weight percent variation for wet samples, different silks show a different tendency to absorb the sanitising solution over 30 minutes. White wet samples increased their weight of only 30-38%, while Querini silks increased it by 70 -100% and red Finzi silks by over 140%. These extremely different behaviours are ascribable to the

intrinsic characteristics of the fabric. As a matter of fact, each analysed fabric presents a characteristic thickness of thread and a different weaving technique.

Weight fluctuations in dry samples presented several differences too: white silk and Querini silk barely increased their final weight (around +5%); final weight for Finzi silk resulted slightly higher than initial one (+5 /+26%). Sample F3, however, presented a decrease in weight (-7%); this tendency greatly differs from all other data, suggesting an anomaly in the sample. These variations are most likely ascribable to benzalkonium chloride residues deposited on the silk surface.

Table 6: weight variation for samples immersed in sanitising solution for 30 minutes

	before treatment	wet 30 min			dry (24h drying)			dry (1 month)		
	weight (g)	weight (g)	Δw (g)	Δw%	weight (g)	weight (g)	Δw (g)	Δw%	weight (g)	weig ht (g)
B1_t2	0,1869	0,2541	0,0672	36%	0,196	0,0091	5%	0,1939	0,007	4%
B2_t2	0,1662	0,2281	0,0619	37%	0,1759	0,0097	6%	0,1752	0,009	5%
B3_t2	0,1467	0,202	0,0553	38%	0,1553	0,0086	6%	0,1545	0,0078	5%
B4_t2	0,1528	0,1999	0,0471	31%	0,1618	0,009	6%	0,161	0,0082	5%
F1_t2	0,2831	0,6892	0,4061	143%	0,3074	0,0243	9%	0,3058	0,0227	8%
F2_t2	0,2886	0,741	0,4524	157%	0,362	0,0734	25%	0,3124	0,0238	8%
F3_t2	0,3356	0,873	0,5374	160%	0,3135	-0,0221	-7%	0,3621	0,0265	8%
F4_t2	0,2841	0,7464	0,4623	163%	0,306	0,0219	8%	0,308	0,0239	8%
Q1_t2	0,2429	0,4967	0,2538	104%	0,2588	0,0159	7%	0,2571	0,0142	6%
Q2_t2	0,2283	0,444	0,2157	94%	0,2441	0,0158	7%	0,2564	0,0281	12%
Q3_t2	0,2385	0,4078	0,1693	71%	0,2416	0,0031	1%	0,2414	0,0029	1%
Q4_t2	0,2247	0,3943	0,1696	75%	0,2397	0,015	7%	0,2368	0,0121	5%

24 hours (treatment 3)

Table 7 reports the weight variations for samples which undertook the immersion treatment in sanitising solution for 24 hours. As noticed before for treatment 2, different silks show a different tendency to absorb sanitising solution, also in the long term. White wet sample, in fact, increased its weight of 60-70%, while Querini silk increased it of 140-170% and red Finzi silk by over 230%. If compared to the variations observed for treatment 2 it appears clear that the weight increase percentage has almost doubled for every sample

Weight fluctuations in dry samples, instead, were almost constant for each type of fabric: depending on the size of samples, each silk presented a final weight increase between 5 and 20%, even after 1 month. As mentioned before, these variations are most likely ascribable to benzalkonium chloride

residues deposited on the silk surface and to water, which might have been retained thanks to benzalkonium action.

Table 7: weight variation for samples immersed in sanitising solution for 24 hours

	before treatment	wet 24 hours			dry (24h drying)			dry (1 month)		
	weight (g)	weight (g)	Δw (g)	Δw%	weight (g)	Δw (g)	Δw%	weight (g)	Δw (g)	Δw%
B5_t3	0,0789	0,1246	0,0457	58%	0,0833	0,0044	6%	0,0828	0,0039	5%
B6_ t3	0,0812	0,1406	0,0594	73%	0,0948	0,0136	17%	0,0952	0,014	17%
B7 t3	0,0809	0,137	0,0561	69%	0,0945	0,0136	17%	0,0903	0,0094	12%
B8 t3	0,0732	0,1226	0,0494	67%	0,0843	0,0111	15%	0,0836	0,0104	14%
F5_ t3	0,1552	0,5675	0,4123	266%	0,1903	0,0351	23%	0,1882	0,033	21%
F6_t3	0,1761	0,5891	0,413	235%	0,1906	0,0145	8%	0,1912	0,0151	9%
F7_t3	0,1986	0,6897	0,4911	247%	0,2195	0,0209	11%	0,2183	0,0197	10%
F8_t3	0,182	0,6511	0,4691	258%	0,2127	0,0307	17%	0,2124	0,0304	17%
Q5_t3	0,1634	0,395	0,2316	142%	0,172	0,0086	5%	0,1783	0,0149	9%
Q6_t3	0,1679	0,4361	0,2682	160%	0,185	0,0171	10%	0,183	0,0151	9%
Q7_t3	0,1609	0,3948	0,2339	145%	0,164	0,0031	2%	0,1702	0,0093	6%
Q8_t3	0,1503	0,3707	0,2204	147%	0,157	0,0067	4%	0,1545	0,0042	3%

Samples immersed in sanitising solution showed a general tendency to absorb liquid (increasing their weight) with different rates based on sample's characteristics, and to retain a certain amount of product (most likely benzalkonium chloride, as ethanol and water tend to evaporate) as reported on Figure 10. However, considering that weigh of wet samples is not directly related to weight variation for dry samples, it can be concluded that also residue humidity contributed to determine the final weight.

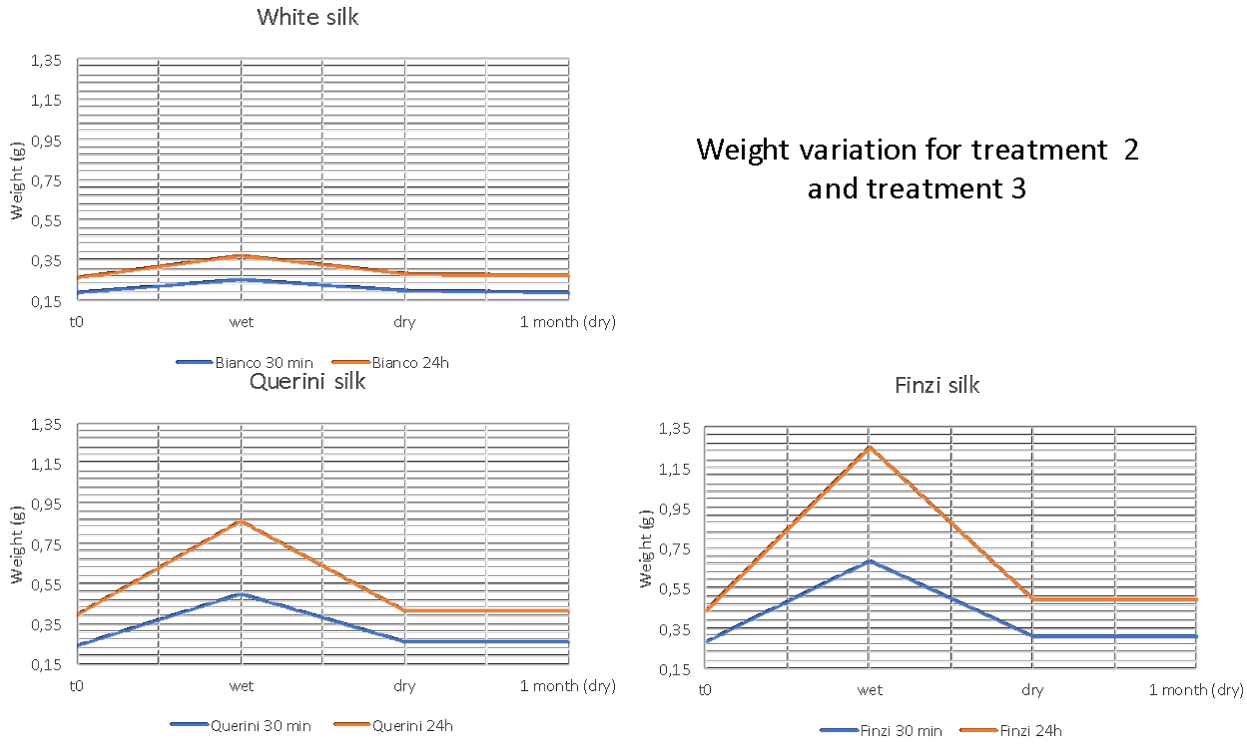

Figure 10: comparison of weight variation under treatment 2 and 3 for each treated sample

3.2.1.3 IMMERSION IN DEIONIZED WATER (treatment 4)

Table reports the weight variations for the samples which undertook the immersion treatment in water for 24 hours. As noticed before for treatment t2 (immersion in sanitising solution for 30 minutes) and t3 (immersion in sanitising solution for 24 hours), different silks show a different tendency to absorb solutions. We therefore notice here a consistent increase of weight, as follows: +125% for white silk, +240% for yellow and Querini silk, +310% for Finzi silk and + 338% for red Velvet. If compared to the sanitising solution levels, it appears clearly that lower values of weight increase were reported before, due to the presence of volatile ethanol in the solution. The samples, in fact, after each treatment were left dripping for 5 minutes to avoid weighting unabsorbed drops of solution.

The dry samples showed two different tendencies: white and Finzi silk appeared to increase their final weight, probably because of water retention. On the contrary, Querini silk decreased its final weight, presenting a decrease of -10 after 24 hours and of -58% after one month, which is most likely due to loss of dust and other incoherent material deposited on the surface.

Table 8:weight variation for samples immersed in deionized water for 24 hours

	before treatment	wet 24 hours			dry (24h drying)			dry (1 month)		
	weight (g)	weight (g)	Δw (g)	Δw%	weight (g)	Δw (g)	Δw%	weight (g)	Δw (g)	Δw%
B_t4	0,0812	0,183	0,1018	125%	0,0956	0,0144	18%	0,0954	0,0142	17%
Q_t4	0,1377	0,4714	0,3337	242%	0,1244	-0,0133	-10%	0,0575	-0,0802	-58%
F_t4	0,1881	0,7734	0,5853	311%	0,2018	0,0137	7%	0,2031	0,0150	8%

3.2.1.4 IMMERSION IN ETHANOL ABSOLUTE (treatment 5)

Table reports the weight variations for samples which undertook the immersion treatment in ethanol for 24 hours. As underlined before for other treatments, different silks show a different tendency to absorb solutions. We can, however, notice here a less consistent increase of weight, if compared to previous treatments. Indeed, weight increase of the wet samples report the following values: +64% for white silk, +120% approximately for Querini silk and +30% for Finzi silk.

Weight fluctuations in dry samples, instead, were almost constant for every type of fabric: depending on the size of samples, each silk presented a final weight increase between 4 and 15%,

White silk and Finzi silk presented a final weight similar to that obtained after immersion in water, while Querini silk increased here its weight, differing from the previous treatment.

Weight increase may be due to the bonding of ethanol in the peptide chain which appears here not to completely evaporate. However, chemical analyses did not provide evidence to confirm this hypothesis. Differing from white and Finzi silk, Querini silk after one month appears to have lost 3% of its initial weight, probably due to loss of water which got substituted by alcohol on peptide linking sites.

Table9: weight variation for samples immersed in ethanol for 24 hours

	before treatment	wet 24 hours			dry (24h drying)			dry (1 month drying)		
	weight (g)	weight (g)	Δw (g)	Δw%	weight (g)	weight (g)	Δw (g)	Δw%	weight (g)	weight (g)
B_t5	0,0757	0,1245	0,0488	64%	0,087	0,0113	15%	0,0870	0,0113	15%
Q_t5	0,1177	0,2628	0,1451	123%	0,1224	0,0047	4%	0,1145	-0,0032	-3%
F_t5	0,195	0,2536	0,0586	30%	0,2086	0,0136	7%	0,2102	0,0152	8%

3.2.1.5 IMMERSION IN WATER/ETHANOL BLENDS (treatments 6-9)

Table presents weight variation for samples treated with ethanol in different concentrations.

Each type of sample shows a different behaviour related to the type of treatment: white silk tends to increase wet weight as ethanol concentration decreases, meaning probably that the less

concentrated, the more water it tends to absorb. This type of sample tends to regain its original weight when dry, except after treatment 7.

Finzi silk, instead, presents a constant weight increase for wet samples (between +300% and +375%), while dry samples show different behaviour. In fact, while for t6 and t8 the weight slightly decreases, for t9 we have a consistent weight loss (-15%) and for t7 (as seen also for other samples) the final weight moderately increases (+6%).

As regards Querini silk, weight increases of 220-290% for all treatments but t9 (where the increase is around +150%). Also, dry samples behaviour seems inconstant showing moderate weight decrease (between -10 and -19%) for t6 and t8, almost constant weight for t9 (only -2%) and moderate increase for t7 (+9%).

This tendency to lose weight for the dry samples might be due to some losses during the treatment; for instance, several samples showed a fading in colour, resulting in a consistent variation of the colour of the solution itself, as it will be described in paragraph 2.3.2. Weight increasing, instead, might be related to the above described mechanism of water retaining. Interestingly, only the 70% ethanol treatment presented this weight increase. Possible explications both for weight increase (water retention) and weight decrease (loss of colour and loose fibres; dehydration of structure) have been provided before. These different tendencies related to different ethanol concentration lead to hypothesise that under a specific threshold (ethanol 50%) no consistent effects have been detected (only the Querini silk lost weight probably due to loss of incoherent deposits). In a defined range (ethanol 70%), instead, water most likely retains into the structure, resulting in a weight increase. In the end, weight loss over a defined concentration (ethanol 75% and 79%) is most likely ascribable to the loss of colour or incoherent deposits or to the action of ethanol replacing water and dehydrating the structure. Samples treated with ethanol 75%, however, appear to increase their weight after one month, probably because the treatment have modified samples' tendency to absorb ambient humidity. It must however be underlined that, due to the limited amount of silk available, treatments with ethanol in different concentrations were carried out on one set of samples for each type of solution. This condition may have affected the reliability of the results. Further investigations should therefore be conducted to confirm such observations.

Table 10: weight variation for samples immersed in different ethanol concentrations for 24 hours

treatment	sample	before treatment	wet 24 hours			dry (24h drying)			dry (1 month drying)		
		weight (g)	weight (g)	Δw (g)	Δw%	weight (g)	Δw (g)	Δw%	weight (g)	Δw (g)	Δw%
EtOH 50% (t6)	B_t6	0,1235	0,2898	0,1663	135%	0,1232	-0,0003	0%	0,1233	-0,0002	0%
	Q_t6	0,1266	0,4023	0,2757	218%	0,1025	-0,0241	-19%	0,0985	-0,0281	-22%
	F_t6	0,1369	0,5884	0,4515	330%	0,1356	-0,0013	-1%	0,136	-0,0009	-1%
EtOH 70% (t7)	B_t7	0,0605	0,1382	0,0777	128%	0,0736	0,0131	22%	0,0741	0,0136	22%
	Q_t7	0,0974	0,383	0,2856	293%	0,1062	0,0088	9%	0,104	0,0066	7%
	F_t7	0,148	0,6558	0,5078	343%	0,1568	0,0088	6%	0,1573	0,0093	6%
EtOH 75% (t8)	B_t8	0,0665	0,1298	0,0633	95%	0,0656	-0,0009	-1%	0,1148	0,0483	73%
	Q_t8	0,1299	0,4393	0,3094	238%	0,1164	-0,0135	-10%	0,1410	0,0111	9%
	F_t8	0,175	0,6982	0,5232	299%	0,1712	-0,0038	-2%	0,1957	0,0207	12%
EtOH 79% (t9)	B_t9	0,0831	0,162	0,0789	95%	0,0821	-0,001	-1%	0,0813	-0,0018	-2%
	Q_t9	0,1344	0,3327	0,1983	148%	0,132	-0,0024	-2%	0,0964	-0,0380	-28%
	F_t9	0,1165	0,5539	0,4374	375%	0,0995	-0,017	-15%	0,1323	0,0158	14%

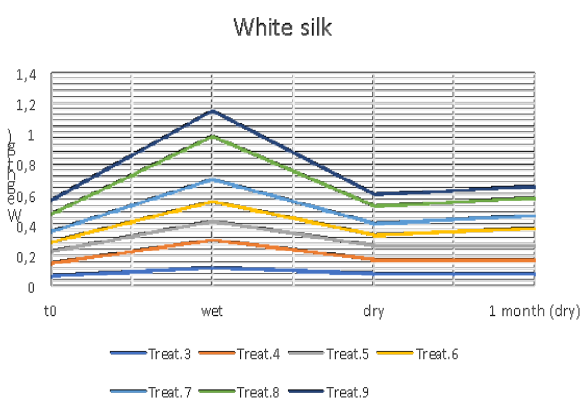

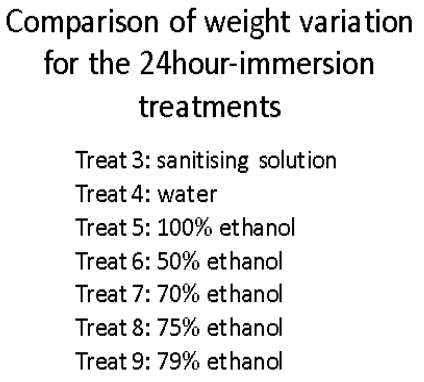

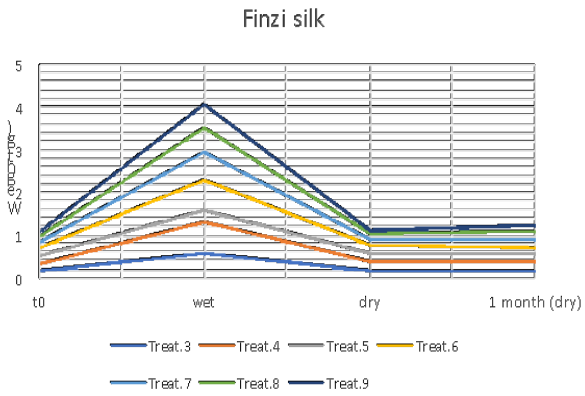

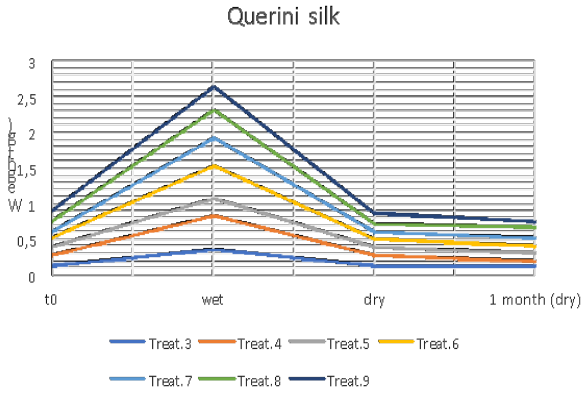

Figure 11 shows, for each silk, a comparison of the weight variation under different treatment. Weights are here reported in different scale among the graphs to better appreciate the related differences. As it can be easily noticed, white silk increases the tendency to gain (and maintain)

weight for concentrations of ethanol between 50% and 79%. A similar behaviour is presented by Finzi silk but not by Querini silk, whose tendency is to almost decrease weight.

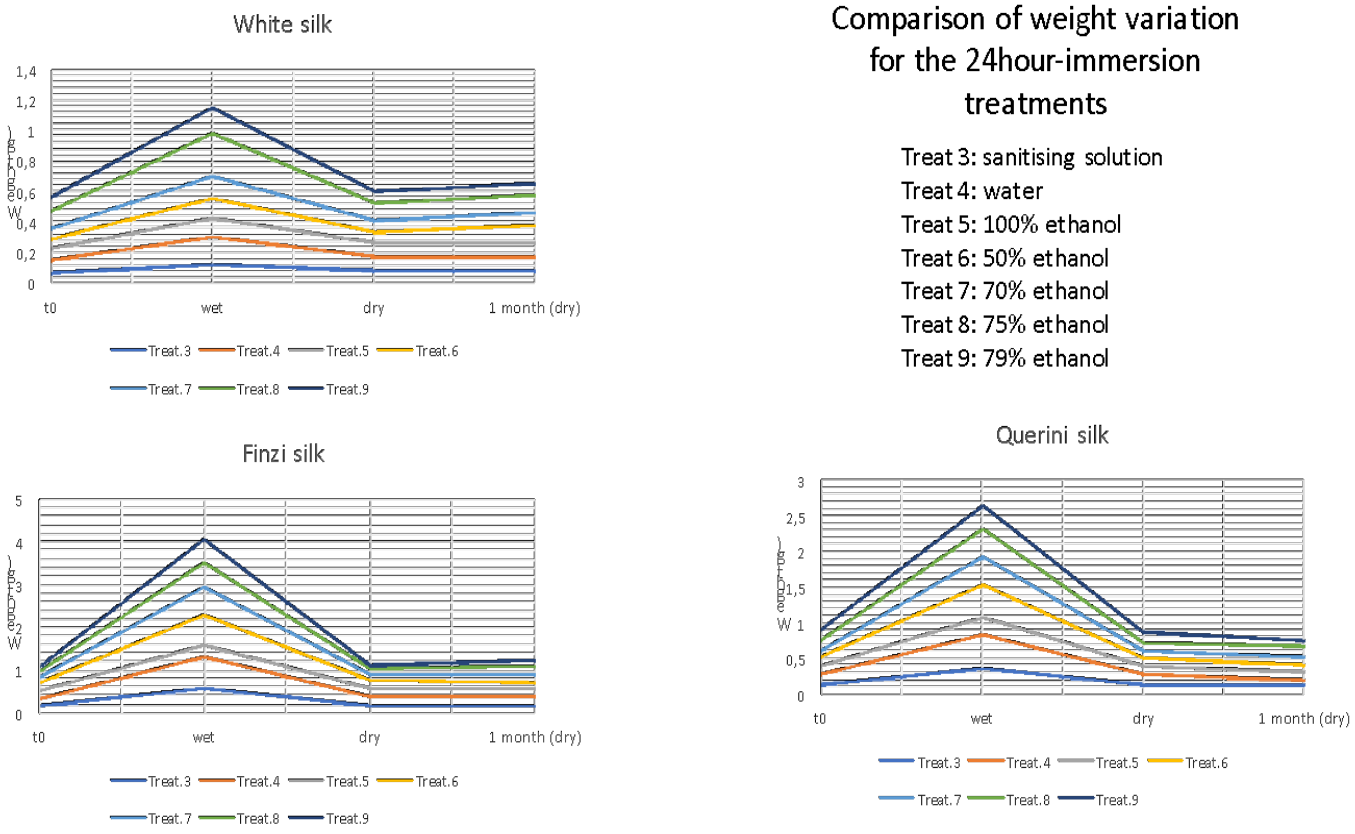

Figure 11: comparison of weight variation for the seven 24-hours treatments

3.2.1.6 IMMERSION IN BENZALKONIUM CHLORIDE (treatment 10)

Samples immersed in benzalkonium chloride presented similar tendency in weight variation, but with specific behaviours for each sample. As can be easily noticed by looking at Table , each sample tended to increase its wet weight, but with completely different tendencies; in fact, white and Querini silk showed an increasing of +800/1.000%, while Finzi silk had a weight increase of 302%.

Since treatment t10 consisted in the immersion of samples in a 50% solution of benzalkonium chloride in water, it appears clearly that, once water evaporated from treated samples, residues of benzalkonium chloride deposited on samples determined a net weight increase for all samples. After one month, however, while white and Querini silk show a decreasing in weight (most likely due to further loss of water), Finzi silk increases its weight. This behaviour might be explained by air humidity absorption.

These results are quite interesting because they show completely different tendencies of different fabrics with different waving characteristics to absorb benzalkonium chloride. Interestingly, this

tendency is not completely reflected in the results from t2 and t3, giving a hint about how absorption also depends on the solution type and combination of different elements.

Table 11: weight variation for samples immersed in 50% benzaklonium chloride for 24 hours

sample	before treatment	wet 24 hours			dry (24h drying)			dry (1 month drying)		
	weight (g)	weight (g)	Δw (g)	Δw%	weight (g)	Δw (g)	Δw%	weight (g)	Δw (g)	Δw%
B_t10	0,1059	1,3183	1,2124	1145%	0,5038	0,3979	376%	0,4218	0,3159	298%
Q_t10	0,3509	3,3115	2,9606	844%	1,6608	1,3099	373%	0,8980	0,5471	156%
F_t10	0,5238	2,108	1,5842	302%	0,9651	0,4413	84%	1,5318	1,0080	192%

Weight variation after each treatment was discussed above, underlying inherent differences in each type of silk's behaviour. Generally speaking, vapour treatment did not significantly affect samples' weight. Immersion treatments, instead, tended to either increase (most likely due to product deposition or water absorption) or decrease (probably because of the loss of colour, loose fibres, dust or retained water) final dry weight of samples, indicating that some sort of modifications occurred during the treatment.

3.2.1.7 EXPOSURE TO CONTROLLED HUMIDITY ENVIRONMENT (treatment 11)

As illustrated in paragraph 2.1.2.3, four sets of samples (untreated, treatment 3, treatment 5 and treatment 10) have been exposed to a humid environment (RH=80%). The aim of the test was to observe if the treated samples had modified their tendency to absorb water vapour in air. Samples exposed to controlled humidity presented different behaviours based on the previous treatments they had undergone.

Table 12: weight variation for samples exposed to humid environment for two weeks

TREATMENT	SAMPLE	weight (g)	weight variation Δw (g)							
		t0	48H	96H	168H	192H	216H	240H	264H	312h
untreated	B	0,2248	0,0054	0,0051	0,0048	0,0054	0,0067	0,0063	0,0069	0,0068
	F	0,4624	0,0088	0,0089	0,0075	0,0087	0,0124	0,0134	0,0151	0,0191
	Q	0,3450	0,0090	0,0112	0,0102	0,0115	0,0148	0,0143	0,0162	0,0163
t3	B	0,0942	0,0014	0,0016	0,0019	0,0017	0,0018	0,0015	0,0015	0,0020
	F	0,1900	0,0021	0,0031	0,0032	0,0034	0,0028	0,0018	0,0026	0,0030
	Q	0,1622	0,0106	0,0265	0,2813	0,2102	0,1721	0,1416	0,1354	0,1251
t5	B	0,0870	0,0040	0,0035	0,0032	0,0035	0,0046	0,0044	0,0047	0,0042
	F	0,2102	0,0046	0,0047	0,0035	0,0054	0,0326	0,0603	0,0420	0,0430
	Q	0,1145	0,0045	0,0050	0,0042	0,0043	0,0051	0,0054	0,0053	0,0058

TREATMENT	SAMPLE	weight (g)	weight variation Δw (g)							
		t0	48H	96H	168H	192H	216H	240H	264H	312h
t10	B	0,4218	0,0362	0,0312	0,0260	0,0241	0,0212	0,0166	0,0142	0,0144
	F	1,5318	0,1841	0,1726	0,1610	0,1677	0,1592	0,1528	0,1470	0,1507
	Q	0,8980	0,1126	0,1127	0,1014	0,1084	0,1071	0,0996	0,0992	0,0365

As reported in Table , untreated samples showed constant weight in both white silk and Finzi silk all over the exposure, with only a slight increase probably due to some water absorption. Untreated querini silk, instead, after a sharp increase in weight, decreased back almost to its initial values, presenting only a slight increase during the rest of the treatment. This sharp increasing value may be attributed to the initial absorption of water by both silk and incoherent material there deposited, which, thanks to the stable environment, got to equilibrium after some time.

Samples treated with t3 (immersion in sanitising solution for 24h hours) showed almost no variation for white and Finzi silk, presenting behaviour similar to that of untreated sample. For Querini silk the sharp weight increase, however, takes place only after 168h, taking also longer to stabilising with a moderate weight decrease. The same hypothesis suggested before can be formulated to explain this behaviour, with the addition that benzalkonium chloride may have interacted with water crystallizing and thus modifying the total weight of the sample.

Moving to samples from treatment 5, a general tendency to maintain weight univariate for almost 200h can be observed for all samples. However, after 216h white sample maintains the described behaviour, while Querini and Finzi silk moderately increase their weight to reach a maximum and then a plateau. This phenomenon shows how silk fibres employ relatively long times to incorporate water, and that this tendency may have been affected by alcohol treatment.

In the end, samples treated with benzalkonium chloride showed a slight initial increase in weight due to water absorption, which was then maintained for the whole period of treatment.

Figure 12 reports a graphical comparison of the different behaviours here described.

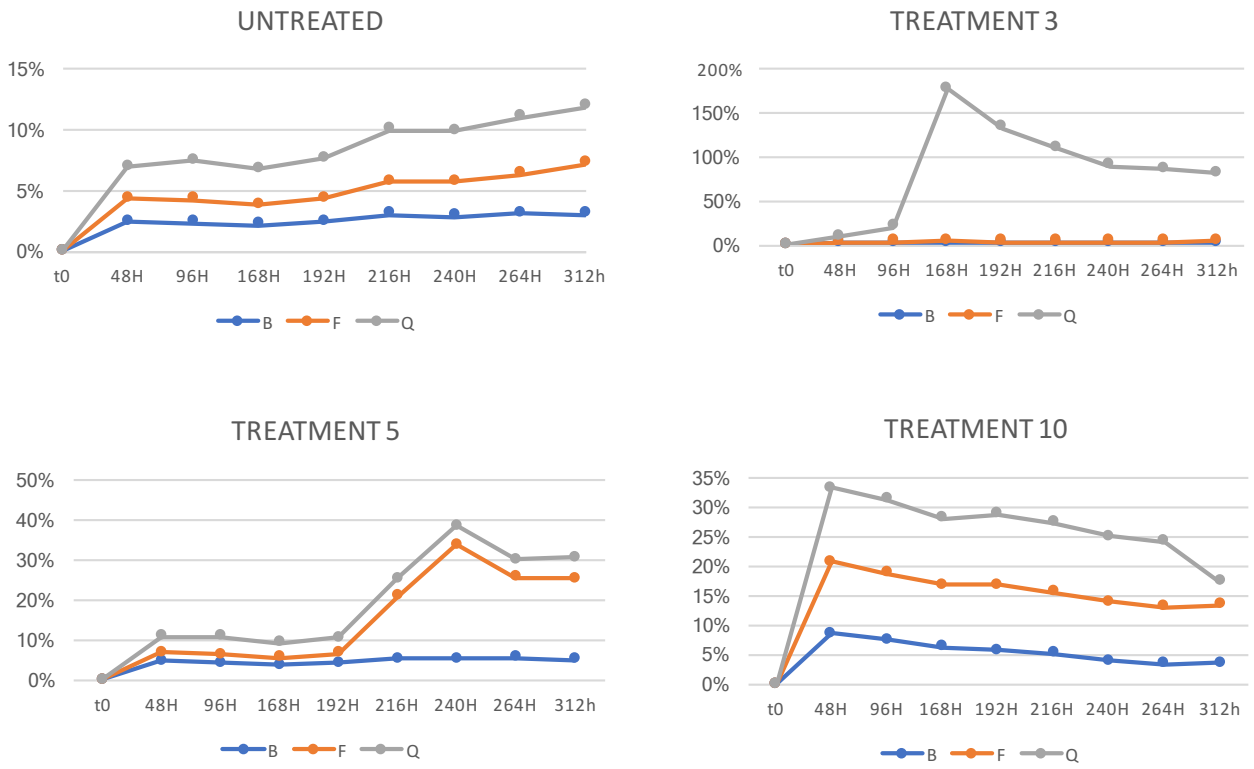

Figure 12:comparison of weight variation of the four sets of samples during exposure to elevated humidity levels

3.2.2 MORPHOLOGICAL CHARACTERIZATION

3.2.2.1 OPTICAL MICROSCOPY

3.2.2.1.1 EXPOSURE TO SANITISING SOLUTION VAPOURS (treatment 1)

Morphology of vapour-treated samples was investigated via portable contact microscope observations, and the photographs taken (both in UV and VIS light at two different magnifications, 50x and 220x) were compared to the images collected of specimens as such.

Figure 13 shows a comparison between images taken at 50x magnification both in VIS and UV light before and after vapour treatment. From the observation of the images, no specific differences can be spotted and it can be therefore stated that no significant morphological variations occurred during vapour treatment.

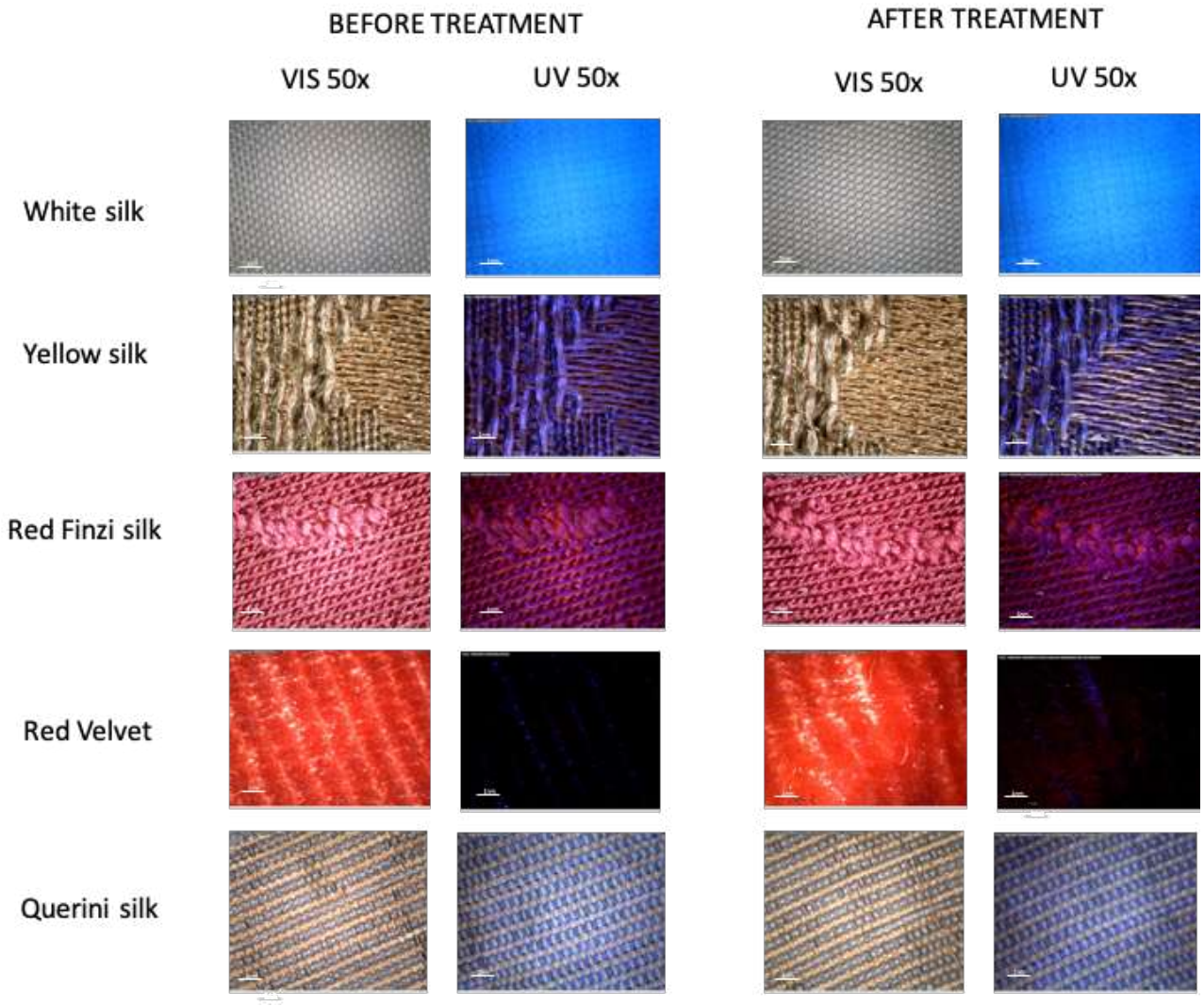

Figure 13: comparison of samples' morphology before and after treatment 1

3.2.2.2.2 IMMERSION IN SANITISING SOLUTION (treatments 2 and 3)

The morphology of samples immersed in sanitising solution was investigated both for treatment 2 (30 minutes immersion) and for treatment 3 (24 hours immersion).

Image 14a shows a comparison between images taken at 50x magnification both in VIS and UV light before and after treatment 3. From the observation of the images, the first clear difference that appears is the consistent colour variation for yellow silk, Finzi silk and red velvet. After treatment colours result greatly faded, and the yellow sample presents threads that completely changed their appearance (from yellowish to silver). This colour variation will however be discussed more in detail in par. 3.2.3.2.

From further observation of image 14b where comparisons of two magnifications are presented, it can be noticed that no specific other modifications occurred, neither to threads nor to weaving.

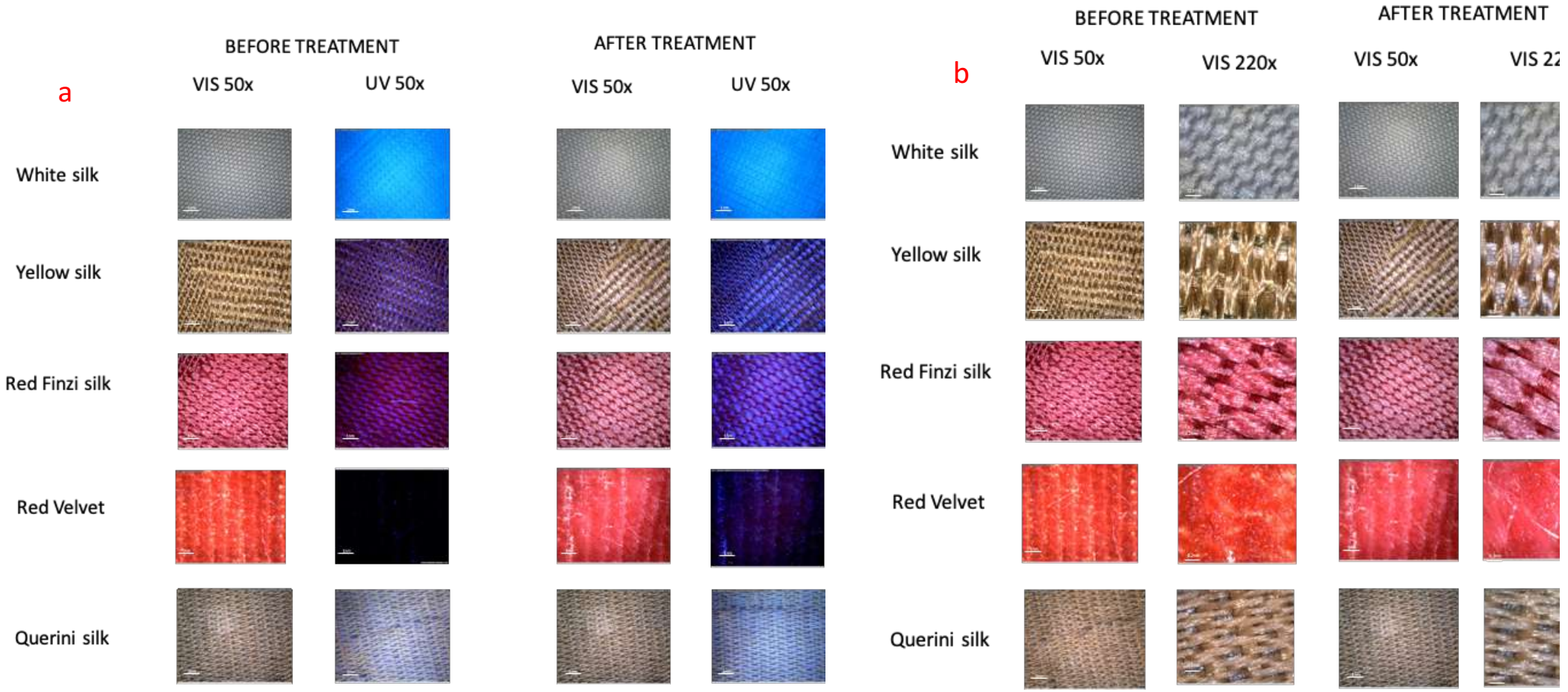

Figure 14: comparisons of samples' morphology before and after treatment 3; a) comparison of visible and UV lights observation; b)comparison of 50x and 220x magnifications

3.2.2.2.3 IMMERSION IN DEIONIZED WATER (treatment 4)

The morphology of samples immersed in water for 24 is presented in image 15; from the observation of the photographs taken at 50x magnification before and after treatment, we can conclude that no significant changes occurred and that no particular signs of fluorescence can be spotted .

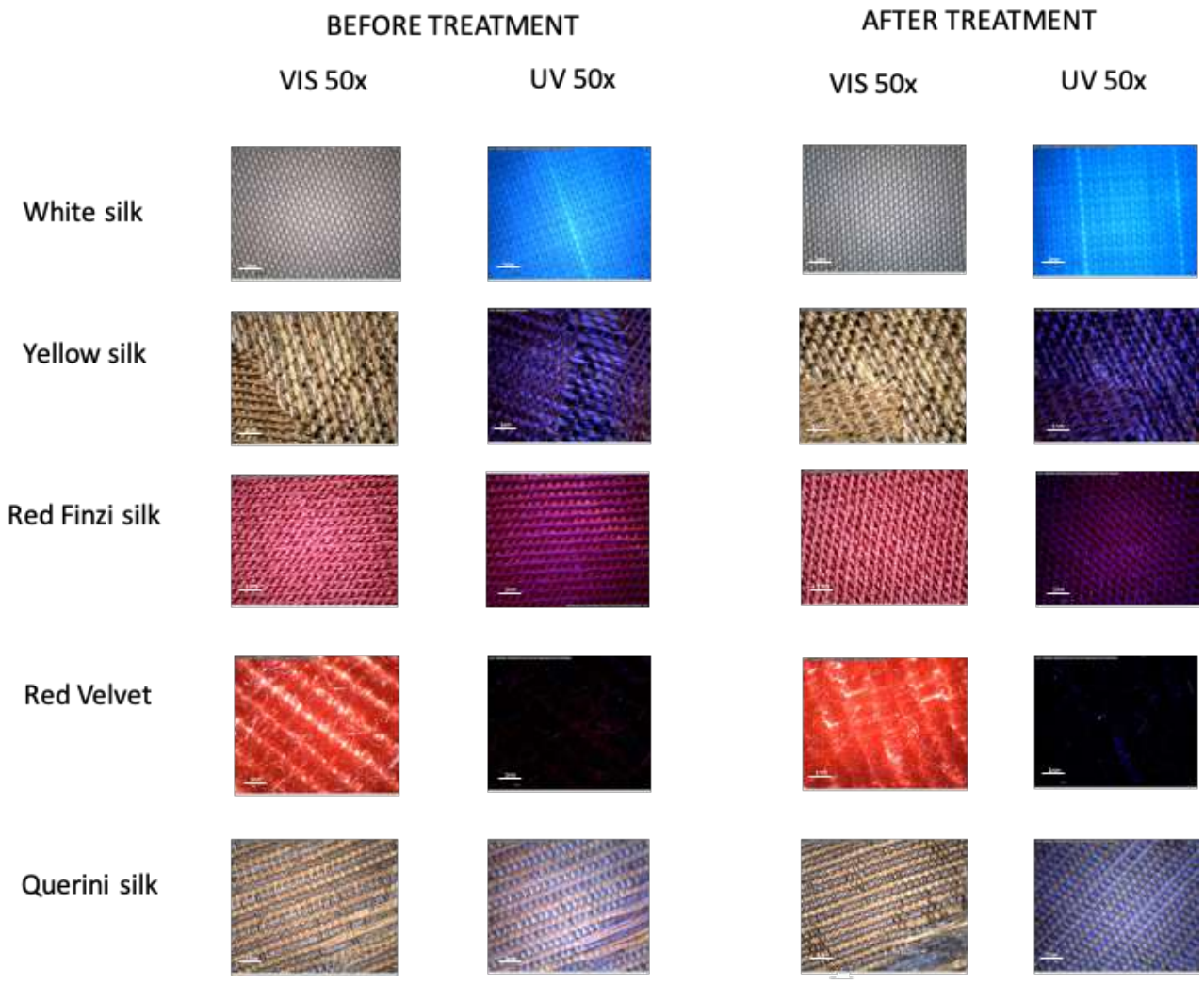

Figure 15: comparison of samples' morphology before and after treatment 4

3.2.2.2.4 IMMERSION IN ETHANOL ABSOLUTE (treatment 5)

The morphology of samples immersed in ethanol absolute for 24 is presented in figure 16; from the observation of the photographs taken at 50x magnification before and after treatment, we can conclude that no significant changes occurred and that no particular signs of fluorescence can be spotted .

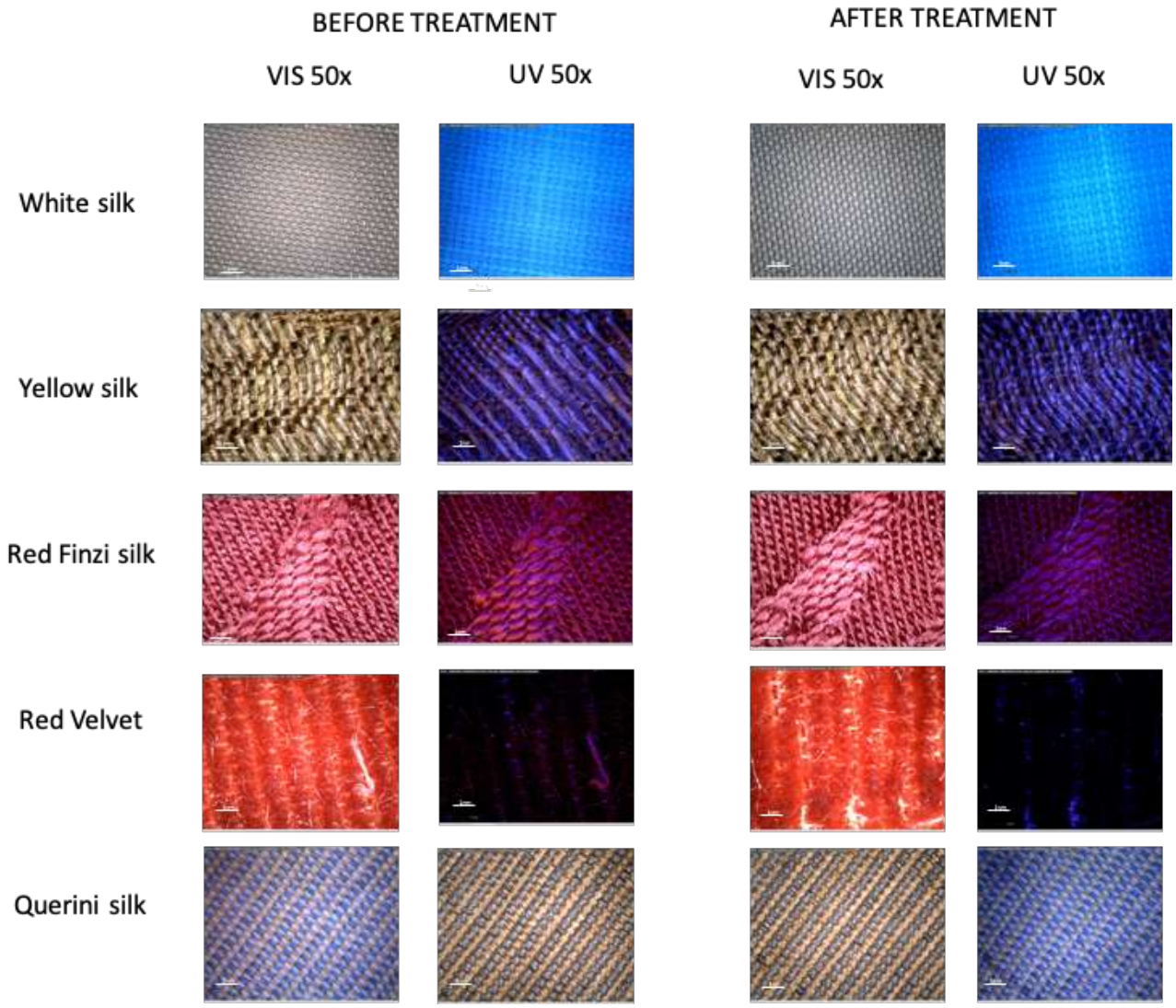

Figure 16: comparison of samples' morphology before and after treatment 5

3.2.2.5 IMMERSION IN WATER/ETHANOL BLENDS (treatments 6-9)

Figure 17 shows a comparison between silk samples' morphology before and after immersion in solutions with four different ethanol concentrations.

Once again, no significant morphological variation occurred among treatments, apart from consistent fading proportionally to the ethanol concentration. The samples most affected by this discolouring are for sure yellow and Finzi silk but, as mentioned before, colour variation will be treated extensively in the dedicated section.

IMMERSION IN 50% EtOH

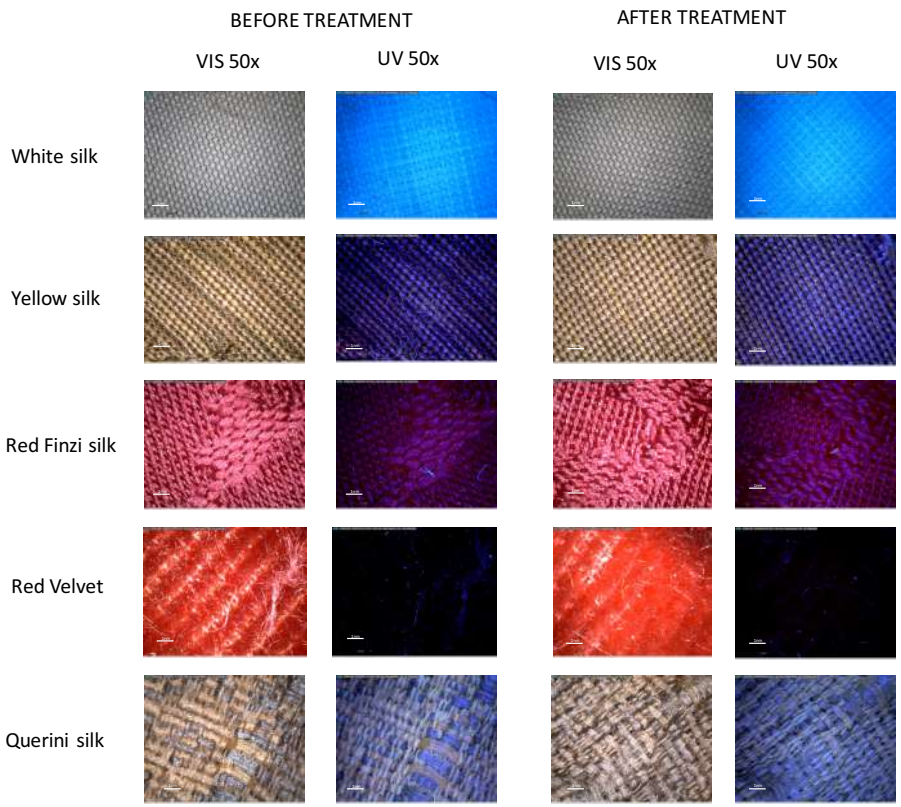

IMMERSION IN 70% EtOH

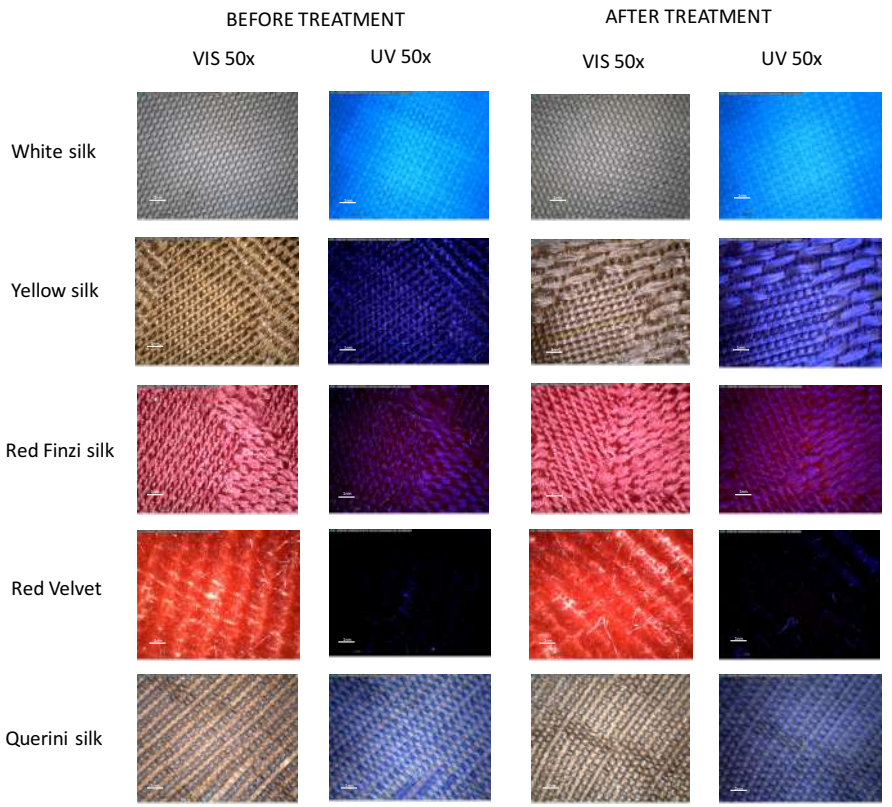

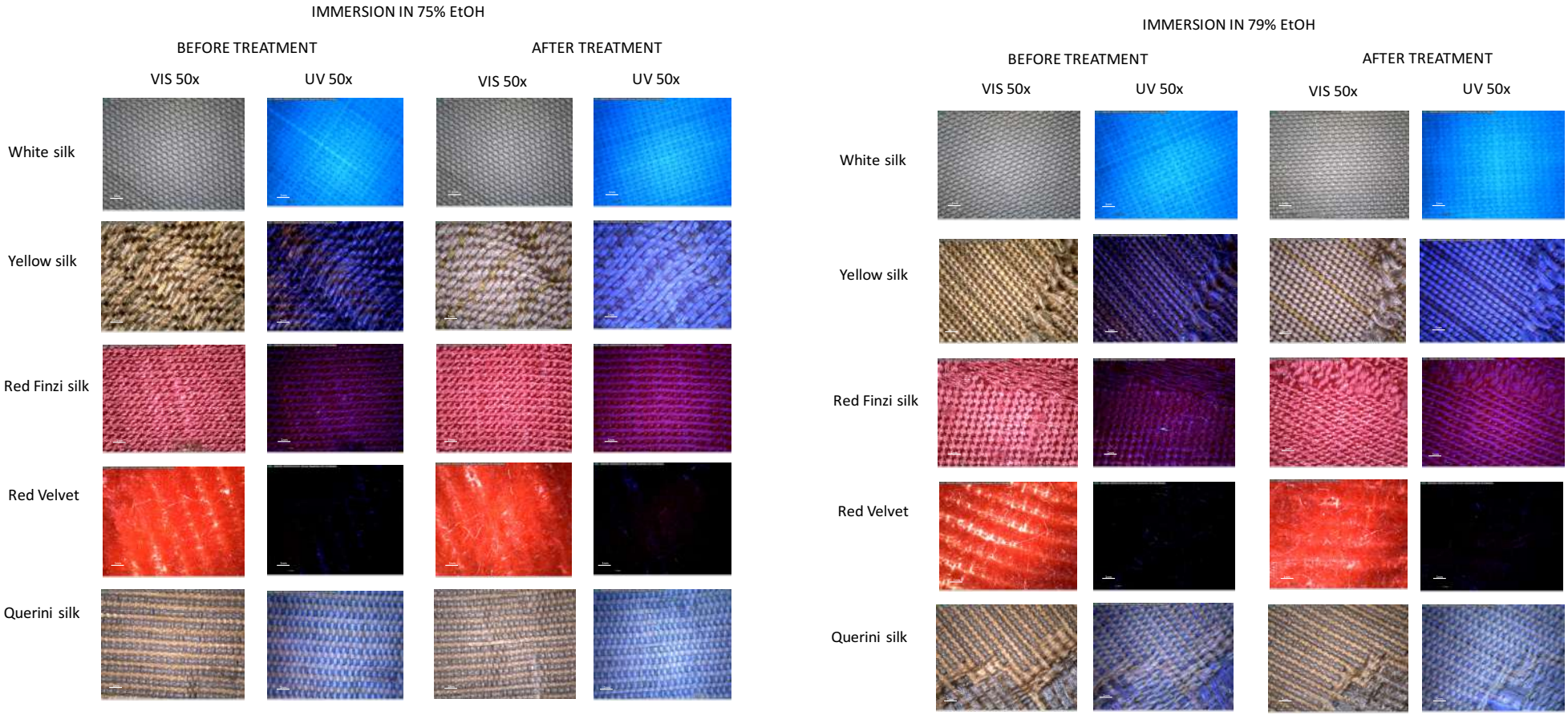

Figure 17: comparisons of samples' morphology after treatments 6, 7, 8 and 9.

3.2.2.6 IMMERSION IN BENZALKONIUM CHLORIDE (treatment 10)

Figure 18 shows a comparison of images taken at magnification 50x before and after treatment 10, after immersion in benzalkonium chloride.

It appears clearly that a significant morphological variation occurred. Benzalkonium chloride, in fact, deposited on silk samples forming a sticky and glossy coating. This coating deposited homogeneously on all samples but velvet. This type of material, in fact, thanks to its particular structure and constitution, retained benzalkonium mainly on the top side of its fibres.

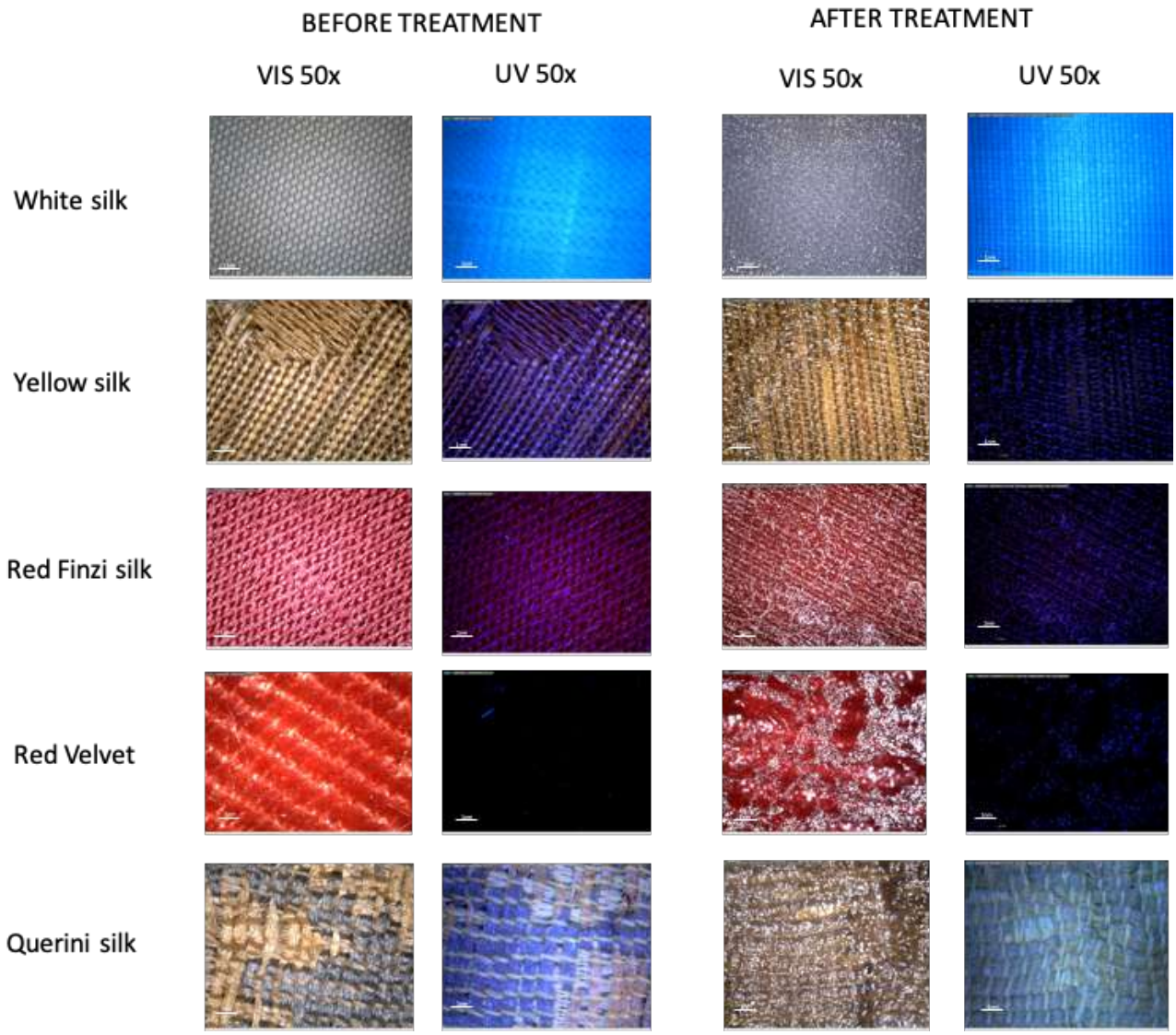

Figure 18: comparison of samples' morphology before and after treatment 10

3.2.2.7 EXPOSURE TO CONTROLLED HUMIDITY ENVIRONMENT (treatment 11)

Figures 19 reports the comparison of optical observation performed before and after treatment 11. Images taken at 220x magnification under visible light are here reported as representative of the morphology of samples.

Untreated samples and treatment-5 samples did not show significant variations after exposure to 77%RH. Samples treated via immersion in sanitising solution (treatment 3), instead, showed some significant changes. Especially for Querini silk, crystallization of salts (most likely benzalkonium chloride) can be observed on the surface of the sample, which is detectable also by naked eye, and which caused the fabric to stiffen.

As regards benzalkonium chloride treated silks, it is possible to notice that samples are here slightly less brilliant, which corresponded also to a moderate decrease in stickiness, probably as a result of a partial drying of benzalkonium solution.

Untreated samples – exposure to controlled RH% environment
VIS LIGHT – 220X

a

Treatment 3 – exposure to controlled RH% environment
VIS LIGHT – 220X

b

	White silk	Finzi silk	Querini silk
BEFORE TREATMENT 11			
AFTER TREATMENT 11		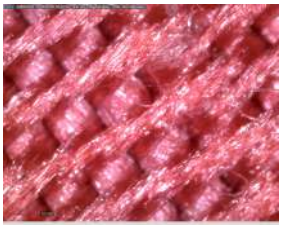	

Treatment 5 – exposure to controlled RH% environment
VIS LIGHT – 220X

c

	White silk	Finzi silk	Querini silk
BEFORE TREATMENT 11			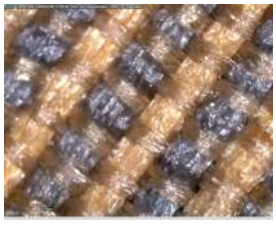
AFTER TREATMENT 11			

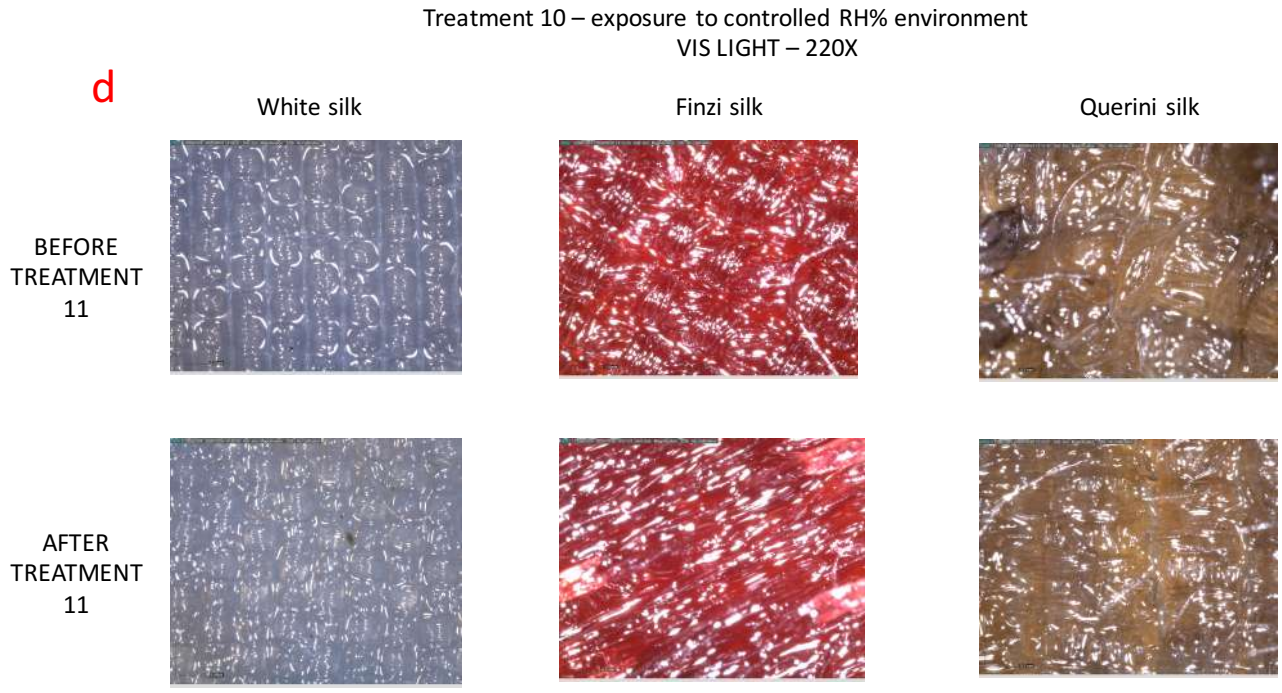

Figure 19: comparisons of samples' morphologies after exposure to humid environment (treatment11); a - untreated samples; b - samples after treatment 3; c - samples after treatment 5; d - samples after treatment 10

3.2.2.2 SCANNING ELECTRON MICROSCOPY

In order to investigate microscopic variations on sample morphology not detectable by optical microscopy, SEM observations were performed on the three reference silks (white silk, Finzi silk and Querini silk). Untreated samples were compared to samples immersed in sanitising solution for 24 hours (treatment 3).

As can be observed in figure 20 a and b, benzalkonium chloride, as previously supposed, deposited on treated surfaces. Figure 20b highlights the visibility of benzalkonium deposits at different magnifications (250x, 500x, 1.000x) on Finzi silk. The salt appears to be distributed unevenly on the surface, forming several aggregations but not defined crystals. Figure 20 a, instead, presents the comparison of treated and untreated silk at greater magnifications (1.000 and 25.000x), with the aim of understanding the distribution of quaternary ammonium salt deposits at nanometric scale. Benzalkonium seems here to have filled some “holes”, leaving emerging residues. This observation was then confirmed by AFM analyses, as will be described in the following paragraph.

Figure 20 c was instead reported to describe the conservation state of Querini silk. As noticeable in also in Finzi silk, Q samples present several broken fibres, together with portions of fabric lacking of several threads. Moreover, incoherent residues (probably dust) can be observed on the surface.

Despite these observations, however, no signs of increased fibres degradation could be observed after treatment 3; we can therefore suppose that, despite this consistent surface modification, the treatment did not cause further degradation phenomena on silk structure.

In order to evaluate the presence of characteristic elements (e.g. from mordants, degumming process or incoherent deposits) EDS point analysis was performed on all samples. However, beside the presence of C, O and N (characteristic of both silk and benzalkonium chloride) no other elements were detected. No characteristic signals for chloride were observed, as it probably evaporated due to its volatility. Figure 20 d reports EDS spectra of treated silk as example.

In some SEM images bright areas are observed. This is due to the sample charging during the measurements, despite the Au metallic coating on top of the surface.

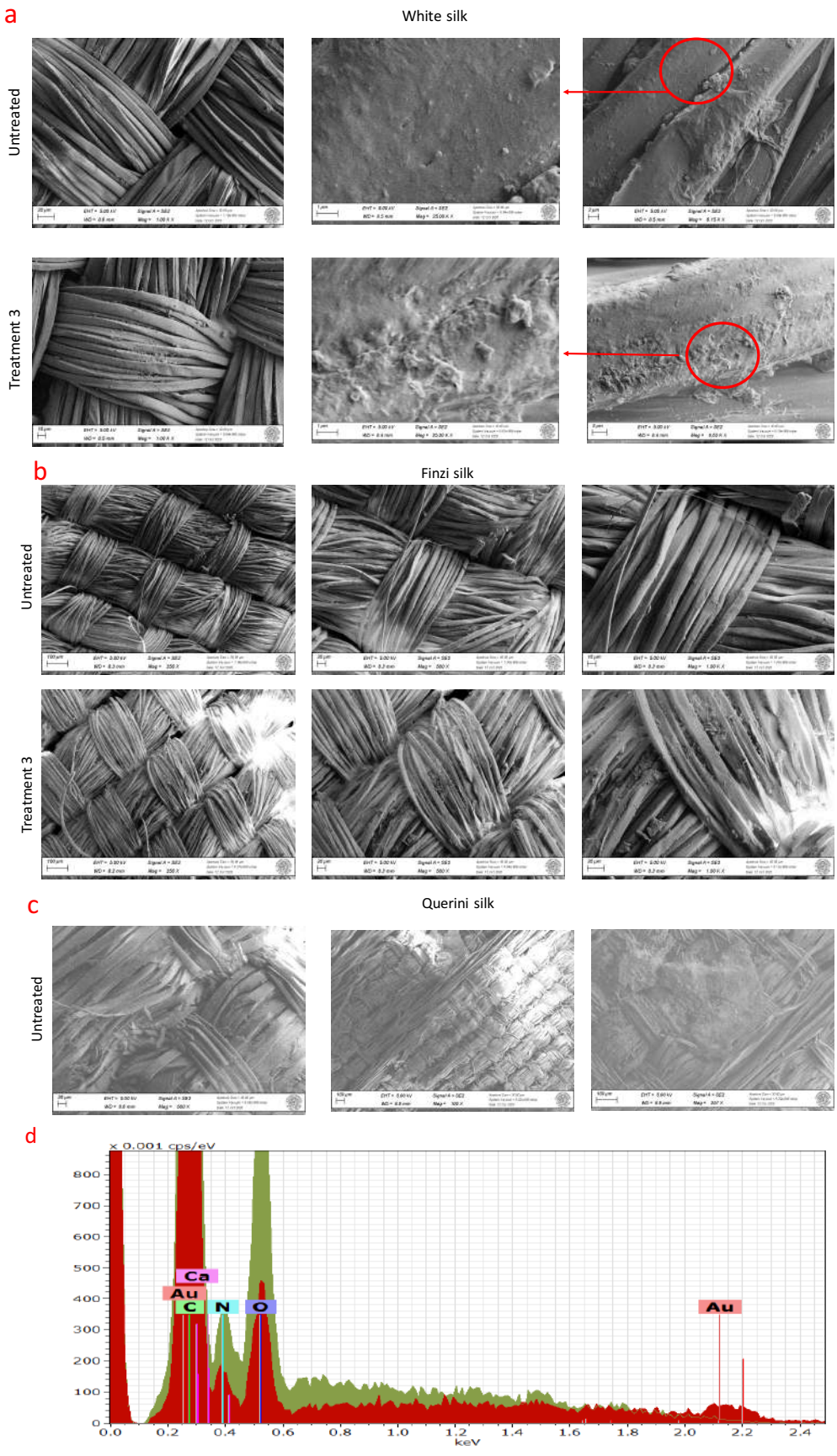

Figure 20: SEM images of white silk before and after treatment 3 (immersion in sanitising solution)

3.2.2.3 AFM ANALYSES

In order to investigate possible microscopic variations on sample morphology, AFM analyses on tapping mode were conducted on white silk, before the Au coating process. The AFM probe utilized was a RTESPA-300 silicon cantilever (nominal spring constant ~40 N/m, nominal tip radius ~8 nm, measured resonance frequency 325,3 kHz).

Treated (t3 – immersion in sanitising solution for 24 hours) and untreated samples images were compared as shown in figure 21.

Tapping mode analyses provided greatly magnified images of silk surface structure. The analysis, as mentioned in the experimental part, was performed on a portion of fabric rather than on a single thread (as reported by other literature studies). This choice was made to test the possibility of investigating the unaltered sample, considering that cultural heritage samples are often valuable and should not undergo consistent modifications in order to study them. This choice, however, made it necessary to correctly check the point of analysis (centre of the thread) in order to avoid interference from other neighbour threads.

First attempts to perform analysis also in other modes, like “PeakForce Tapping” mode, in order to evaluate mechanical properties of the selected area, failed because of the nanometric composition of silk threads. The AFM probe utilized in this case was a SNL silicon tip on nitride lever (nominal spring constant ~0.06 N/m, nominal tip radius ~2 nm). The surface of the threads, as noticed by SEM observations, is characterized by *valleys, craters and humps*. Moreover, the thread is not isolated, but still contained in the fabric surrounded by other threads. These morphology and surroundings create consistent interference and instability on the probe, resulting in the impossibility to correctly perform the analysis in this mode. Further investigations, if foreseen, could be carried out on the isolated thread properly kept fixed, using dedicated probes and carefully selected.

As a general tendency, from the results of tapping mode analysis, it was possible to notice how the untreated sample presented a surface characterized by *valleys* and *craters,* while the treated sample not only did not show this characteristic morphology, but also presented several emerging structures. A possible explanation for this behaviour might be due to the deposition on the surface of benzalkonium chloride present in the sanitising solution. Benzalkonium might have filled the holes, leaving some residues on the surface, as noticed thank to scanning electron microscopy analyses at lower magnification with respect to AFM magnification.

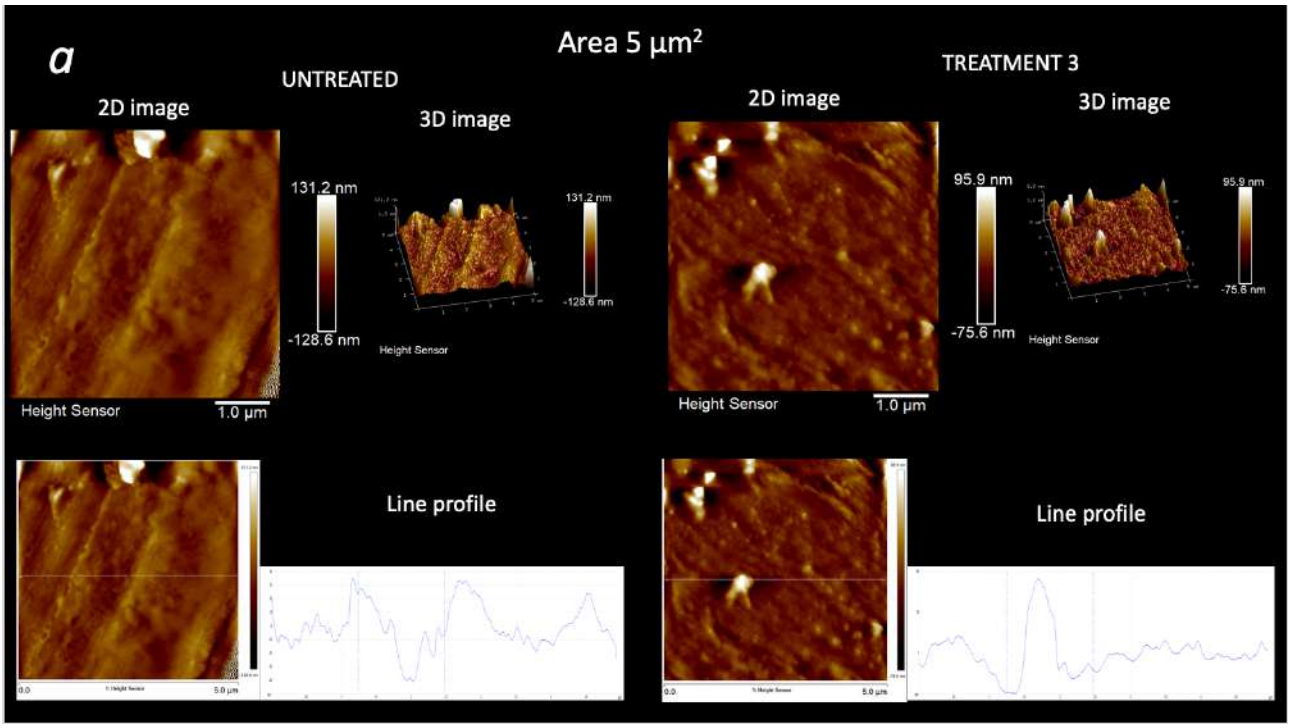
a
Area 5 µm²
UNTREATED
TREATMENT 3
2D image
3D image
2D image
3D image
131.2 nm
-128.6 nm
Height Sensor
95.9 nm
-75.6 nm
Height Sensor
1.0 µm
Line profile
Line profile

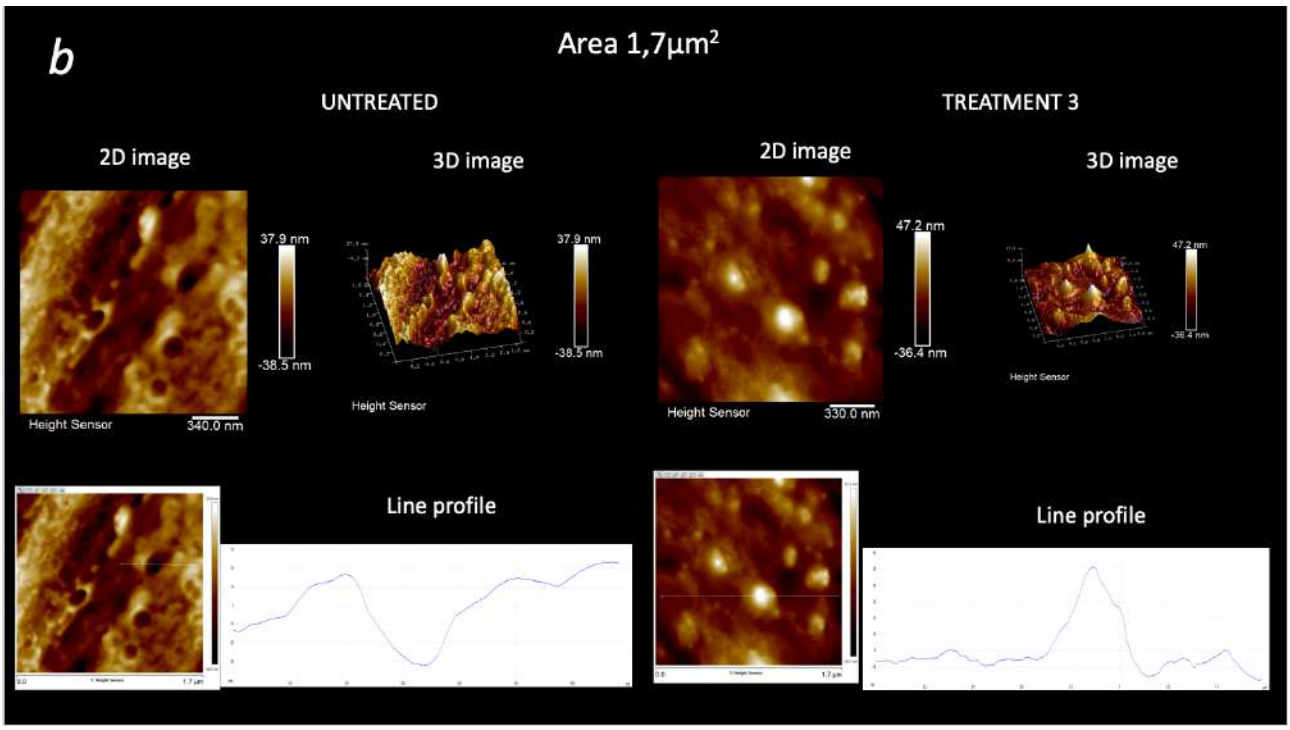
b
Area 1,7µm²
UNTREATED
TREATMENT 3
2D image
3D image
2D image
3D image
37.9 nm
-38.5 nm
Height Sensor
340.0 nm
47.2 nm
-36.4 nm
Height Sensor
330.0 nm
Line profile
Line profile

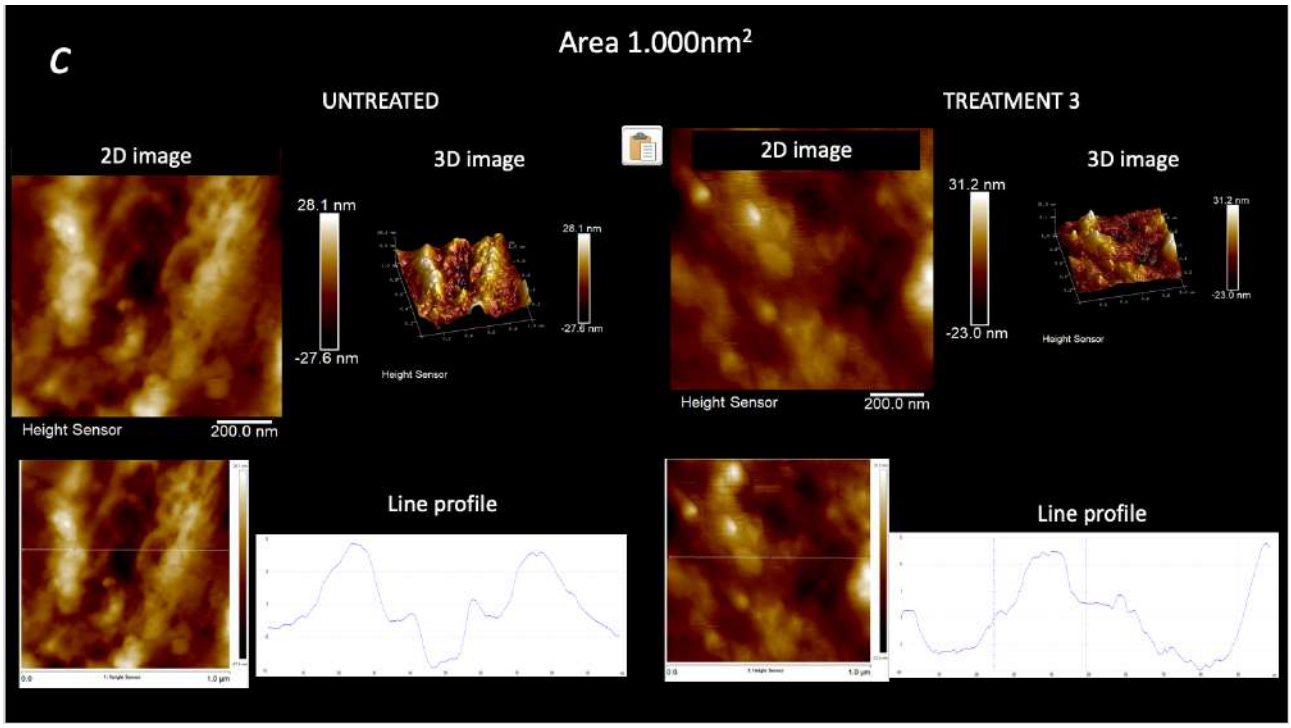

Figure21: results from AFM analyses at different magnifications (a: 5µm; b:1,7 µm, c:100nm). 2D and 3D images are presented, together with a line profile for 2D image

3.2.3 COLORIMETRIC VARIATIONS

As mentioned above, to present results in the clearest possible way, three silks are taken as representative of characteristic behaviour: white silk (B), Finzi silk (F) and Querini silk (Q).

Moreover, colorimetric variations reported here include only the SCI component, as mentioned in the experimental part.

3.2.3.1.1 EXPOSURE TO SANITISING SOLUTION VAPOURS (treatment 1)

Table 13 reports the colour coordinates related to silk samples exposed to vapour treatments for 10 days.

As we can easily notice, for the white samples no great differences can be detected, since ΔE values are all below 1,5 points, being therefore barely detectable by the human eye. White silk colour variations are ascribable mainly to L* component decreasing, and to b* component increasing towards yellow coordinate.

As regards Finzi silk, ΔE levels are slightly higher, but they remain below the level of tolerance (except for the sample F4, whose colour coordinates can be considered outliers). The reason for the higher ΔE values is due to a consistent variation in the L* component.

Querini silk, instead, presents a highly inhomogeneous behaviour as regards to colour variation; ΔE levels vary from 0,74 to 6,43, and the variation of the single components goes from -0,30 to 1,20 for a*, from –0,28 to 5,72 for b* and -0,25/2,38 for L*. This tendency might be explained because Querini silk resulted to be highly inhomogeneous as it is composed of two different types of threads and because it shows, in some areas, a faded flower pattern. Moreover, Querini silk was originally covered with a layer of dust and incoherent material, which probably contributed to the inhomogeneous colour variation.

We can therefore conclude that only minor specific colour variation can be ascribed to this treatment.

Table 13: colour variations for silk samples after treatment 1

sample	L*	*a	b*	ΔE	ΔL*(D65)	Δa*(D65)	Δb*(D65)
B_TALQ	80,56	0,77	3,09				
B_vap_1	79,14	0,58	3,75	1,58	-1,42	-0,19	0,66
B_vap_2	80,39	0,70	4,29	1,21	-0,17	-0,07	1,20
B_vap_3	80,21	0,60	3,66	0,69	-0,35	-0,17	0,57
B_vap_4	79,94	0,54	3,80	0,97	-0,62	-0,23	0,71
F_TALQ	33,55	37,31	5,6				
F_vap_1	33,13	35,15	5,54	0,91	-0,88	-0,16	0,19
F_vap_2	31,73	34,71	5,70	2,38	-2,28	-0,60	0,35
F_vap_3	33,17	35,52	5,55	0,89	-0,84	0,21	0,20
F_vap_4	40,22	25,13	9,22	12,53	6,21	-10,18	3,87
Q_talq	52,89	4,18	17,45				
Q_vap_1	48,66	2,09	13,84	1,52	1,14	-0,62	-0,79
Q_vap_2	48,70	2,41	14,88	1,24	1,18	-0,30	0,25
Q_vap_3	47,27	2,07	14,35	0,74	-0,25	-0,64	-0,28
Q_vap_4	49,90	4,42	20,35	6,43	2,38	1,71	5,72

3.2.3.1.2 IMMERSION IN SANITISING SOLUTION (treatments 2 and 3)

30 MINUTES (treatment 2)

Table 14 reports the colour parameters related to silk samples immersed in sanitising solution for 30 minutes.

White samples did not show consistent colour variation, apart from two parameters of sample B1, which appear to have undertaken a noticeable colour variation due to increase of both L* (+ 2,68 in average) and b* (+ 1,13 in average) components.

Finzi silk presented a similar (but more homogeneous) behaviour, losing its brilliant red, with a* increasing on average of 2,61 points and b* increasing of 3,43 points on average. The total ΔE variation appears to lie on the threshold of human eye perception. Querini silk, instead, presented less homogeneous but still detectable colour variation, with ΔE ranging from 3,01 to 6,68. Querini silk, in fact, presented a less consistent colour loss in the solution (as reported in table 16), and the treatment mainly removed incoherent material deposited on the samples.

Table 14: colour variations for silk samples after treatment 2

sample	L*	*a	b*	ΔE	ΔL*(D65)	Δa*(D65)	Δb*(D65)
b as such	80,84	0,83	3,75				
b1	83,52	1,12	4,88	2,92	2,68	0,29	1,13
b2	80,65	0,90	3,46	0,35	-0,19	0,07	-0,29
b3	80,00	1,01	3,54	0,88	-0,84	0,18	-0,21
b4	80,36	0,85	3,28	0,67	-0,48	0,02	-0,47
f as such	32,87	37,32	5,45				
f1	32,34	39,90	9,44	4,78	-0,53	2,58	3,99
f2	34,15	40,13	8,86	4,60	1,28	2,81	3,41
f3	34,18	40,14	8,68	4,48	1,31	2,82	3,23
f4	34,31	39,56	8,54	4,08	1,44	2,24	3,09
q as such	55,82	4,41	19,68				
q1	51,48	4,35	18,12	4,61	-4,34	-0,06	-1,56
q2	53,41	5,51	21,11	3,01	-2,41	1,10	1,43
q3	51,51	3,97	16,96	5,11	-4,31	-0,44	-2,72
q4	49,54	4,35	17,40	6,68	-6,28	-0,06	-2,28

24 HOURS (treatment 3)

Table 15 reports colour parameters related to silk samples immersed in sanitising solution for 24 hours.

White samples did not show consistent variation, with ΔE levels maintained below 2, and with L* as main component responsible for this variation (-1,49 points in average)

Finzi silk presented a considerably stronger loss, with an average ΔE of 16,60. In this case L results to be the component with the strongest variation (+15,55 points in average), followed by a* with 4,2 points on average.

Querini silk, instead, presented a less evident but still detectable colour variation, with ΔE ranging from 1,77 to 2,74. Querini silk, in fact, presented a less consistent colour loss in the solution, and the treatment mainly removed incoherent material deposited on the samples.

Table 15: colour variations for silk samples after treatment 3

sample	L*	*a	b*	ΔE	ΔL*(D65)	Δa*(D65)	Δb*(D65)
b as such	80,84	0,87	3,02				
b5	78,97	0,71	3,19	1,89	-1,87	-0,16	0,17
b6	80,00	1,63	3,62	1,28	-0,84	0,76	0,60
b7	79,25	0,63	2,81	1,62	-1,59	-0,24	-0,21
b8	79,16	0,61	3,55	1,78	-1,68	-0,26	0,53
f as such	29,96	37,44	5,82				
f5	45,33	40,45	7,74	15,78	15,37	3,01	1,92
f6	46,36	41,89	7,75	17,11	16,40	4,45	1,93
f7	45,47	41,70	8,04	16,24	15,51	4,26	2,22
f8	44,88	42,65	8,31	16,00	14,92	5,21	2,49
q as such	51,45	2,64	15,47				
q5	53,28	3,30	17,06	2,51	1,83	0,66	1,59
q6	52,46	3,35	16,68	1,73	1,01	0,71	1,21
q7	50,88	3,56	16,87	1,77	-0,57	0,92	1,40
q8	54,14	2,13	15,46	2,74	2,69	-0,51	-0,01

Values of colour variations for sanitising solution after treatment are reported in table 16. As it can easily be noticed, the solution employed for the treatment of the white silk did not consistently modify its colour, while those used for Finzi and Querini treatment showed a colour variation increasing with the increase of the exposure time. In particular, this variation is most probably related to fading of silk colour and, for the Querini silk, also to the removal of dust. Finzi treatment solutions, in fact, increase consistently their red component, while Finzi silk sample showed a combined slight increase in red and yellow values, together with a consistent increase in whiteness. Querini treatment solutions, instead, increase their yellow component. Querini silk samples show two different behaviours: samples treated for 30 minutes increase their blue level, while samples treated for 24 hours increase their yellow component. These behaviours, however, can also be ascribed to the

weaving of the fabric: as observed by optical microscopy, Querini silk is composed of yellow and blue threads interlaced together.

Table 16: colour variations for treating solutions (before and after treatment 2 and 3).

treatment	sample	L*	a*	b*	ΔL	Δa	Δb	ΔE
	target	37,15	0,34	1,27				
immersion in sanitising solution, 30min	B	38,46	-0,52	3,25	1,31	-0,86	1,98	2,53
	F	28,32	6,93	1,03	-8,83	6,59	-0,24	11,02
	Q	38,69	-0,48	4,83	1,54	-0,82	3,56	3,96
immersion in sanitising solution, 24h	B	38,46	-0,52	3,25	1,31	-0,86	1,98	2,53
	F	20,86	2,28	0,35	-16,29	1,94	-0,92	16,43
	Q	30,18	-0,39	9,67	-6,97	-0,73	8,4	10,94

3.2.3.1.3 IMMERSION IN DEIONIZED WATER (treatment 4)

Table 17 presents colour variation for samples that underwent t4, immersion in deionized water for 24 hours. White sample did not show consistent variation (ΔE variation is, on average, 1,24) with L* as the main varying component (-1,22 points on average). Finzi silk, instead, had an even less consistent colour variation (average ΔE=0,47), being b* the main varying component (-0,46 on average). Querini silk, on the other hand, presented higher levels of ΔE, but always under the human eye detection threshold. Querini silk, indeed, showed an average ΔE of 2,01 with average b* value increasing up to 1,75 points.

Table 17: colour variations for silk samples after treatment 4

sample	L*	*a	b*	ΔE	ΔL*(D65)	Δa*(D65)	Δb*(D65)
b as such	79,3	0,78	3,16				
b_water	78,08	0,80	2,93	1,24	-1,22	0,02	-0,23
f as such	29,61	36,39	5,71				
f_water	29,53	36,45	5,25	0,47	-0,08	0,06	-0,46
q as such	52,09	4,83	20,05				
q_water	51,47	5,60	21,80	2,01	-0,62	0,77	1,75

Table 18 reports value of colour variation collected for treatment solution. Results show that no significant colour changing occurred on solutions after this treatment. Querini silk treatment solution presents the higher value of ΔE, probably due to dissolution of incoherent material deposited.

Table 18: colour variation for treating solution after treatment 4

	sample	L*	a*	b*	ΔL*	Δa*	Δb*	ΔE
	target	39	0,36	1,55				
treatment 4	B	41,26	-0,59	3,6	3,20	2,26	-0,95	2,05
	F	39,45	-0,4	3,9	2,51	0,45	-0,76	2,35
	Q	40,28	-0,73	6,01	4,77	1,28	-1,09	4,46

3.2.3.1.4 IMMERSION IN ETHANOL (treatment 5)

Results of colour variation for silk samples after t5 are reported in table 19.

From these results we can notice that both white and Finzi silk presented negligible colour variation (average ΔE below 2 points), while Querini silk presented higher ΔE variation, but always below the tolerance threshold [44]. In all cases, L* results to be the more affected component.

Table 19: colour variation of silk samples after treatment 5

sample	L*	*a	b*	ΔE	ΔL*(D65)	Δa*(D65)	Δb*(D65)
b as such	77,51	0,8	3,35				
b_EtOH	79,04	0,89	2,74	1,65	1,53	0,09	-0,61
f as such	30,02	37,07	5,85				
f_EtOH	31,77	36,98	5,18	1,87	1,75	-0,09	-0,67
q as such	56,04	4,49	19,97				
q_EtOH	53,02	6,46	22,58	4,45	-3,02	1,97	2,61

Table 20 shows results of solutions colour variation. The solution did not show colour variation when applied on the white silk samples. On the contrary, Finzi and Querini treatment solutions (red and yellow samples) appeared to increase red component in the first case and yellow component in the second. We can therefore conclude that the colour variation observed on silk samples is reflected also on solutions, as observed for treatment 3. In this case, however, the colour variation appears to be less consistent than the one caused by sanitising solution.

Table 20: colour variation for treating solution after treatment 5

		L*	a*	b*	ΔE	ΔL	Δa	Δb
	target	37,9	0,31	1,29				
treatment 5	**B**	41,25	-0,49	3,71	4,21	3,35	-0,8	2,42
	F	34,46	5,08	3,37	6,24	-3,44	4,77	2,08
	Q	37,87	-1,11	11,06	9,87	-0,03	-1,42	9,77

3.2.3.1.5 IMMERSION IN WATER/ETHANOL BLEND (treatments 6-9)

EtOH 50% (treatment 6)

Table 21 shows colour variation for samples immersed for 24 hours in 50% ethanol solution.

The different types of silk present three different behaviours: while white silk has a negligible colour variation (average ΔE below 2 points) mainly related to the decrease of L* level, Finzi silk presented a consistent but not high average ΔE (5,18). This variation is ascribable to an increase both in L* (average + 3,35) and in a* (+3,95 on average) parameter. Querini silk showed a more consistent colour variation with increase in average L* (+7,30) and decrease in a* (-1,95).

As reported above, also in this case it was possible to observe the variation of colours on the solutions (table 22) correlated to fading of the silk colours. In particular, the solution used for treating the sample F (Finzi red silk) became consistently red and Querini treatment solution appear to yellow.

Table 21: colour variation for silk samples after treatment 6

sample	L*	*a	b*	ΔE	ΔL*(D65)	Δa*(D65)	Δb*(D65)
B as such	80,44	0,74	2,75				
B_EtOH 50%	79,08	0,68	3,16	1,42	-1,36	-0,06	0,41
F as such	30,26	37,49	6,34				
F_EtOH 50%	33,61	41,44	6,22	5,18	3,35	3,95	-0,12
Q as such	46,13	4,6	18,7				
Q_EtOH 50%	53,43	2,65	18,43	7,56	7,30	-1,95	-0,27

Table 22: colour variation for treating solutions after treatment 6

		L*	a*	b*	ΔL*	Δa*	Δb*	ΔE
	target	36,84	0,32	1,16				
treatment 6	**B**	39,67	0,12	3,34	3,58	2,83	-0,2	2,18
	F	27,03	10,84	1,44	14,39	-9,81	10,52	0,28
	Q	34,81	-2,09	8,89	8,35	-2,03	-2,41	7,73

EtOH 70% (treatment 7)

Colour parameters collected for samples that underwent treatment t7 are presented in table 23.

White silk and Finzi silk presented a negligible colour variation (less than 2,5 points) mainly related to the variation of L* level. Querini silk, instead presented a consistent but not high average ΔE (3,23).

This variation is ascribable to the increase of L* (+2,80 on average) and the decrease of a* (-1,58 on average).

Table 23: colour variation for silk samples after treatment 7

sample	L*	*a	b*	ΔE	ΔL*(D65)	Δa*(D65)	Δb*(D65)
B as such	80,08	0,78	3,49				
B_EtOH 70%	79,23	0,65	3,20	0,91	-0,85	-0,13	-0,29
F as such	32,96	39,29	5,63				
F_EtOH 70%	33,87	41,42	6,22	2,39	0,91	2,13	0,59
Q as such	49,19	4,55	18,33				
Q_EtOH 70%	51,99	2,97	18,64	3,23	2,80	-1,58	0,31

As reported above, also in this case it was possible to observe the variation of colours on the solutions (table 24) correlated to fading of the silk colours. In particular, the solution used for treating the sample F (Finzi red silk) became consistently red and Querini treatment solution increased its yellow component.

Table 24: colour variation for treating solution after treatment 7

		L*	a*	b*	ΔL*	Δa*	Δb*	ΔE
	target	37,1	0,3	1,14				
treatment 7	**B**	39,91	-0,56	3,74	3,92	2,81	-0,86	2,6
	F	24	9,08	2,18	15,80	-13,1	8,78	1,04
	Q	35,1	-0,91	6,54	5,88	-2	-1,21	5,4

EtOH 75% (treatment 8)

Colour parameters collected for samples that underwent treatment t8 are presented in table 25.

White silk presented a low colour variation (average ΔE =2,54) mainly related to the decrease of L* level (-2,49 on average). Finzi and Querini silk, instead, presented a consistent average ΔE (10,00 for Finzi silk and 11,06 for Querini silk).

Table 25: colour variation of silk samples after treatment 8

sample	L*	*a	b*	ΔE	ΔL*(D65)	Δa*(D65)	Δb*(D65)
B as such	80,2	0,75	2,97				
B_EtOH 75%	77,71	0,52	3,42	2,54	-2,49	-0,23	0,45
F as such	30,26	36,15	5,4				
F_EtOH 75%	35,84	44,38	6,47	10,00	5,58	8,23	1,07
Q as such	57,54	7,28	25,18				

sample	L*	*a	b*	ΔE	ΔL*(D65)	Δa*(D65)	Δb*(D65)
Q_EtOH 75%	55,30	2,30	15,57	11,06	-2,24	-4,98	-9,61

As reported above, also in this case it was possible to observe the variation of colours on treating solutions (table 26).

Once again, Finzi silk underwent a consistent colour loss, but also solution for Querini silk treatment increased its yellowness. As can easily be observed, the solutions appear to vary their colour more consistently as the concentration of ethanol increases.

Table 26: colour variations of treating solutions after treatment 8

		L*	a*	b*	ΔL*	Δa*	Δb*	ΔE
	target	37,06	0,29	1,13				
treatment 8	**B**	39,72	-0,56	3,82	3,88	2,66	-0,85	2,69
	F	26,39	12,11	2,93	16,03	-10,67	11,82	1,8
	Q	35,83	-1,55	9,36	8,52	-1,23	-1,84	8,23

EtOH 79% (treatment 9)

Colour parameters collected for samples that underwent treatment t9 are presented in table 27.

White silk presented a low colour variation (average ΔE =1,42) mainly related to the decrease of L* level (-1,36 on average). Querini silk, instead presented a consistent average ΔE (7,56). This variation is ascribable mainly to the increase of L* (+7,30 on average).

Finzi silk, instead, presented a less consistent average ΔE (5,18).

Table 27: colour variation for silk samples after treatment 9

sample	L*	*a	b*	ΔE	ΔL*(D65)	Δa*(D65)	Δb*(D65)
B as such	79,82	0,86	2,81				
B_EtOH 79%	79,08	0,68	3,16	1,42	-1,36	-0,06	0,41
F as such	29,13	37,52	6,14				
F_EtOH 79%	33,61	41,44	6,22	5,18	3,35	3,95	-0,12
Q as such	52,32	4,65	19				
Q_EtOH 79%	53,43	2,65	18,43	7,56	7,30	-1,95	-0,27

Both Finzi and Querini silk treatment solutions (table 28) showed a consistent colour variation, increasing red (in the first case) and yellow (in the second case) components. However, differently from what observed before, the colour variation is less consistent here if compared to 75% EtOH

solution. It can be therefore concluded that colour fading in silk is more effective in a defined range of ethanol concentration, and decreases its effectiveness moving away from those values.

Table 28: colour variation for treating solutions after treatment 9

		L*	a*	b*	ΔL	Δa	Δb	ΔE
	target	36,02	0,25	1,03				
treatment 9	**B**	39,41	-0,57	2,7	3,87	3,39	-0,82	1,67
	F	22,69	6,31	2,01	14,68	-13,33	6,06	0,98
	Q	31,51	-0,21	9,83	9,90	-4,51	-0,46	8,8

3.2.3.1.6 IMMERSION IN BENZALKONIUM CHLORIDE (treatment 10)

As can be easily noticed by observing table 29, treatment 10 strongly modified colour parameters for all the samples. In particular, the elevated ΔE values are due to the variation of L* component.

Each sample presents also a strong variation on another component, and, in particular: Finzi silk presents a strong variation for a* component (on average -28,38), while Querini silk showed a consistent decrease in b* value (on average -12,37 for Querini silk). White silk, instead, presented a moderate decrease of b* (on average -4,28).

These variations are due to the fact that a layer of benzalkonium is probably deposited on samples' surfaces, altering their aspects.

Table 29: colour variation of silk samples after treatment 10

sample	L*	*a	b*	ΔE	ΔL*(D65)	Δa*(D65)	Δb*(D65)
B as such	82,58	1,12	4,96				
B_EtOH 50%	40,99	0,81	0,68	41,81	-41,59	-0,31	-4,28
F as such	30,56	36,92	5,47				
F_EtOH 50%	22,22	8,54	1,80	29,80	-8,34	-28,38	-3,67
Q as such	52,57	3,92	17,85				
Q_EtOH 50%	24,08	2,09	5,48	31,12	-28,49	-1,83	-12,37

It is interesting to notice that also in this case the Finzi silk underwent some colour loss, as can be noticed by looking at table 30.

Table 30: colour variation for silk samples after treatment 9

		L*	a*	b*	ΔL	Δa	Δb	ΔE
	target	36,97	-0,28	3,53				
treatment 10	**B**	40,45	-0,53	3,37	3,49	-0,25	-0,16	3,50

		L*	a*	b*	ΔL	Δa	Δb	ΔE
	F	26,19	17,47	6,23	-10,78	17,75	2,71	20,94
	Q	35,34	-1,37	6,93	-1,62	-1,09	3,41	3,93

3.2.3.1.7 EXPOSURE TO CONTROLLED HUMIDITY ENVIRONMENT (treatment 11)

Table 31 reports colour variation for samples before and after treatment 11. As observed by naked eye, only a couple of consistent colour variations are here reported. In particular, for treatment 3 Querini silk shows a consistent increase in L* component, due to benzalkonium chloride efflorescence. The other relevant case is represented by treatment 10, where sample B varied its L* component of 3,92 points; this variation is most likely ascribable to partial drying of benzalkonium on surface, as detected also by the decrease in stickiness.

As a general tendency, the most relevant component variation is ascribable to L*, which is reported to vary moderately in all samples.

Table 31: colour variation of silk samples after treatment 11

TREATMENT	SAMPLE	ΔL*	Δa*	Δb*	ΔE
Untreated	B	-1,18	-0,03	0,54	1,30
	F	-1,63	-1,45	-0,34	2,21
	Q	-1,20	-0,51	-2,55	2,86
Treatment 3	B	-2,38	-0,79	0,25	2,53
	F	2,37	-1,60	-0,72	2,95
	Q	3,10	-0,83	-2,85	4,29
Treatment 5	B	-0,49	-0,17	-0,35	0,62
	F	-2,09	-2,04	-0,81	3,03
	Q	-3,02	0,99	0,96	3,32
Treatment 10	B	3,92	0,65	0,35	3,99
	F	2,20	1,07	-0,01	2,44
	Q	-1,67	-1,42	-0,06	2,19

Generally speaking, a few conclusions can be drawn from the observation of colour variation under the different treatments.

The first conclusion is that ethanol/water blends, with a concentration of ethanol between 50% and 79%, are responsible for consistent loss of colour which is dissolved into the treating solution. This happens both with and without the addition of benzalkonium chloride, which affects only partially the

final colour modification of the samples. It was observed also that within specific EtOH concentrations, the colour loss is more effective.

The second conclusion is related to the effects of pure water or pure ethanol. The two separate components, as observed before, do not affect the colour of silk samples as much as when they are mixed together. Ethanol/water blends result to be more effective on silk than pure water or pure alcohol, as mentioned before. Dilution of ethanol in water, in fact, modifies the ability of alcohol to interact with other components.

The last conclusion regards benzalkonium chloride: the colour variation for samples that underwent t10 is not related to the interaction between silk and the solution but, rather, to the way in which benzalkonium deposited on the sample itself, changing its morphology and colour (also partially dissolving it).

3.2.4 CHEMICAL CHARACTERIZATION

3.2.4.1 FTIR ANALYSES

As described in detail in paragraph 2.1.2.3.4, IR analyses were carried out both in ATR and ER modes on treated and untreated samples to investigate possible variations occurred.

3.2.4.1.1 EXPOSURE TO SANITISING SOLUTION VAPOUR (treatment 1)

IR spectra were collected for all the silk samples both before and after exposure to sanitising solution vapours.

As a result from this analysis, no significant differences can be spot on white and Finzi silk both in ATR and ER mode, as presented in figure 22. Querini silk, instead, presents some variations reported in table 32 and observable in figure 21.

Querini silk

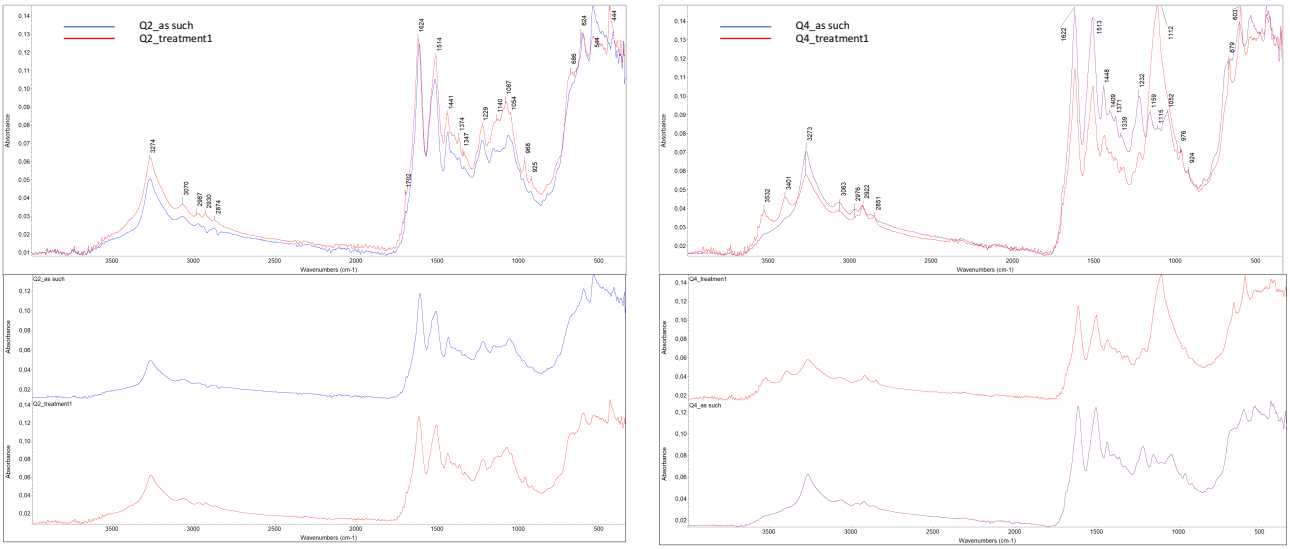

Figure 22: comparison of ATR spectra of querini silk before and after treatment 1. Both sample Q2_t1 and Q2_t1 are here presented

Table 32: Silk characteristic ATR peaks' variation after treatment 1

FTIR PEAKS VARIATION AFTER VAPOUR EXPOSURE – QUERINI SILK sample 4				
untreated silk		**peak variation on treated silk**		
cm^{-1}	**peak attribution**	**cm^{-1}**	**ATR**	**ER**
-	-	3532	OH stretching	-
-	-	3401	OH stretching	-
3275	stretching C=O	-	*unvaried*	-
1699	Amide I (stretching C=O, C-N, N-H)	1737	*unvaried*	shape variations for Q
1665	Amide I in antiparallel β sheet conformation		-	*unvaried*
1656	Amide I in random coil and α helical conformation		-	*unvaried*
1620	Amide I in parallel β sheet conformation		*unvaried*	*unvaried*
1595	C-C-C tryptophan stretching		-	*unvaried*
1511-1524	Amide II (peptide bond N-H bending and C-N bending)		*unvaried*	*unvaried*
1442	CH_2 e CH_3 Alanine bending		*unvaried*	*unvaried*
1405	CH_2 Aspargine bending		*unvaried*	*unvaried*
1367	CH bending		-	*unvaried*
1334	CH bending; phenylalanine		*unvaried*	*unvaried*
1261-1277	Amide III in β sheet conformation		*unvaried*	*unvaried*
1230-1236	Amide III in random coil conformation		*unvaried*	*unvaried*
1160-1164	CN Tyrosine stretching	1112	broad band covering characteristic	*unvaried*
1083	CN Alanine stretching			*unvaried*

FTIR PEAKS VARIATION AFTER VAPOUR EXPOSURE – QUERINI SILK sample 4				
untreated silk		**peak variation on treated silk**		
cm^{-1}	**peak attribution**	**cm^{-1}**	**ATR**	**ER**
1065	CH_3 rocking + CN stretching in amide III		absorptions	*unvaried*
1035	CN Phenylalanine stretching		*unvaried*	*unvaried*
997	CH_3 rocking		*unvaried*	*unvaried*
977	CC skeletal stretching in Glycine-Glycine and Glycine-Alanine		*unvaried*	*unvaried*
800	CC skeletal stretching + CH out of plane deformation in aromatic rings of tryptophan		*unvaried*	*unvaried*
605	Amide III mode		*unvaried*	*unvaried*
540	Deformation CCN mode		*unvaried*	*unvaried*
442	Deformation CCN mode		*unvaried*	*unvaried*

As it can easily be noticed from the observation of figure 23, different ATR analysis of two samples obtained from the same silk provided different two slightly responses. In particular, spectra for sample Q2 did not show great variation before and after vapour exposure, while spectra of sample Q4 present several differences: two peaks in the OH stretching region (3500-3200 cm^{-1}) and a strong absorption peak at 1112 cm^{-1} that covers the characteristic peaks at 1159 cm^{-1} (CN stretching in tyrosine) and 1052 cm^{-1} (amide III).

ER spectra for Querini sample, instead, presented some noticeable variations only in the 1740-1650 cm^{-1} region, where the shape of the 1737cm^{-1} broad band varies among the different spectra. This region corresponds to the amide I region, and these variations correspond to those observed and reported above in the ATR analysis.

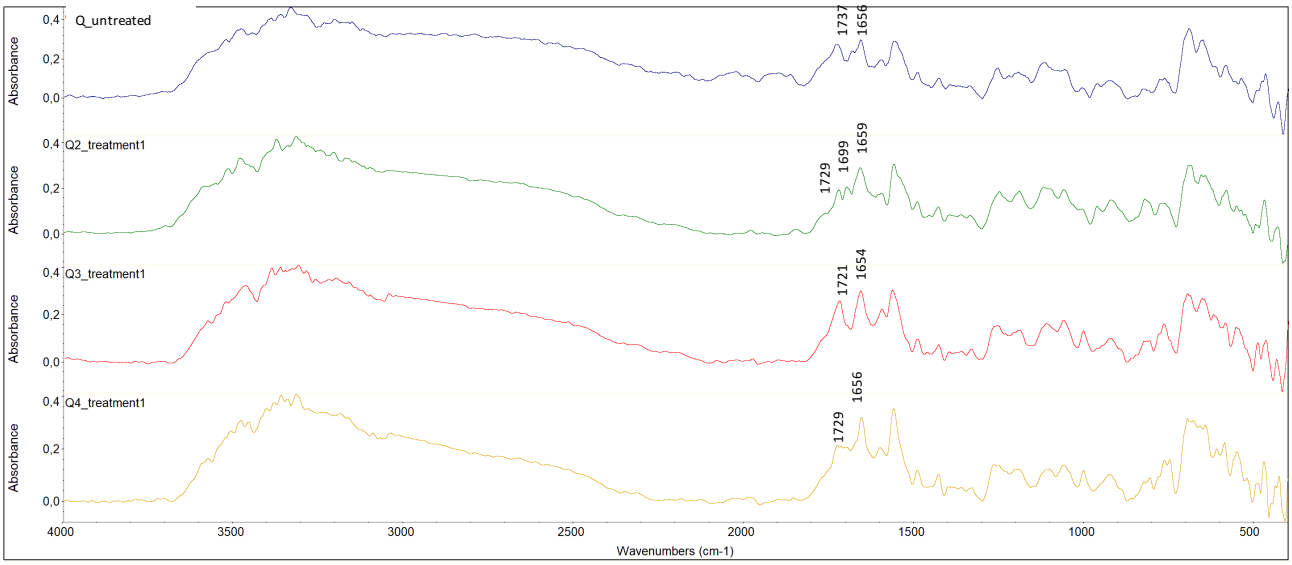

Figure 23: ER spectra of Querini silk before and after treatment 1

ATR technique is an extremely useful tool for non-invasive analysis of cultural heritage materials, but its characteristic surface punctual analyses can sometimes represent a drawback. The abovementioned variations, in fact, are most likely related to where the analysis was performed; therefore,- inhomogeneous samples can highly affect the analysis. Querini silk did not undergo any preparation before treatments and presented thus incoherent deposits on its surface. The different ATR spectra among similar samples might be due either to chemical modifications of surface deposits on the silk or to local chemical modification on the silk itself.

3.2.4.1.2 IMMERSION IN SANITISING SOLUTION (treatment 2 and 3)

Immersion of silk samples in sanitising solution caused some alteration, as described previously for weight, morphological and colorimetric analyses.

Therefore, ATR analyses were performed in order to evaluate chemical variations after treatment 2 (immersion in sanitising solution for 30 minutes) and 3 (immersion in sanitising solution for 24h).

ATR spectra collected for samples B, F and Q are shown here, for they are representative of three silk conditions, as explained before. Treatment 3 was preferentially showed here over treatment 2 for longer exposure times lead to stronger and more easily detectable variations.

ATR spectra for B, F and Q samples, however, presented only few differences, thus indicating that the above-mentioned alterations do not have numerous correspondence on chemical bond variation (table 33).

Table 33: silk characteristic peaks' variation after treatment 3

FTIR SILK CHARACTERISTIC PEAKS		ATR AFTER TREATMENT			ER AFTER TREATMENT		
cm^-1	**peak attribution**	**WIHTE SILK**	**FINZI SILK**	**QUERINI SILK**	**WIHTE SILK**	**FINZI SILK**	**QUERINI SILK**
-	-	-	-	new absorptions at 3035 and 3409 cm-1	-	-	-
3275	stretching C=O	*unvaried*	*unvaried*	*unvaried*	*unvaried*	*unvaried*	*unvaried*
-	-	new absorptions at 2924 and 2952 cm^{-1} – benzalkonium chloride peaks	absorptions at 2924 and 2952 cm^{-1} – benzalkonium chloride peaks	new absorptions at 2924 and 2952 cm^{-1} – benzalkonium chloride peaks	new absorptions at 2938 cm^{-1} and 2855 cm^{-1} - benzalkonium chloride peaks	new absorptions at 2938 cm^{-1} and 2855 cm^{-1} - benzalkonium chloride peaks	new absorptions at 2938 cm^{-1} and 2855 cm^{-1} - benzalkonium chloride peaks
1699	Amide I (stretching C=O, C-N, N-H)	*unvaried*	*unvaried*	*unvaried*	*unvaried*	*unvaried*	*unvaried*
1665	Amide I in antiparallel β sheet conformation	-	-	-	*unvaried*	*unvaried*	*unvaried*
1656	Amide I in random coil and α helical conformation	-	-	-	shift to 1710 cm^{-1}	shift to 1710 cm^{-1}	shift to 1710 cm^{-1}
1620	Amide I in parallel β sheet conformation	*unvaried*	*unvaried*	*unvaried*	shift to 1660 cm^{-1} and increase in intensity	shift to 1660 cm^{-1} and increase in intensity	shift to 1660 cm^{-1} and increase in intensity
1595	C-C-C tryptophan stretching	-	-	-	*unvaried*	*unvaried*	*unvaried*
1511-1524	Amide II (peptide bond N-H bending and C-N bending)	*unvaried*	*unvaried*	*unvaried*	*unvaried*	*unvaried*	*unvaried*
1442	CH_2 e CH_3 Alanine bending	*unvaried*	*unvaried*	*unvaried*	*unvaried*	*unvaried*	*unvaried*
1405	CH_2 Aspargine bending	*unvaried*	*unvaried*	*unvaried*	*unvaried*	*unvaried*	*unvaried*
1367	CH bending	*unvaried*	*unvaried*	*unvaried*	*unvaried*	*unvaried*	*unvaried*
1334	CH bending; phenylalanine	*unvaried*	*unvaried*	*unvaried*	*unvaried*	*unvaried*	*unvaried*

1261-1277	Amide III in β sheet conformation	*unvaried*	*unvaried*	*unvaried*	*unvaried*	*unvaried*	*unvaried*
1230-1236	Amide III in random coil conformation	*unvaried*	*unvaried*	broad band covering characteristic absorptions at 1112 cm^{-1}	*unvaried*	*unvaried*	*unvaried*
1160-1164	CN Tyrosine stretching	*unvaried*	*unvaried*		*unvaried*	*unvaried*	*unvaried*
1083	CN Alanine stretching	*unvaried*	*unvaried*		*unvaried*	*unvaried*	*unvaried*
1065	CH_3 rocking + CN stretching	*unvaried*	*unvaried*		*unvaried*	*unvaried*	*unvaried*
1035	CN Phenylalanine stretching	*unvaried*	*unvaried*	*unvaried*	*unvaried*	*unvaried*	*unvaried*
997	CH_3 rocking	*unvaried*	*unvaried*	*unvaried*	*unvaried*	*unvaried*	*unvaried*
977	CC skeletal stretching in Glycine-Glycine and Glycine-Alanine	*unvaried*	*unvaried*	*unvaried*	*unvaried*	*unvaried*	*unvaried*
800	CC skeletal stretching + CH out of plane deformation in aromatic rings of tryptophan	*unvaried*	*unvaried*	*unvaried*	*unvaried*	*unvaried*	*unvaried*
605	Amide III mode	*unvaried*	*unvaried*	*unvaried*	*unvaried*	*unvaried*	*unvaried*
540	Deformation CCN mode	*unvaried*	*unvaried*	*unvaried*	*unvaried*	*unvaried*	*unvaried*
442	Deformation CCN mode	*unvaried*	*unvaried*	*unvaried*	*unvaried*	*unvaried*	*unvaried*

It is worth reminding that the after-treatment spectra here presented were collected on dry samples; therefore, the peaks modification can be due either to possible residues of benzalkonium chloride or to bond modification of the treated sample.

Figure 24 shows the FTIR benzalkonium chloride spectra, where the peaks at 2925 and 2850 cm^{-1} correspond to the absorption detected in the treated silk samples. Benzalkonium chloride seems to be able to deposit on the surface of samples, not interacting with it but only modifying samples' properties (e.g. colour, wettability).

As regards Querini silk ATR analysis, some new peaks are present on the treated samples, as reported in table33. The signals lay at 3035, 3409 and 1122 cm^{-1}, which correspond to the peaks appeared on the same type ok silk after treatment 1, suggesting a probable interaction with components present on sample surface.

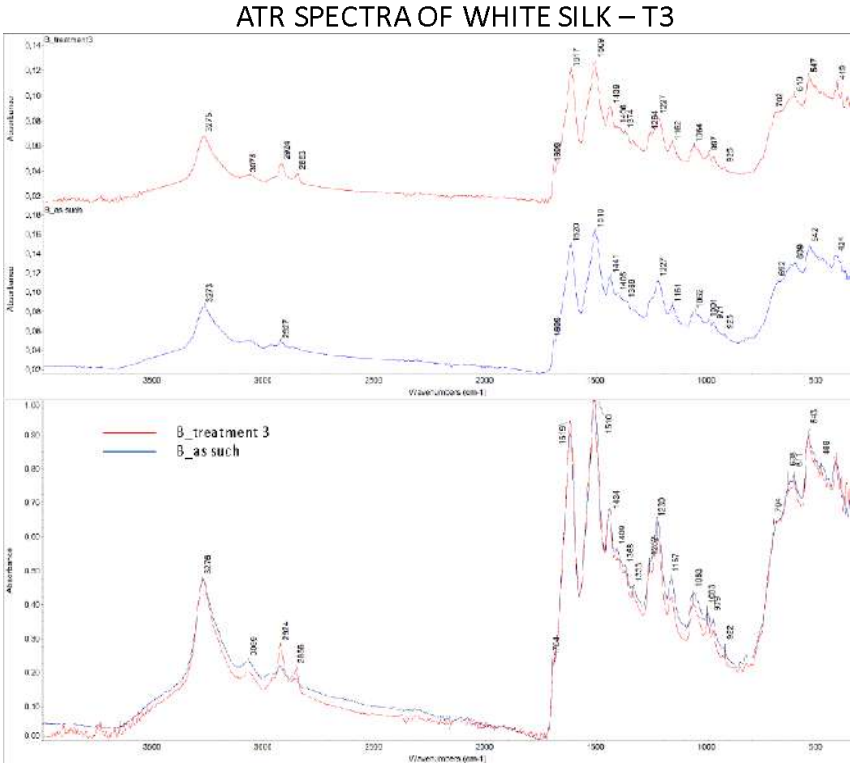

Figure 24: ATR spectra of Finzi silk before and after treatment 3

ER spectra confirmed the detectability of benzalkonium chloride on samples treated by immersion in sanitising solution. Figure 25 shows a comparison between ER spectra of untreated and treated silk, together with ATR spectra for treated silk. Two strong absorption at 2938 cm^{-1} and 2855 cm^{-1} correspond most likely to benzalkonium chloride peaks, as seen before (table 33). No other significant variations could be spotted between treated and untreated ER spectra, beside the intensity increase of amide I in parallel β sheet conformation (1665cm^{-1}). As observed elsewere, however, this intensity variation appears to happen quite frequently. Further researches should be conducted in order to provide an explication for this phenomenon.

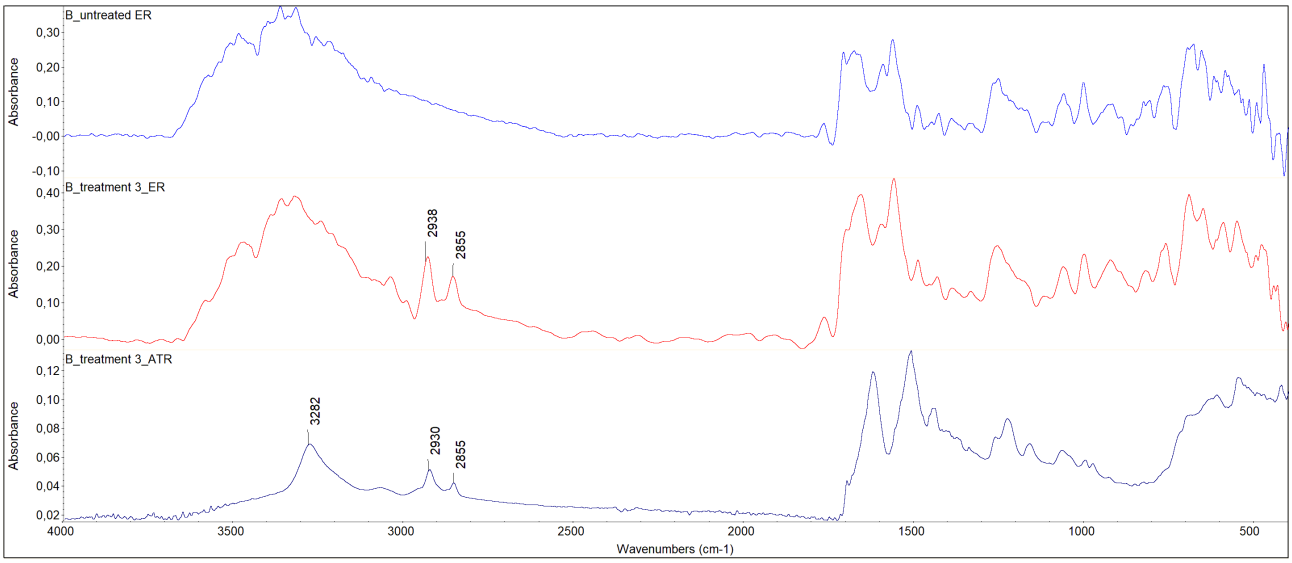

Figure 25: ATR and ER spectra of white silk before and after treatment 3

3.2.4.1.3 IMMERSION IN DEIONIZED WATER (treatment 4)

Representative results from ATR spectra analyses of samples immersed in deionized water for 24 hours are presented in table 34. No major variations could be detected via IR analyses for white silk samples.

Finzi and Querini silk, instead, presented as the only difference a relative intensity variations for the peaks at 1620 cm^{-1} (Amide I) and 1515 cm^{-1} (Amide II). This modification, however, was detected on several others comparisons, also between spectra collected on the same sample. Therefore it can be concluded that this variation in intensity cannot be related to silk treatments here performed. The difference in intensity, in fact, could be related to the type of analyses

performed. As above mentioned, ATR analysis is conducted on a small portion of sample where a consistent pressure is applied. Therefore, by compressing the surface, the analysis may reflect an interior portion of the sample rather than the outer (more degraded) side.

Table 34: silk characteristic peaks' variation after treatment 4

FTIR SILK CHARACTERISTIC PEAKS		ATR AFTER TREATMENT			ER AFTER TREATMENT		
cm^-1	**peak attribution**	**WIHTE SILK**	**FINZI SILK**	**QUERINI SILK**	**WIHTE SILK**	**FINZI SILK**	**QUERINI SILK**
3275	stretching C=O	*unvaried*	*unvaried*	*unvaried*	reduced noise in the 3700-3000 cm^{-1} region		
1699	Amide I (stretching C=O, C-N, N-H)	*unvaried*	*unvaried*	*unvaried*	*unvaried*	*unvaried*	*unvaried*
1665	Amide I in antiparallel β sheet conformation	-	-	-	*unvaried*	*unvaried*	*unvaried*
1656	Amide I in random coil and α helical conformation	-	-	-	variation intensity in the 1600 cm^{-1} region		
1620	Amide I in parallel β sheet conformation	*unvaried*	*unvaried*	*unvaried*			
1595	C-C-C tryptophan stretching	-	-	-	one broad band at 1570cm^{-1}		
1511-1524	Amide II (peptide bond N-H bending and C-N bending)	*unvaried*	slight increase in intensity	slight increase in intensity			
1442	CH_2 e CH_3 Alanine bending	*unvaried*	*unvaried*	*unvaried*	*unvaried*	*unvaried*	*unvaried*
1405	CH_2 Aspargine bending	*unvaried*	*unvaried*	*unvaried*	*unvaried*	*unvaried*	*unvaried*
1367	CH bending	*unvaried*	*unvaried*	*unvaried*	*unvaried*	*unvaried*	*unvaried*
1334	CH bending; phenylalanine	*unvaried*	*unvaried*	*unvaried*	*unvaried*	*unvaried*	*unvaried*
1261-1277	Amide III in β sheet conformation	*unvaried*	*unvaried*	*unvaried*	*unvaried*	*unvaried*	*unvaried*
1230-1236	Amide III in random coil conformation	*unvaried*	*unvaried*	*unvaried*	*unvaried*	*unvaried*	*unvaried*
1160-1164	CN Tyrosine stretching	*unvaried*	*unvaried*	*unvaried*	*unvaried*	*unvaried*	*unvaried*
1083	CN Alanine stretching	*unvaried*	*unvaried*	*unvaried*	*unvaried*	*unvaried*	*unvaried*
1065	CH_3 rocking + CN stretching	*unvaried*	*unvaried*	*unvaried*	*unvaried*	*unvaried*	*unvaried*
1035	CN Phenylalanine stretching	*unvaried*	*unvaried*	*unvaried*	*unvaried*	*unvaried*	*unvaried*
997	CH_3 rocking	*unvaried*	*unvaried*	*unvaried*	*unvaried*	*unvaried*	*unvaried*
977	CC skeletal stretching in Glycine-Glycine and Glycine-Alanine	*unvaried*	*unvaried*	*unvaried*	*unvaried*	*unvaried*	*unvaried*
800	CC skeletal stretching + CH out of plane deformation in aromatic rings of tryptophan	*unvaried*	*unvaried*	*unvaried*	*unvaried*	*unvaried*	*unvaried*
605	Amide III mode	*unvaried*	*unvaried*	*unvaried*	*unvaried*	*unvaried*	*unvaried*
540	Deformation CCN mode	*unvaried*	*unvaried*	*unvaried*	*unvaried*	*unvaried*	*unvaried*
442	Deformation CCN mode	*unvaried*	*unvaried*	*unvaried*	*unvaried*	*unvaried*	*unvaried*

ER spectra, presented also in table 34 and in figure 26, show two main variations between untreated silk and silk immersed in deionized water. The first is related to the consistent decrease of noise in the 3700-3000 cm^{-1} region that makes it hard to distinguish NH amide band at 3325 cm^{-1}. The abovementioned region corresponds to hydrogen bonding and therefore the increased signal can be due to OH vibration. The second, instead, is represented by the fact that treated samples present only one broader band at 1570 cm^{-1}, while silk as such showed to absorption at 1597 cm^{-1} and 1562 cm^{-1}. As mentioned before, peak's intensity variations in the 1700-1550 cm^{-1} region should be object of further studies.

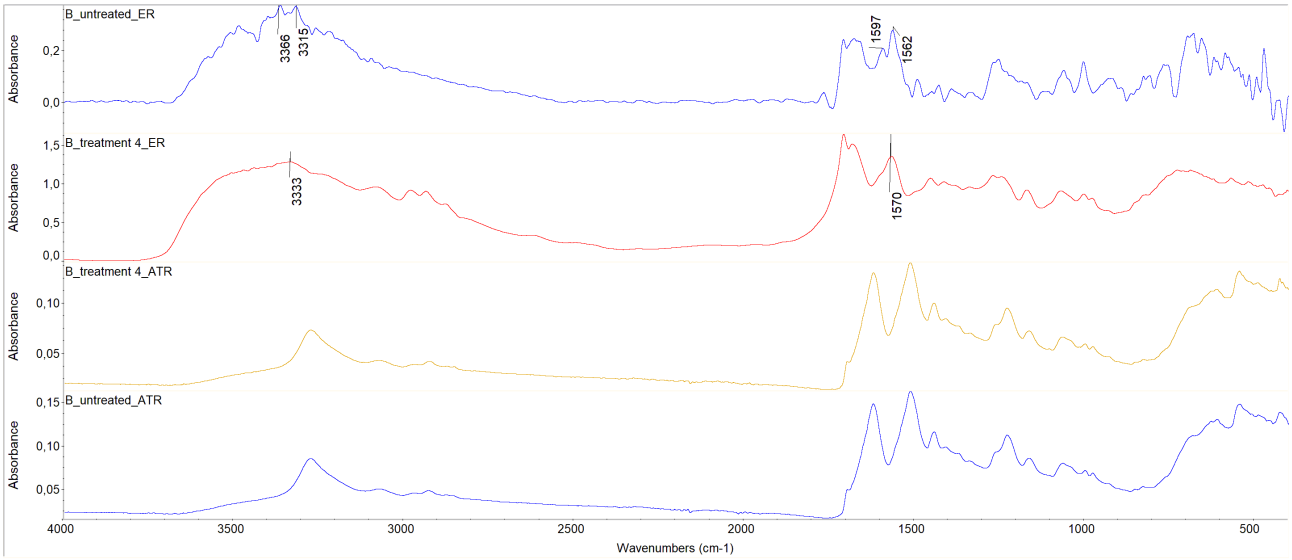

Figure 26: ATR and ER spectra of white silk before and after treatment 4

3.2.4.1.4 IMMERSION IN ETHANOL WITH DIFFERENT CONCENTRATIONS (treatments 5-9)

In order to verify the effects of pure and diluted alcohol, immersion tests were conducted both with pure ethanol and with ethanol/water blends at different alcohol concentrations (50%, 70%, 75%, 79%).

As mentioned before, alcohol does not chemically react with proteins, but interacts with them by destabilizing planar peptide bonds; therefore the variation that occurs is not chemical but rather structural, thus providing a reason to explain the lack of variations in ATR spectra before and after treatments. The only differences that can be spotted are, in fact, related to the relative intensity variation of 1620-1515 cm^{-1} peaks, as discussed above. Moreover, Querini silk presents the same peak appearance reported in previous observations.

Table 35 reports a comparison of the ATR and ER spectra collected for B (white silk), F (Finzi silk) and Q (Querini silk) samples collected before and after treatments with solutions with various EtOH concentrations.

Table 35: silk characteristic peaks' variation after treatment 5-9

FTIR SILK CHARACTERISTIC PEAKS		ATR AFTER TREATMENT			ER AFTER TREATMENT		
cm^-1	**peak attribution**	**WIHTE SILK**	**FINZI SILK**	**QUERINI SILK**	**WIHTE SILK**	**FINZI SILK**	**QUERINI SILK**
3275	stretching C=O	*unvaried*	*unvaried*	*unvaried*	reduced noise in the 3700-3000 cm^{-1} region (all treatments)		
1699	Amide I (stretching C=O, C-N, N-H)	*unvaried*	*unvaried*	*unvaried*	*unvaried*	*unvaried*	*unvaried*
1665	Amide I in antiparallel β sheet conformation	-	-	-	*unvaried*	*unvaried*	*unvaried*
1656	Amide I in random coil and α helical conformation	-	-	-	*unvaried*	*unvaried*	*unvaried*
1620	Amide I in parallel β sheet conformation	*unvaried*	*unvaried*	*unvaried*	*unvaried*	*unvaried*	*unvaried*
1595	C-C-C tryptophan stretching	-	-	-	one broad band at 1570cm^{-1} (all treatments)		
1511-1524	Amide II (peptide bond N-H bending and C-N bending)	*unvaried*	slight decrease in intensity for treatment 5 and 8	slight decrease in intensity for treatment 5 and 8			
1442	CH_2 e CH_3 Alanine bending	*unvaried*	*unvaried*	*unvaried*	*unvaried*	*unvaried*	*unvaried*
1405	CH_2 Aspargine bending	*unvaried*	*unvaried*	*unvaried*	*unvaried*	*unvaried*	*unvaried*
1367	CH bending	*unvaried*	*unvaried*	*unvaried*	*unvaried*	*unvaried*	*unvaried*
1334	CH bending; phenylalanine	*unvaried*	*unvaried*	*unvaried*	*unvaried*	*unvaried*	*unvaried*
1261-1277	Amide III in β sheet conformation	*unvaried*	*unvaried*	*unvaried*	*unvaried*	*unvaried*	*unvaried*
1230-1236	Amide III in random coil conformation	*unvaried*	*unvaried*	*unvaried*	*unvaried*	*unvaried*	*unvaried*
1160-1164	CN Tyrosine stretching	*unvaried*	*unvaried*	*unvaried*	*unvaried*	*unvaried*	*unvaried*
1083	CN Alanine stretching	*unvaried*	*unvaried*	*unvaried*	*unvaried*	*unvaried*	*unvaried*
1065	CH_3 rocking + CN stretching	*unvaried*	*unvaried*	*unvaried*	*unvaried*	*unvaried*	*unvaried*
1035	CN Phenylalanine stretching	*unvaried*	*unvaried*	*unvaried*	*unvaried*	*unvaried*	*unvaried*
997	CH_3 rocking	*unvaried*	*unvaried*	*unvaried*	*unvaried*	*unvaried*	*unvaried*
977	CC skeletal stretching in Glycine-Glycine and Glycine-Alanine	*unvaried*	*unvaried*	*unvaried*	*unvaried*	*unvaried*	*unvaried*
800	CC skeletal stretching + CH out of plane deformation in aromatic rings of tryptophan	*unvaried*	*unvaried*	*unvaried*	*unvaried*	*unvaried*	*unvaried*
605	Amide III mode	*unvaried*	*unvaried*	*unvaried*	*unvaried*	*unvaried*	*unvaried*
540	Deformation CCN mode	*unvaried*	*unvaried*	*unvaried*	*unvaried*	*unvaried*	*unvaried*

FTIR SILK CHARACTERISTIC PEAKS		ATR AFTER TREATMENT			ER AFTER TREATMENT		
cm^-1	peak attribution	WIHTE SILK	FINZI SILK	QUERINI SILK	WIHTE SILK	FINZI SILK	QUERINI SILK
442	Deformation CCN mode	*unvaried*	*unvaried*	*unvaried*	*unvaried*	*unvaried*	*unvaried*

3.2.4.1.5 IMMERSION IN BENZALKONIUM CHLORIDE (treatment 10)

Immersion in benzalkonium chloride caused the deposition of the product on the sample surface, as expected and described before. All the samples, therefore, presented a benzalkonium chloride sticky layer, whose presence is also observable in ATR spectra of treated silk (table 36; figure 27).

Table 36: silk characteristic peaks' variation after treatment 10

FTIR SILK CHARACTERISTIC PEAKS		ATR AFTER TREATMENT		
cm^-1	peak attribution	WIHTE SILK	FINZI SILK	QUERINI SILK
-	-	broad band at 3400cm^{-1}		
3275	stretching C=O	*unvaried*	*unvaried*	*unvaried*
-	-	new absorptions at 2925 cm^{-1} and 2850 cm^{-1} – benzalkonium chloride		
1699	Amide I (stretching C=O, C-N, N-H)	*unvaried*	*unvaried*	*unvaried*
1620	Amide I in parallel β sheet conformation	*unvaried*	*unvaried*	*unvaried*
1511-1524	Amide II (peptide bond N-H bending and C-N bending)	*unvaried*	*unvaried*	*unvaried*
-	-	benzalkonium chloride peaks at 1486 cm^{-1} and 1455 cm^{-1}		
1442	CH_2 e CH_3 Alanine bending	*unvaried*	*unvaried*	*unvaried*
1405	CH_2 Aspargine bending	*unvaried*	*unvaried*	*unvaried*
1367	CH bending	*unvaried*	*unvaried*	*unvaried*
1334	CH bending; phenylalanine	*unvaried*	*unvaried*	*unvaried*
1261-1277	Amide III in β sheet conformation	*unvaried*	*unvaried*	*unvaried*
1230-1236	Amide III in random coil conformation	*unvaried*	*unvaried*	*unvaried*
1160-1164	CN Tyrosine stretching	*unvaried*	*unvaried*	*unvaried*
1083	CN Alanine stretching	*unvaried*	*unvaried*	*unvaried*
1065	CH_3 rocking + CN stretching	*unvaried*	*unvaried*	*unvaried*
1035	CN Phenylalanine stretching	*unvaried*	*unvaried*	*unvaried*
997	CH_3 rocking	*unvaried*	*unvaried*	*unvaried*
977	CC skeletal stretching in Glycine-Glycine and Glycine-Alanine	*unvaried*	*unvaried*	*unvaried*
800	CC skeletal stretching + CH out of plane deformation in aromatic rings of tryptophan	*unvaried*	*unvaried*	*unvaried*
-	-	benzalkonium peaks at 710 cm^{-1}		

FTIR SILK CHARACTERISTIC PEAKS		ATR AFTER TREATMENT		
cm^-1	peak attribution	WIHTE SILK	FINZI SILK	QUERINI SILK
		and 700 cm^{-1}		
605	Amide III mode	*unvaried*	*unvaried*	*unvaried*
540	Deformation CCN mode	*unvaried*	*unvaried*	*unvaried*
442	Deformation CCN mode	*unvaried*	*unvaried*	*unvaried*

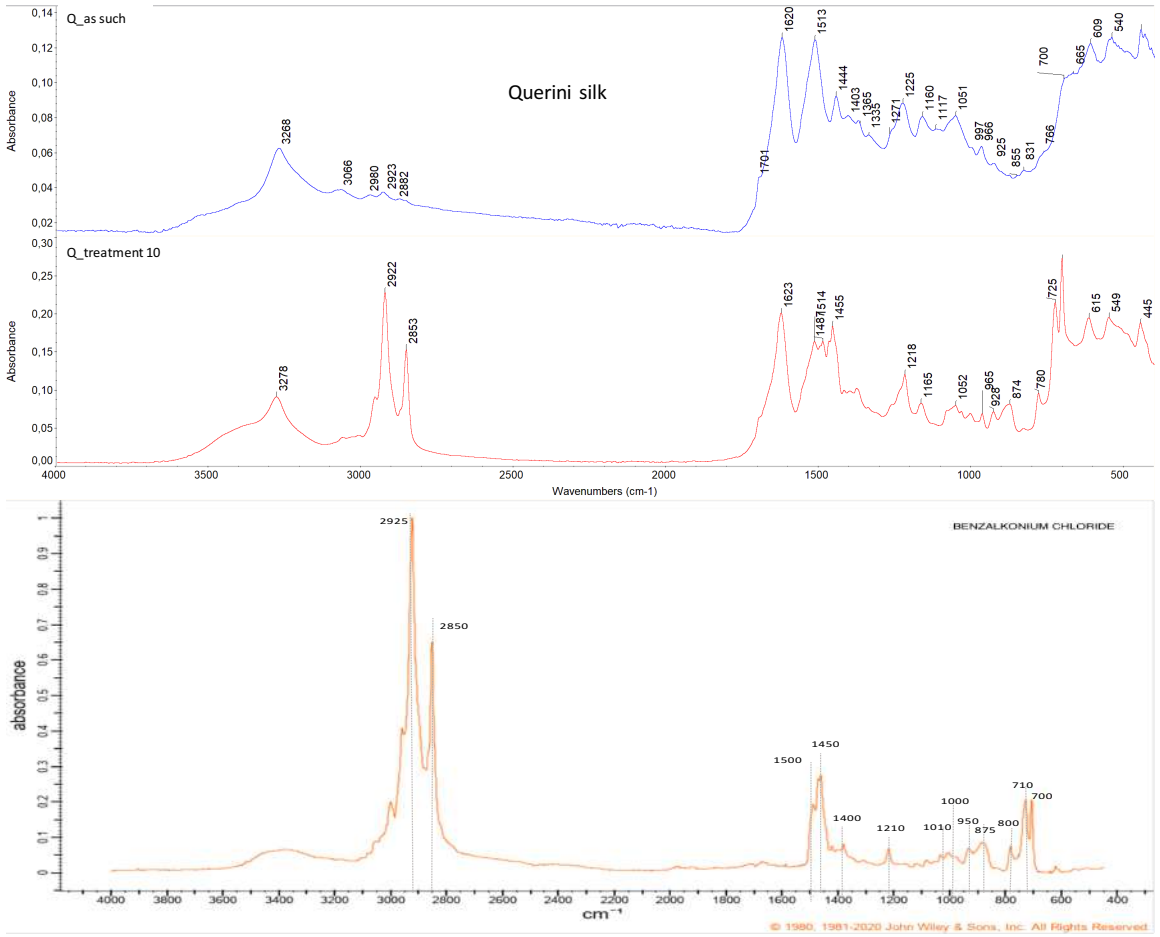

Figure 27: ATR spectra of white silk before and after treatment 10, compared to benzalkonium chloride spectrum

3.2.4.1.6 EXPOSURE TO CONTROLLED HUMDITY ENVIRONMENT (treatment 11)

Table 37 reports silk characteristic's peaks variation after exposure to humid environment. Silks that had undergone the same treatment showed here the same behaviour when exposed to high humidity levels. No significant differences could be spot on spectra after treatment 11, with few exception.

Samples treated by immersion in sanitising solution appeared here to be covered by a crystallized layer of benzalkonium chloride whose signals (for both ATR and ER 2925 cm^{-1} - 2850 cm^{-1}) are clearly detectable both in ATR and ER modes. ER variation for 1660 – 1597 cm-1 peaks instead can be compared with the same variation observed for treatment 4. Therefore we can concluded that the increase is related to the presence of water.

Table 37: silk characteristic peaks' variation after treatment 11

FTIR SILK CHARACTERISTIC PEAKS		ATR AFTER TREATMENT			ER AFTER TREATMENT		
cm^-1	**WIHTE SILK**	**untreated silk**	**treatment 3**	**treatment 5**	**untreated silk**	**treatment 3**	**treatment 5**
3275	stretching C=O	*unvaried*	*unvaried*	*unvaried*	*unvaried*	*unvaried*	*unvaried*
-	-	-	new absorptions at 2925 cm^{-1} and 2850 cm^{-1} _ benzalkonium chloride	-	-	new absorptions at 2925 cm^{-1} and 2860 cm^{-1} _ benzalkonium chloride	-
1699	Amide I (stretching C=O, C-N, N-H)	*unvaried*	*unvaried*	*unvaried*	*unvaried*	*unvaried*	*unvaried*
1665	Amide I in antiparallel β sheet conformation	-	-	-	*unvaried*	*unvaried*	*unvaried*
1656	Amide I in random coil and α helical conformation	-	-	-	*unvaried*	*unvaried*	*unvaried*
1620	Amide I in parallel β sheet conformation	*unvaried*	*unvaried*	*unvaried*	*unvaried*	increase in intensity of the shifted peak at 1660 cm^{-1}	*unvaried*
1595	C-C-C tryptophan stretching	*unvaried*	*unvaried*	*unvaried*	*unvaried*	one single broad peak at 1597 cm^{-1}	*unvaried*
1511-1524	Amide II (peptide bond N-H bending and C-N bending)	*unvaried*	*unvaried*	*unvaried*	*unvaried*		*unvaried*
1442	CH_2 e CH_3 Alanine bending	*unvaried*	*unvaried*	*unvaried*	*unvaried*	*unvaried*	*unvaried*
1405	CH_2 Aspargine bending	*unvaried*	*unvaried*	*unvaried*	*unvaried*	*unvaried*	*unvaried*
1367	CH bending	*unvaried*	*unvaried*	*unvaried*	*unvaried*	*unvaried*	*unvaried*
1334	CH bending; phenylalanine	*unvaried*	*unvaried*	*unvaried*	*unvaried*	*unvaried*	*unvaried*
1261-1277	Amide III in β sheet conformation	*unvaried*	*unvaried*	*unvaried*	*unvaried*	*unvaried*	*unvaried*
1230-1236	Amide III in random coil conformation	*unvaried*	*unvaried*	*unvaried*	*unvaried*	*unvaried*	*unvaried*

FTIR SILK CHARACTERISTIC PEAKS		ATR AFTER TREATMENT			ER AFTER TREATMENT		
cm^-1	WIHTE SILK	untreated silk	treatment 3	treatment 5	untreated silk	treatment 3	treatment 5
1160-1164	CN Tyrosine stretching	*unvaried*	*unvaried*	*unvaried*	*unvaried*	*unvaried*	*unvaried*
1083	CN Alanine stretching	*unvaried*	*unvaried*	*unvaried*	*unvaried*	*unvaried*	*unvaried*
1065	CH_3 rocking + CN stretching	*unvaried*	*unvaried*	*unvaried*	*unvaried*	*unvaried*	*unvaried*
1035	CN Phenylalanine stretching	*unvaried*	*unvaried*	*unvaried*	*unvaried*	*unvaried*	*unvaried*
997	CH_3 rocking	*unvaried*	*unvaried*	*unvaried*	*unvaried*	*unvaried*	*unvaried*
977	CC skeletal stretching in Glycine-Glycine and Glycine-Alanine	*unvaried*	*unvaried*	*unvaried*	*unvaried*	*unvaried*	*unvaried*
800	CC skeletal stretching + CH out of plane deformation in aromatic rings of tryptophan	*unvaried*	*unvaried*	*unvaried*	*unvaried*	*unvaried*	*unvaried*
605	Amide III mode	*unvaried*	*unvaried*	*unvaried*	*unvaried*	*unvaried*	*unvaried*
540	Deformation CCN mode	*unvaried*	*unvaried*	*unvaried*	*unvaried*	*unvaried*	*unvaried*
442	Deformation CCN mode	*unvaried*	*unvaried*	*unvaried*	*unvaried*	*unvaried*	*unvaried*

Comparing the results obtained with FTIR analyses, some conclusions can be drawn.

First, the benzalkonium chloride present in the sanitising solution actually deposited on the silk surface, without producing detectable chemical interaction. This hypothesis was confirmed by the observation of spectra after treatment 10: silk (e.g. amide signals at 1629 and 1515 cm^{-1}) and benzalkonium (e.g. 2920, 2850 and 1004 cm^{-1}) characteristic peaks both appear, without showing the presence of new peaks, suggesting that no new components were produced following chemical reactions among them.

Second, despite the observed morphological variations for ethanol/water blend treatments, no significant chemical modifications have been observed on the FTIR spectra collected. Ethanol is known to show stronger interactions when diluted with water, as mentioned before. Therefore, some characteristic vibrations due to the structural change of peptide planar bonds induced by ethanol can be expected. However, in our case, no significant modifications were detected on spectra before and after treatments 5-9. This phenomena may have two possible explanations: the first is that these vibrations are not easily detectable via ATR (for ER spectra lack of reference to be easily interpreted). The second is that, according to what Badillo-Sanchez reported [47], the pressure exerted on the samples to collect ATR spectra may alter the fibres' structure, showing not the response of the surface, but the spectra for a more internal layer, not affected by the

solution interactions. Silk is a flexible material and can be easily modified when pressure is applied as in ATR measurements.

3.2.4.2 RAMAN ANALYSES

As described in detail in paragraph 2.1.2.3.5, Raman analyses were carried out on treated and untreated samples to investigate possible chemical variations occurred.

3.2.4.2.1 EXPOSURE TO SANITISING SOLUTION VAPOURS (treatment 1)

Table 38 reports the variation of Raman characteristic signals for silk before and after treatment 1. The spectra collected do not show significant variations after the treatment, apart from the peak at 2870 cm^{-1} for white silk (CH_3 symmetric stretching), which, after the treatment, shifts to 2880 cm^{-1}. This tendency can be detected (even if it is less intense) on Finzi silk. This phenomena may be attributed to the signal of hydroxyl groups derived from solution (water) residues which led the shift and broadening of the signal.

Table 38: Variation of Raman characteristic peaks for silk after treatment 1

RAMAN CHARACTERISTIC SILK PEAKS		**RAMAN PEAKS AFTER TREATMENT**		
cm^-1	**peak attribution**	**white silk**	**Finzi silk**	**Querini silk**
622	Phenylalanine	*unvaried*	*unvaried*	*unvaried*
645-54	Tyrosine ring-breathing mode	*unvaried*	*unvaried*	*unvaried*
760	Tryptophan	*unvaried*	*unvaried*	*unvaried*
830	Tyrosine (bending of ring)	*unvaried*	*unvaried*	*unvaried*
855	Tyrosine (bending of ring)	*unvaried*	*unvaried*	*unvaried*
885	CC skeletal stretch, Tryptophan	*unvaried*	*unvaried*	*unvaried*
900-960	skeletal mode	*unvaried*	*unvaried*	*unvaried*
979	CC skeletal stretch	*unvaried*	*unvaried*	*unvaried*
1004	COC stretching vibration of tryptophan ring and phenyl ring of phenylalanine	*unvaried*	*unvaried*	*unvaried*
1087	CN stretch	*unvaried*	*unvaried*	*unvaried*
1159	CN stretch	*unvaried*	*unvaried*	*unvaried*
1232	Amide III in β sheet conformation (bending)	*unvaried*	*unvaried*	*unvaried*
1269	Amide III in β sheet conformation and disordered (bending)	*unvaried*	*unvaried*	*unvaried*
1308	CH bend	*unvaried*	*unvaried*	*unvaried*
1337	CH bend, Phenylalanine	*unvaried*	*unvaried*	*unvaried*
1449	CH_2, CH_3 bending modes	*unvaried*	*unvaried*	*unvaried*
1585	Phenylalanine	*unvaried*	*unvaried*	*unvaried*
1605	Phenylalanine	*unvaried*	*unvaried*	*unvaried*

RAMAN CHARACTERISTIC SILK PEAKS		RAMAN PEAKS AFTER TREATMENT		
cm^-1	**peak attribution**	**white silk**	**Finzi silk**	**Querini silk**
1616	Tryosine, Tryptophane	*unvaried*	*unvaried*	*unvaried*
1668	Amide I in β sheet conformation (stretching)	*unvaried*	*unvaried*	*unvaried*
1675	Amide I	*unvaried*	*unvaried*	*unvaried*
2875	CH_3 symmetrical stretch	shift to 2880 cm^{-1}	shift to 2880 cm^{-1}	*unvaried*
2934	CH_3 stretch asymmetrical	*unvaried*	*unvaried*	*unvaried*
3063	CNH bend overtone	*unvaried*	*unvaried*	*unvaried*
3286	NH stretch	*unvaried*	*unvaried*	*unvaried*

3.2.4.2.2 IMMERSION IN SANITISING SOLUTION (treatments 2 and 3)

Immersion of silk samples in sanitising solution caused some colour alteration, and ATR results assessed the presence of benzalkonium chloride residues on the silk surface. Therefore, the comparison of Raman spectra for silk before and after treatment 2 and 3 is key to confirm such modifications. In order to successfully do so, Raman spectra of samples B, F and Q were take once again into consideration as they are believed to provide a representative insight of the processes occurred. Treatment 3 was preferentially shown here over treatment 2 for longer exposure times might lead to stronger and more easily detectable variations.

Raman spectra for B, F and Q samples presented some differences, probably related both to benzalkonium chloride deposits and to possible alterations related to the silk dyes, as reported in table 39.

Table 39: Variation of Raman characteristic peaks for silk after treatment 3

RAMAN CHARACTERISTIC SILK PEAKS		RAMAN PEAKS AFTER TREATMENT		
cm^-1	**peak attribution**	**white silk**	**Finzi silk**	**Querini silk**
622	Phenylalanine	*unvaried*	*unvaried*	*unvaried*
645-54	Tyrosine ring-breathing mode	*unvaried*	*unvaried*	*unvaried*
760	Tryptophan	*unvaried*	*unvaried*	*unvaried*
830	Tyrosine (bending of ring)	*unvaried*	*unvaried*	*unvaried*
855	Tyrosine (bending of ring)	*unvaried*	*unvaried*	increase in intensity
885	CC skeletal stretch, Tryptophan	*unvaried*	*unvaried*	*unvaried*
900-960	skeletal mode	*unvaried*	*unvaried*	*unvaried*

RAMAN CHARACTERISTIC SILK PEAKS		RAMAN PEAKS AFTER TREATMENT		
cm^-1	**peak attribution**	**white silk**	**Finzi silk**	**Querini silk**
979	CC skeletal stretch	*unvaried*	*unvaried*	*unvaried*
1004	COC stretching vibration of tryptophan ring and phenyl ring of phenylalanine	increase in intensity	slight increase in intensity	increase in intensity
1087	CN stretch	*unvaried*	*unvaried*	*unvaried*
1159	CN stretch	*unvaried*	*unvaried*	*unvaried*
1232	Amide III in β sheet conformation (bending)	*unvaried*	*unvaried*	*unvaried*
1269	Amide III in β sheet conformation and disordered (bending)	*unvaried*	*unvaried*	*unvaried*
1308	CH bend	*unvaried*	*unvaried*	*unvaried*
1337	CH bend, Phenylalanine	*unvaried*	slight increase in intensity	*unvaried*
1449	CH_2, CH_3 bending modes	*unvaried*	*unvaried*	*unvaried*
1585	Phenylalanine	*unvaried*	*unvaried*	*unvaried*
1605	Phenylalanine	*unvaried*	*unvaried*	*unvaried*
1616	Tryosine, Tryptophane	*unvaried*	*unvaried*	*unvaried*
1668	Amide I in β sheet conformation (stretching)	*unvaried*	*unvaried*	*unvaried*
1675	Amide I	*unvaried*	*unvaried*	*unvaried*
2875	CH_3 symmetrical stretch	increase in intensity	increase in intensity	*unvaried*
2934	CH_3 stretch asymmetrical	*unvaried*	increase in intensity	*unvaried*
3063	CNH bend overtone	*unvaried*	increase in intensity	increase in intensity
3286	NH stretch	*unvaried*	*unvaried*	*unvaried*

For white silk, in fact, peaks at 2875 cm^{-1} and 1004 cm^{-1} appear more intense after treatment; these peaks correspond to two characteristic signals of benzalkonium chloride, and can therefore be attributed to its deposition on the surface.

Finzi silk, instead, shows an increase in the intensity for the peaks in the region between 3064-2875 cm^{-1}, which might be attributed to the presence of benzalkonium chloride once again. Benzalkonium might have given a contribution also to the increase in the intensity for the peaks at 1035 cm^{-1} and 1004 cm^{-1} (figure 26).

Peak variations at 1666 cm^{-1}, 1598 cm^{-1} and 1310 cm^{-1} can be related to the interaction of the solution with silk dye, as observed in previous tests (colorimetric analyses).

Raman spectra for Querini silk (figure 28), in the end, shows some significant variations worth discussing. First, the spectrum of the untreated silk results quite noisy, while Raman signal for silk after immersion in sanitising solution is remarkably more defined. This might be due to the loss of incoherent deposits that made the collection of the spectrum difficult. Second, not all the variations observed in the treated sample can be attributed to benzalkonium chloride presence. While the sharp peak arising at 3083 cm^{-1} in the treated sample and the increase of the peaks at 1009 cm^{-1} and 860 cm^{-1} correspond to benzalkonium chloride absorption bands, the variation of the peaks in the region 1730-1220 cm^{-1} cannot be attributed to the same cause.

Based on the Raman data, it is possible to hypothesise that benzalkonium chloride deposited on the surface of samples, not interacting with it but only modifying samples' properties (e.g. wettability, colour and morphology variation). Furthermore, the variations observed for dyed samples leads to the hypothesis that the ethanol/water blend (that constitutes the main component of the sanitising solution) may have interacted with silk dying components. As observed and discussed in the previous paragraphs, in fact, silk samples faded their colour after treatments; this phenomenon was indeed reflected also in colour variation of treatment solutions.

Finzi silk

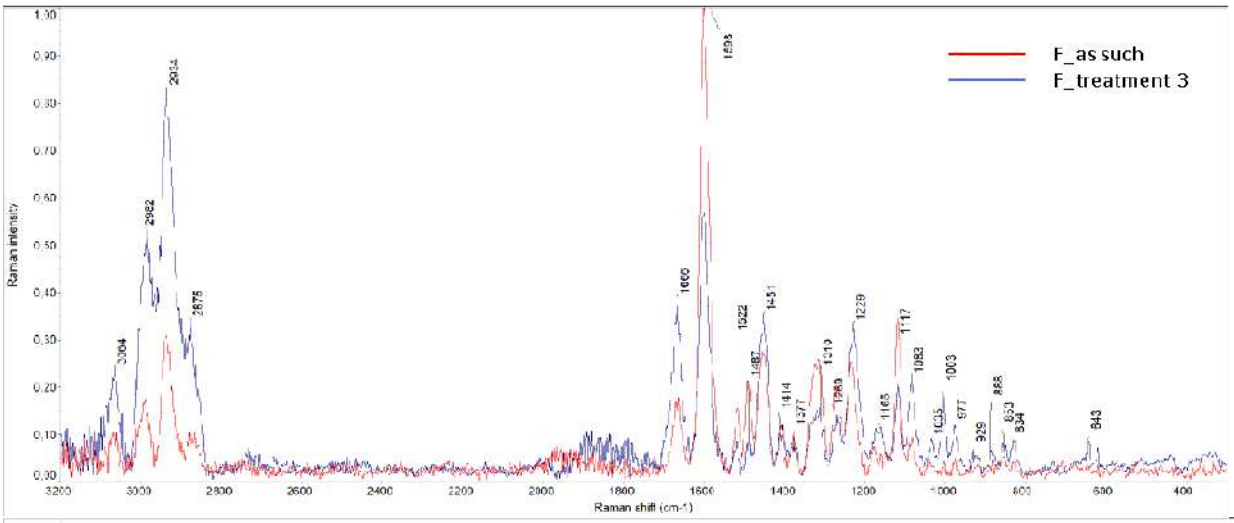

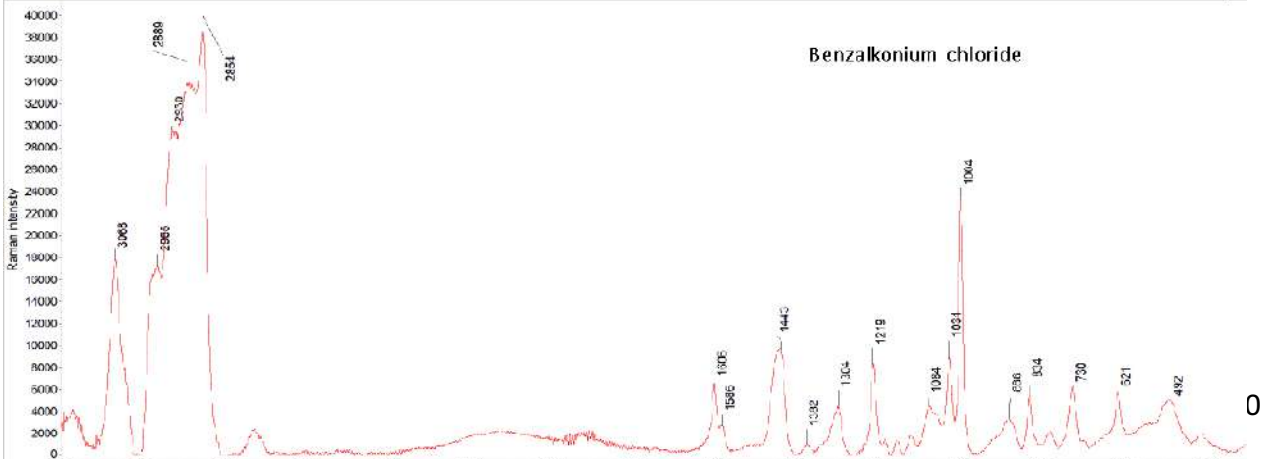

0

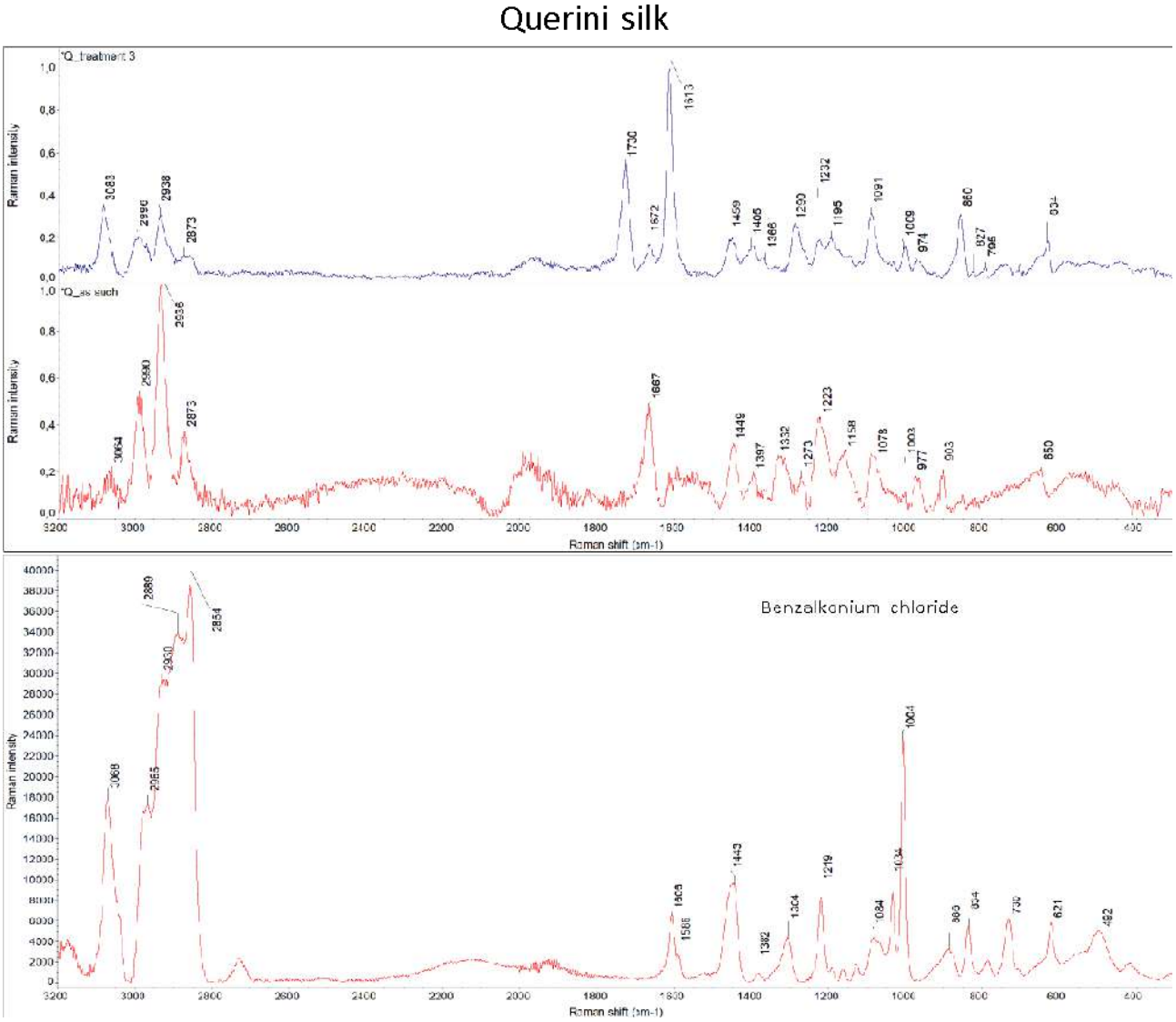

Figure 28: Raman spectra of Querini and Finzi silk before and after treatment 3, compared with Raman spectrum of benzalkonium chloride

3.2.4.2.3 IMMERSION IN DEIONIZED WATER (treatment 4)

Results from Raman spectra analyses of samples immersed in deionized water for 24 hours are presented in table 40.

Table 40: Variation of Raman characteristic peaks for silk after treatment 4

Raman		After treatment		
cm^-1	**Peak attribution**	**White silk**	**Finzi silk**	**Querini silk**
622	Phenylalanine	*unvaried*	*unvaried*	noisy broad absorption between 600 and 300 cm^{-1}
645-54	Tyrosine ring-breathing mode	*unvaried*	*unvaried*	*unvaried*
760	Tryptophan	*unvaried*	*unvaried*	*unvaried*
830	Tyrosine (bending of ring)	*unvaried*	*unvaried*	*unvaried*
855	Tyrosine (bending of ring)	*unvaried*	*unvaried*	*unvaried*
885	CC skeletal stretch, Tryptophan	increase in intensity	*unvaried*	*unvaried*
900-960	skeletal mode	*unvaried*	*unvaried*	*unvaried*
979	CC skeletal stretch	*unvaried*	*unvaried*	*unvaried*
1004	COC stretching vibration of tryptophan ring and phenyl ring of phenylalanine	increase in intensity	*unvaried*	*unvaried*
-	-	weak signal at 1036 cm^{-1}	-	-
1087	CN stretch	slight increase in intensity	*unvaried*	*unvaried*
1159	CN stretch	*unvaried*	*unvaried*	*unvaried*
1232	Amide III in β sheet conformation (bending)	*unvaried*	*unvaried*	original peak at 1226 shows now to absorptions at 1236-1212 cm^{-1}
1269	Amide III in β sheet conformation and disordered (bending)	*unvaried*	*unvaried*	*unvaried*
1308	CH bend	*unvaried*	*unvaried*	*unvaried*
1337	CH bend, Phenylalanine	*unvaried*	*unvaried*	*unvaried*
-	-	-	-	noisy broad band between 1400 and 950 cm^{-1}
1449	CH_2, CH_3 bending modes	*unvaried*	*unvaried*	*unvaried*
1585	Phenylalanine	*unvaried*	*unvaried*	*unvaried*
1605	Phenylalanine	*unvaried*	*unvaried*	*unvaried*
1616	Tryosine, Tryptophane	*unvaried*	*unvaried*	*unvaried*
1668	Amide I in β sheet conformation (stretching)	*unvaried*	*unvaried*	*unvaried*
1675	Amide I	*unvaried*	*unvaried*	*unvaried*
-	-	-	-	noisy broad band between 2100 and 1800 cm^{-1}
2875	CH_3 symmetrical stretch	*unvaried*	*unvaried*	*unvaried*
2934	CH_3 stretch asymmetrical	*unvaried*	*unvaried*	*unvaried*
3063	CNH bend overtone	*unvaried*	*unvaried*	*unvaried*
3286	NH stretch	*unvaried*	*unvaried*	*unvaried*

White samples showed minor variations such as a slight intensity increase for the peaks at 1086 cm^{-1}, 1036 cm^{-1}, 1006 cm^{-1} (phenylalanine) and 880 cm^{-1}(tryptophan), while Finzi silk did not show specific variation after treatment. Relative intensity variations can be considered either related to water absorption or to an effect caused by the point analysis.

A different behaviour, instead, is shown by Querini silk sample. After-treatment the spectrum results, in fact, extremely noisy, and in three regions (2100-1800 cm^{-1}, 1400-950 cm^{-1} and 600-300 cm^{-1})a broad band appears. These absorptions appear to correspond to water signals, indicating water absorption in the sample. Moreover, the amide III signal at 1226 cm^{-1} gets replaced by a double peak (1236-1212 cm^{-1}); this variation may, also, be related to the presence of water on sample.

3.2.4.2.4 IMMERSION IN ETHANOL WITH DIFFERENT CONCENTRATIONS (treatments 5-9)

Table 41 reports a comparison of RAMAN spectra for B, F and Q samples collected before and after treatments with ethanol solutions. To verify the effects of pure and diluted alcohol, immersion tests were conducted both with pure ethanol and with ethanol/water blends at different concentrations (50%, 70%, 75%, 79%).

Raman spectra for white silk present several differences after treatment 7 (immersion n 70% EtOH). First, two broad bands are present in the treated sample's spectra in the regions between 2400-2000 cm^{-1} and 600-400 cm^{-1}. Second, several peaks show a significant increase in intensity, slightly modifying their shape. In particular this refers to peaks at 1338 cm^{-1} (phenylalanine), 1297 cm^{-1} (CH bend), 1230 cm^{-1} (amide III), 1171 cm^{-1} and 1093 cm^{-1} (CN stretch), 1004 cm^{-1} (phenylalanine, tryptophan), 970 cm^{-1} (CC skeletal stretch).

A similar behaviour is observed for Finzi silk treated with 70% EtOH solution; two broad absorptions at 2400-2200 cm^{-1} and at 600-400 cm^{-1} are present, while several peaks in the region between 1700-800 cm^{-1} increase their intensity. In particular, together with the increase of 1669 cm^{-1}(amide III), 1598 cm^{-1}(phenylalanine), 1273 cm^{-1} (amide III), 1234 cm^{-1} (amide III), 1169 cm^{-1} (CN stretch), 1089 cm^{-1}(CN stretch), 1003 cm^{-1} (phenylalanine, tryptophan), 974 cm^{-1} (CC skeletal stretch) 881 cm^{-1} (tryptophan) peaks, the signals at 1515 cm^{-1} and 1496 cm^{-1} (CH region) are no longer detectable. These signal are likely ascribable to colourant (which appeared to fade, justifying a decrease in signal); the region presents, in fact, characteristic signals typical of several organic dyes. Moreover, the three characteristics peak of silk in the 1400-1200 cm^{-1} region (CH

bending, Amide III) result in a single large shoulder for the treated sample. Few of these variations (specifically the peaks at 1669-1598-1310 cm^{-1}) were the same detected for treatment 3 and attributed to silk dye.

Querini silk, on the contrary, does present a similar behaviour for all the treated samples. Besides some negligible intensity variations (peaks at 1994 cm^{-1} – ascribable to colour or incoherent deposits- and at 1613 cm^{-1} slightly increase for treatment 5; peak at 1091 cm^{-1} slightly increases for treatment 7), no significant changes appear to occur after immersion on these silks in ethanol.

Table 41: Variation of Raman characteristic peaks for silk after treatments 5-9

Raman		treatment 5			treatment 6			treatment 7			treatment 8	treatment 9
cm^-1	peak attribution	B	F	Q	B	F	Q	B	F	Q	all samples	all samples
		unvaried	*unvaried*	*unvaried*	*unvaried*	*unvaried*	*unvaried*	broad band in the 600-400 cm^{-1} region		*unvaried*	*unvaried*	*unvaried*
622	Phenylalanine	*unvaried*	*unvaried*	*unvaried*	*unvaried*	*unvaried*	*unvaried*	*unvaried*	*unvaried*	*unvaried*	*unvaried*	*unvaried*
645-54	Tyrosine ring-breathing mode	*unvaried*	*unvaried*	*unvaried*	*unvaried*	*unvaried*	*unvaried*	*unvaried*	*unvaried*	*unvaried*	*unvaried*	*unvaried*
760	Tryptophan	*unvaried*	*unvaried*	*unvaried*	*unvaried*	*unvaried*	*unvaried*	*unvaried*	*unvaried*	*unvaried*	*unvaried*	*unvaried*
830	Tyrosine (bending of ring)	*unvaried*	*unvaried*	*unvaried*	*unvaried*	*unvaried*	*unvaried*	*unvaried*	*unvaried*	*unvaried*	*unvaried*	*unvaried*
855	Tyrosine (bending of ring)	*unvaried*	*unvaried*	*unvaried*	*unvaried*	*unvaried*	*unvaried*	*unvaried*	*unvaried*	*unvaried*	*unvaried*	*unvaried*
885	CC skeletal stretch, Tryptophan	*unvaried*	*unvaried*	*unvaried*	*unvaried*	*unvaried*	*unvaried*	*unvaried*	increase in intensity	*unvaried*	*unvaried*	*unvaried*
900-960	skeletal mode	*unvaried*	*unvaried*	*unvaried*	*unvaried*	*unvaried*	*unvaried*	*unvaried*	*unvaried*	*unvaried*	*unvaried*	*unvaried*
979	CC skeletal stretch	*unvaried*	*unvaried*	*unvaried*	*unvaried*	*unvaried*	*unvaried*	increase in intensity (peak shifted to 970 cm^{-1})	increase in intensity	*unvaried*	*unvaried*	*unvaried*
1004	COC stretching vibration of tryptophan ring and phenyl ring of phenylalanine	*unvaried*	*unvaried*	*unvaried*	*unvaried*	*unvaried*	*unvaried*	increase in intensity	increase in intensity	*unvaried*	*unvaried*	*unvaried*
1087	CN stretch	*unvaried*	*unvaried*	*unvaried*	*unvaried*	*unvaried*	*unvaried*	increase in intensity (peak shifted to 1093 cm^{-1})	increase in intensity	slight increase in intensity	*unvaried*	*unvaried*
1159	CN stretch	*unvaried*	*unvaried*	*unvaried*	*unvaried*	*unvaried*	*unvaried*	increase in intensity (peak shifted to 1171 cm^{-1})	increase in intensity (peak shifed to 1169 cm^{-1})	*unvaried*	*unvaried*	*unvaried*
1232	Amide III in β sheet conformation (bending)	*unvaried*	*unvaried*	*unvaried*	*unvaried*	*unvaried*	*unvaried*	increase in intensity	increase in intensity	*unvaried*	*unvaried*	*unvaried*

Raman		treatment 5			treatment 6			treatment 7			treatment 8	treatment 9
cm^-1	peak attribution	B	F	Q	B	F	Q	B	F	Q	all samples	all samples
1269	Amide III in β sheet conformation and disordered (bending)	*unvaried*	*unvaried*	*unvaried*	*unvaried*	*unvaried*	*unvaried*	*unvaried*	increase in intensity (peak shifted to 1273 cm^{-1})	*unvaried*	*unvaried*	*unvaried*
1308	CH bend	*unvaried*	*unvaried*	*unvaried*	*unvaried*	*unvaried*	*unvaried*	increase in intensity (peak shifted to 1297 cm^{-1})	*unvaried*	*unvaried*	*unvaried*	*unvaried*
1337	CH bend, Phenylalanine	*unvaried*	*unvaried*	*unvaried*	*unvaried*	*unvaried*	*unvaried*	increase in intensity	*unvaried*	*unvaried*	*unvaried*	*unvaried*
1449	CH_2, CH_3 bending modes	*unvaried*	*unvaried*	*unvaried*	*unvaried*	*unvaried*	*unvaried*	*unvaried*	*unvaried*	*unvaried*	*unvaried*	*unvaried*
1585	Phenylalanine	*unvaried*	*unvaried*	*unvaried*	*unvaried*	*unvaried*	*unvaried*	*unvaried*	increase in intensity (peak shifted to 1598 cm^{-1})	*unvaried*	*unvaried*	*unvaried*
1605	Phenylalanine	*unvaried*	*unvaried*	*unvaried*	*unvaried*	*unvaried*	*unvaried*	*unvaried*	*unvaried*	*unvaried*	*unvaried*	*unvaried*
1616	Tryosine, Tryptophane	*unvaried*	*unvaried*	slight increase in intensity	*unvaried*	*unvaried*	*unvaried*	*unvaried*	*unvaried*	*unvaried*	*unvaried*	*unvaried*
1668	Amide I in β sheet conformation (stretching)	*unvaried*	*unvaried*	*unvaried*	*unvaried*	*unvaried*	*unvaried*	*unvaried*	increase in intensity	*unvaried*	*unvaried*	*unvaried*
1675	Amide I	*unvaried*	*unvaried*	*unvaried*	*unvaried*	*unvaried*	*unvaried*	*unvaried*		*unvaried*	*unvaried*	*unvaried*
		unvaried	*unvaried*	*unvaried*	*unvaried*	*unvaried*	*unvaried*	broad band in the 2400-2000 cm^{-1} region		*unvaried*	*unvaried*	*unvaried*
2875	CH_3 symmetrical stretch	*unvaried*	*unvaried*	*unvaried*	*unvaried*	*unvaried*	*unvaried*	*unvaried*	*unvaried*	*unvaried*	*unvaried*	*unvaried*
2934	CH_3 stretch asymmetrical	*unvaried*	*unvaried*	*unvaried*	*unvaried*	*unvaried*	*unvaried*	*unvaried*	*unvaried*	*unvaried*	*unvaried*	*unvaried*
3063	CNH bend overtone	*unvaried*	*unvaried*	*unvaried*	*unvaried*	*unvaried*	*unvaried*	*unvaried*	*unvaried*	*unvaried*	*unvaried*	*unvaried*
3286	NH stretch	*unvaried*	*unvaried*	*unvaried*	*unvaried*	*unvaried*	*unvaried*	*unvaried*	*unvaried*	*unvaried*	*unvaried*	*unvaried*

3.2.4.2.5 IMMERSION IN BENZALKONIUM CHLORIDE (treatment 10)

Immersion in benzalkonium chloride, as mentioned before, caused the deposition of the product on the sample surface. All samples presented a benzalkonium chloride sticky layer, whose presence is clearly detectable in the Raman spectra of the treated silk, as presented in table 42.

Despite the noisy signal, benzalkonium chloride can be detected on white silk thank to the intense shoulder between 1900 cm^{-1} and 1800 cm^{-1}, the broad band in the 2000-2400 cm^{-1} region and the strong peaks at 1445 cm^{-1}, 1219 cm^{-1}, 1310 $cm^{-1}$and 1005 cm^{-1}.

Raman spectra of both Finzi and Querini treated samples have a great resemblance with benzalkonium chloride spectra, and almost do not present silk characteristic peaks. These phenomena can clearly be explained by the fact that most likely no significant chemical interaction occurred between sample and treating solution, which only deposited on the surface of silk.

Table 42: Variation of Raman characteristic peaks for silk after treatment 10

Raman		
cm^{-1}	**Peak attribution**	**Treated silks**
622	Phenylalanine	*unvaried*
645-54	Tyrosine ring-breathing mode	*unvaried*
760	Tryptophan	*unvaried*
830	Tyrosine (bending of ring)	*unvaried*
855	Tyrosine (bending of ring)	*unvaried*
885	CC skeletal stretch, Tryptophan	*unvaried*
900-960	skeletal mode	*unvaried*
979	CC skeletal stretch	*unvaried*
1004	COC stretching vibration of tryptophan ring and phenyl ring of phenylalanine	increase in intensity
1087	CN stretch	*unvaried*
1159	CN stretch	*unvaried*
1232	Amide III in β sheet conformation (bending)	increase in intensity (peak shifted to 1219cm^{-1})
1269	Amide III in β sheet conformation and disordered (bending)	*unvaried*
1308	CH bend	increase in intensity
1337	CH bend, Phenylalanine	*unvaried*
1449	CH_2, CH_3 bending modes	increase in intensity
1585	Phenylalanine	*unvaried*
1605	Phenylalanine	*unvaried*
1616	Tryosine, Tryptophane	*unvaried*

1668	Amide I in β sheet conformation (stretching)	*unvaried*
1675	Amide I	*unvaried*
-	-	shoulder at 1900-1800 cm^{-1}
-	-	broad absorption between 2400 and 2000 cm^{-1}
2875	CH_3 symmetrical stretch	*unvaried*
2934	CH_3 stretch asymmetrical	*unvaried*
3063	CNH bend overtone	*unvaried*
3286	NH stretch	*unvaried*

3.2.4.2.6 EXPOSURE TO CONTROLLED HUMIDITY ENVIRONMENT (treatment 11)

UNTREATED SAMPLES

For untreated samples, no significant differences can be observed neither in white nor in Finzi silk. Querini silk instead presented some differences mainly related to the increase of peaks' intensity after exposure to controlled RH%.

TREATMENT 3

No significant variations can be spot between the two versions of white and Finzi silk treated with sanitising solution.

Some variation occurred, instead, on Querini sample. It is interesting to note that the spectrum of treated silk after exposure to controlled RH presents mainly benzalkonium chloride signals, instead of silk characteristic peaks. This is most likely because, as seen during optical observation, benzalkonium crystallized on sample's surface.

TREATMENT 5

From the observation of the acquired spectra no significant variation seemed to occur, except for Querini silk, whose noisy spectra suggests that probably some interactions between the sample or its incoherent deposits and moisture occurred. The spectra, in fact, has a consistent resemblance with the one collected for Querini silk after treatment 4 (immersion in deionized water).

Results of Raman analyses conducted on Querini silk treated with sanitising solution, ethanol and benzalkonium chloride and then exposed to treatment 11 are here compared with spectra of untreated silk (table 43).

Table 43: Variation of Raman characteristic peaks for Querini silk after treatment 11

Querini silk				
Raman characteristic silk signals		**After RH exposure**		
cm^-1	**Peak attribution**	**treatment 3**	**treatment 5**	**treatment 10**
-	-	new peak at 475 cm^{-1}	noisy broad band between 600 and 300 cm^{-1}	noisy broad band between 600 and 300 cm^{-1}
622	Phenylalanine	*unvaried*	*unvaried*	*unvaried*
645-54	Tyrosine ring-breathing mode	undetectable	*unvaried*	*unvaried*
760	Tryptophan	undetectable	*unvaried*	*unvaried*
830	Tyrosine (bending of ring)	undetectable	*unvaried*	*unvaried*
855	Tyrosine (bending of ring)	undetectable	*unvaried*	*unvaried*
885	CC skeletal stretch, Tryptophan	undetectable	*unvaried*	*unvaried*
900-960	skeletal mode	undetectable	noisy broad band between 1400 and 950 cm^{-1}	*unvaried*
979	CC skeletal stretch	strong peak		*unvaried*
1004	COC stretching vibration of tryptophan ring and phenyl ring of phenylalanine	undetectable		noisy broad band between 1400 and 1000 cm^{-1}
1087	CN stretch	undetectable		
1159	CN stretch	undetectable		
1232	Amide III in β sheet conformation (bending)	peak at 1223 cm^{-1}		
1269	Amide III in β sheet conformation and disordered (bending)	undetectable		
1308	CH bend	undetectable		
1337	CH bend, Phenylalanine	undetectable		
1449	CH_2, CH_3 bending modes	peak at 1459 cm^{-1}		
1585	Phenylalanine	undetectable	*unvaried*	*unvaried*
1605	Phenylalanine	noisy broad band between 2000 and 1600 cm^{-1}	*unvaried*	noisy broad band between 2100 and 1800 cm^{-1}
1616	Tryosine, Tryptophane		*unvaried*	
1668	Amide I in β sheet conformation (stretching)		*unvaried*	
1675	Amide I		*unvaried*	
-	-	-	noisy broad band between 2100 and 1800	

Querini silk				
Raman characteristic silk signals		**After RH exposure**		
cm^-1	**Peak attribution**	**treatment 3**	**treatment 5**	**treatment 10**
			cm^{-1}	
-	-	-	*unvaried*	noisy broad band between 2500 and 2000 cm-1
-	-	benzalkonium peak at 2854 cm^{-1}	-	benzalkonium peak at 2845 cm^{-1}
2875	CH_3 symmetrical stretch	undetectable	*unvaried*	*unvaried*
2934	CH_3 stretch asymmetrical	*unvaried*	*unvaried*	*unvaried*
3063	CNH bend overtone	noisy region	*unvaried*	v
-	-		*unvaried*	benzalkonium signal at 3044 cm^{-1}
3286	NH stretch		*unvaried*	*unvaried*

TREATMENT 10

Spectra of samples immersed in benzalkonium chloride showed different responses to treatment 11. As shown in table 44, Finzi silk appears almost unchanged after exposure to controlled RH environment. White and Querini silk, instead, present extremely noisy and altered spectra. For both samples some absorptions resemble those of the same sample before treatment 11, but not all the characteristic bands can be detected, and many regions show broad absorptions hard to interpret. Figure 29 reports a comparison of white silk spectra as reference.

Table 44: Variation of Raman characteristic peaks for silk treated with benzalkonium chloride after exposure to elevated humidity levels

White silk		
cm^{-1}	**Raman Peak attribution for silk**	**treated silk – treatment 10**
622	Phenylalanine	shoulder between 600 and 400 cm^{-1}
645-54	Tyrosine ring-breathing mode	
760	Tryptophan	*unvaried*
830	Tyrosine (bending of ring)	*unvaried*
855	Tyrosine (bending of ring)	noisy shoulder between 1050 and 850 cm^{-1}
885	CC skeletal stretch, Tryptophan	
900-960	skeletal mode	
979	CC skeletal stretch	

White silk		
cm^{-1}	**Raman Peak attribution for silk**	**treated silk – treatment 10**
1004	COC stretching vibration of tryptophan ring and phenyl ring of phenylalanine	
1087	CN stretch	noisy shoulder between 1300 and 1100 cm^{-1}
1159	CN stretch	
1232	Amide III in β sheet conformation (bending)	
1269	Amide III in β sheet conformation and disordered (bending)	
1308	CH bend	
1337	CH bend, Phenylalanine	
1449	CH_2, CH_3 bending modes	*unvaried*
1585	Phenylalanine	undetectable
1605	Phenylalanine	undetectable
1616	Tryosine, Tryptophane	undetectable
1668	Amide I in β sheet conformation (stretching)	undetectable
1675	Amide I	*unvaried*
-	-	broad band between 2500 and 1900 cm^{-1}
-	-	noisy region between 3200 and 2500 cm^{-1}
2875	CH_3 symmetrical stretch	
2934	CH_3 stretch asymmetrical	
3063	CNH bend overtone	
3286	NH stretch	

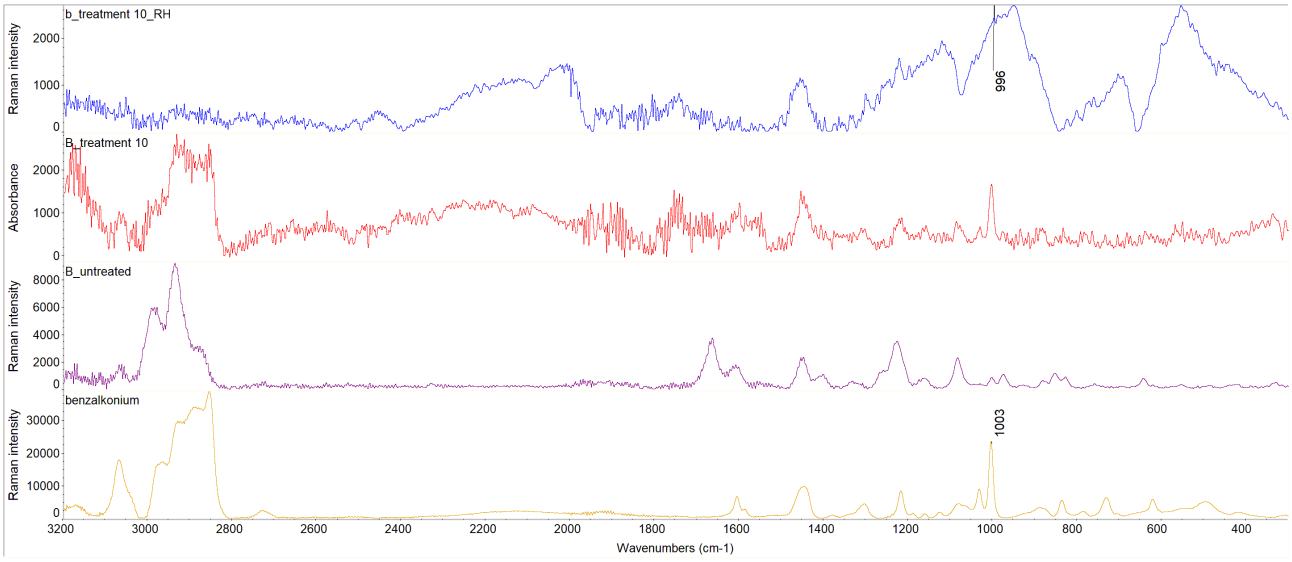

Figure 29: comparison of three white silk Raman spectra (untreated, after treatment 10 and after treatment 11) and Raman spectra of benzalkonium chloride

All these things considered, few conclusions can be made.

First, that, once again, the presence of benzalkonium chloride on samples' surface after treatment 3 was demonstrated. Second, that water treatment (t4) for Querini silk provided some indications of occurred chemical variations. The simplest explication for these observation is, however, related to the interaction between deposits on silk surface and water.

Ethanol treatments, instead, confirmed the hypothesis that the joint effect of water and ethanol (within a certain range of concentration) causes more effects than the single blend's components taken alone.

In the end, benzalkonium chloride was confirmed to deposit on sample surface without chemically interacting with it.

3.2.5 CRISTALLINITY EVALUATION

Crystallinity degree of two representative samples was evaluated via X-Ray Diffraction analysis. The analyses were performed both before and after treatment 3 (immersion in sanitising solution for 24 hours) in order to understand possible variation in crystallinity, as described at paragraph 2.1.2.3.6.

Figure 30 reports XRD diffraction pattern for white silk. Amorphous peaks at 28,2^{o} and 24,7^{o} seem to show no consistent variations, while crystalline peaks at 20,7^{o} and 8,8^{o} present some peculiar differences. Both peaks appear slightly shifted towards smaller angles for the treated samples. Moreover, the region between 15^{o} and 5^{o} shows higher intensity if compared to the untreated sample. The interpretation of this last observation is quite challenging, for the 20,7^{o} peak is, in fact a multi peak [51], containing both the amorphous peak at 19,7^{o} and the crystalline one at 18,9^{o}. Considerations can be made on the fact that for the treated sample, crystalline peak at 8,8^{o} significantly increased its intensity, meaning that a greater amount of detectable crystalline component is present after treatment 3. However, this increase does not correspond to a decrease in amorphous peaks (which would be an indicator of degradation of amorphous regions).

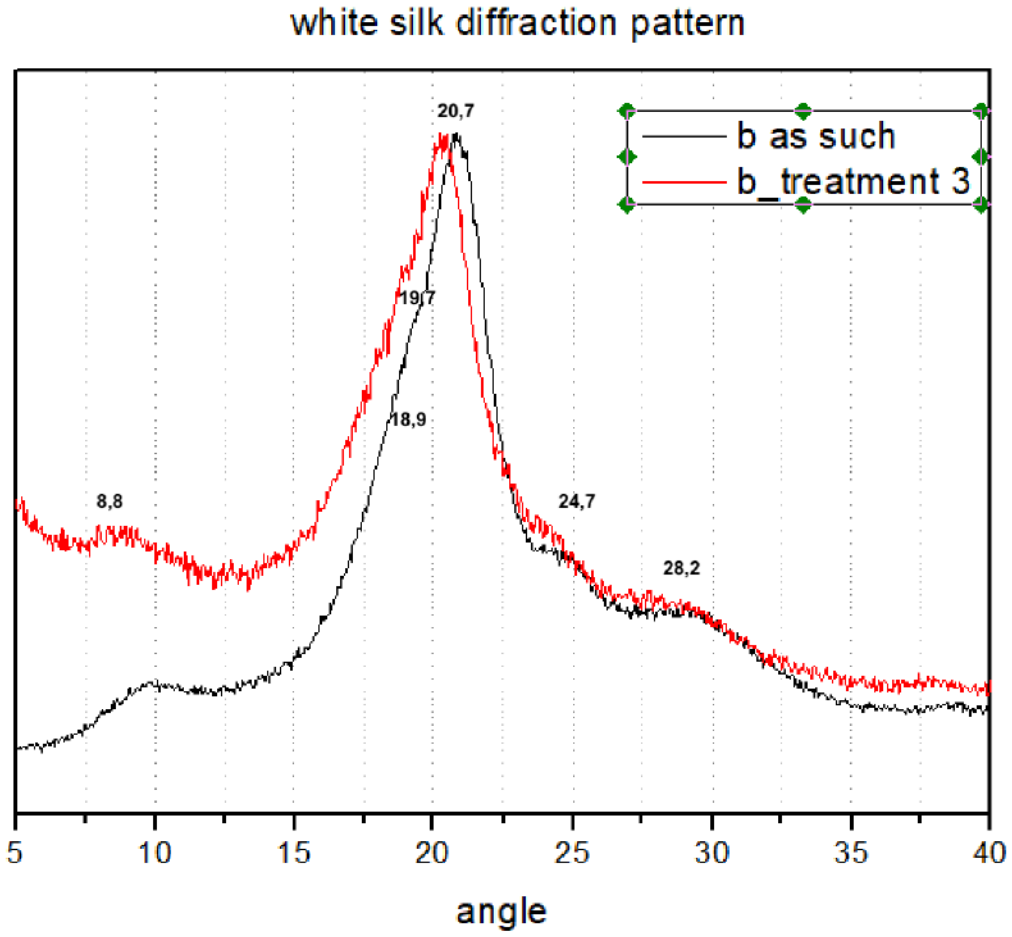

Figure 30: White silk diffraction pattern

Figure 31 shows the diffraction pattern of red velvet before and after treatment 3. The signal, as can be noticed, was extremely noisy, probably due to the heterogeneous sample structure and waving morphology. Therefore, very few considerations can be made upon these results. The first aspect is that these diffraction patterns differ greatly from the white silk ones. Crystalline peak at 8,8° can barely be detected due to the extremely noisy patter. Moreover, the region between 18,9° and 20,7° shows more legible signals for the untreated silk, while the treated Finzi silk does not present significant signals. The presence of an amorphous peak, reported in literature at 24,7°, is here shifted to higher angle values, and has a sharp and intense feature. In the end, amorphous peak at 28,2° is completely covered by the noise

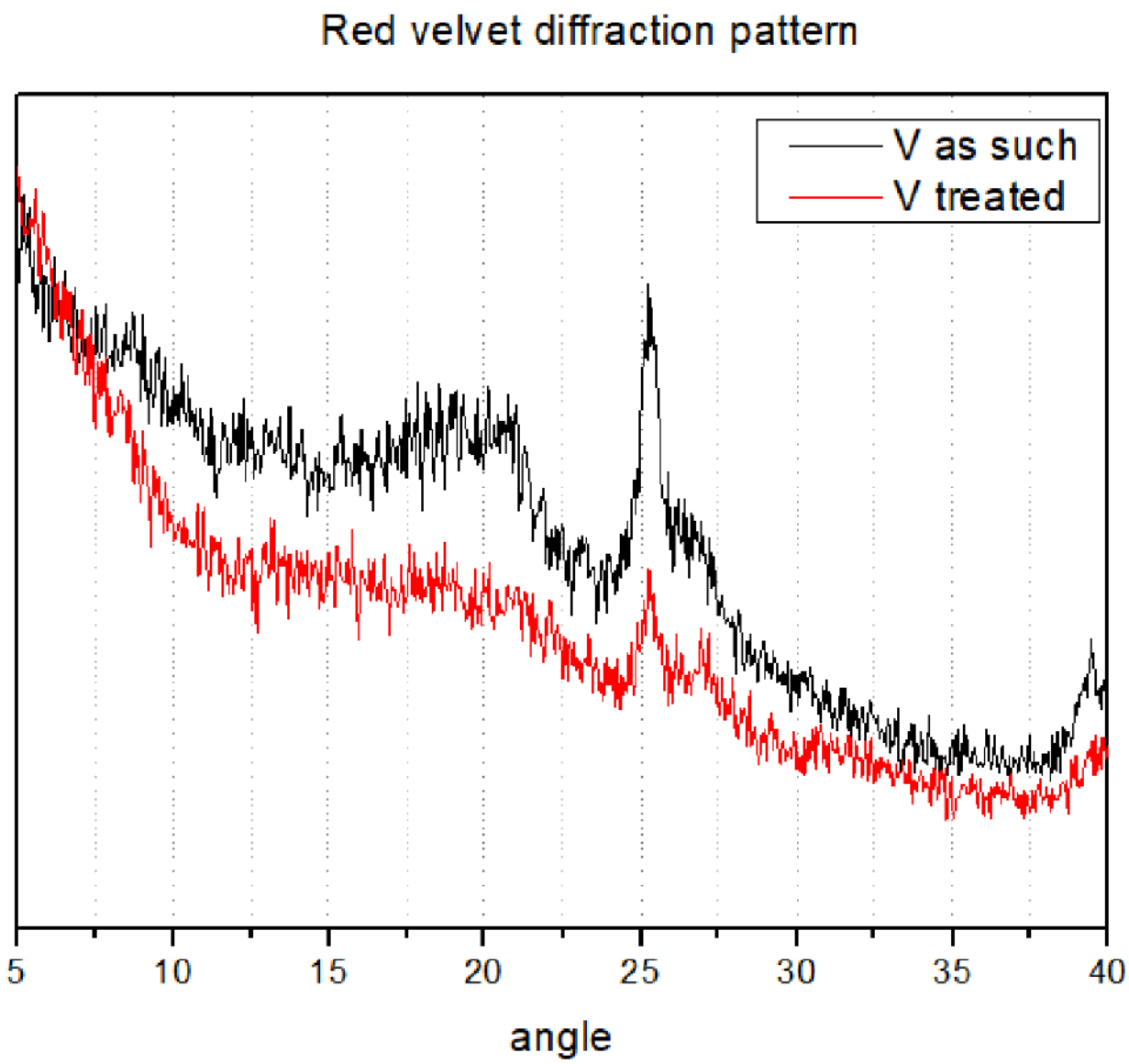

Figure 31: Red velvet diffraction pattern

From these results, few considerations can be made.

XRD analyses revealed a great difference in crystallinity features for the untreated white and red velvet, which lead also to different responses of the samples after treatment 3. These contrasting responses for the two samples analysed are due to the consistently different structure and weaving of white silk and red velvet.

Given this premise, between treated and untreated samples some variations can be observed. White sample, which allows easier peak attribution, presents several peak shifts. These variations can possibly be ascribed to internal structural variation. ATR analyses, however, did not present enough evidence to support and define this hypothesis. We can therefore conclude that no remarkable

variations occurred under the crystalline point of view. To give a possible explanation to the results obtained, further investigations are required.

3.2.6 WETTABILITY

Wettability was measured on samples one week after treatment.

Measures were then repeated after one month, and their results are reported in the following paragraphs. These latter results appear to be slightly different from those collected one week after the treatment, when samples were probably not completely dry yet.

It should be considered, however, that contact angle measurements highly depend on sample's (e.g. humidity absorbed) and measurements conditions. These values, therefore, should be considered as indicative.

3.2.6.1.1 EXPOSURE TO SANITISING SOLUTION VAPOUR (treatment 1)

Wettability variation for samples treated with vapour exposure was evaluated for all samples. An explicative detail for B (Bevilacqua), F (Finzi) and Q (Querini) samples is reported in table 45. All samples show a relative decrease in their contact angle value, ranging from -5,7^{o} to almost -11^{o}.

From this observation, two main conclusions can be drawn. First, contact angle variation is an indicator of the occurrence of some variation after treatment. Second, the decrease of contact angle value corresponds to the increase in wettability for treated samples, resulting in a variation of a property which may affect silk conservation [30]. Increase in wettability, in fact, may lead to further chemical degradation processes in humid conditions, and to mechanical properties modification related to humidity variations.

Table 45: contact angle variation after treatment 1

SAMPLE	α0	α24h	Δα
B	53,4	42,5	-10,9
F	53,3	46,4	-6,9
Q	54,3	48,7	-5,6

3.2.6.1.2 IMMERSION IN SANITISING SOLUTION (treatments 2 and 3)

As reported in table 46, wettability underwent a consistent variation after treatment with the sanitising solution (75% ethanol, 20% water, 5% benzalkonium chloride). For all the samples, in fact, it was not possible to measure the contact angle after treatment. This behaviour can be explained by the presence of benzalkonium chloride in the sanitising solution. Benzalkonium may wither have directly affected the wettability, by interacting with the water drop (benzalkonium chloride, in fact, is known to be a surfactant) or by altering the properties of silk.

Table 46: contact angle variation after treatment 2 and 3

SAMPLE	α0	α30min	α24h
B	53,4	not measurable	not measurable
G	53,3	not measurable	not measurable
F	54,3	not measurable	not measurable

3.2.6.1.3 IMMERSION IN DEIONIZED WATER (treatment 4)

Table 47 shows the contact angle variation for samples treated with deionized water. All samples presented decreasing values of the contact angle.

These variations might be related to the minor chemical variations observed in Raman analyses and related probably to water absorption. Moreover, as in the case of Querini silk, it can be supposed that the immersion in water had the effect of removing part of the dust or incoherent material there deposited, with the resulting effect of surface roughness variation and thus wettability modification.

Table 47: contact angle variation after treatment 4

SAMPLE	α0	α24h	Δα
B	53,4	42,9	-10,5
F	53,3	45,3	-8
Q	54,3	43,8	-10,5

3.2.6.1.4 IMMERSION IN PURE ETHANOL (treatment 5)

Table 48 shows the results of the wettability evaluation for the samples immersed in pure ethanol for 24 hours. In this case as for treatment 4 (immersion in deionised water), all samples showed a similar behaviour, with a decrease of their contact angle, ranging from -4,7 degrees for Finzi silk to -12,9 degrees for Querini silk. This is an indicator of a similar behaviour between all types of silk and

ethanol. As hypothesized above, alcohol may interact with the protein peptide planar bonds, thus probably modifying silk characteristic wettability.

Table 48: contact angle variation after treatment 5

SAMPLE	α0	α24h	Δα
B	53,4	48,05	-5,4
F	53,3	48,63	-4,7
Q	54,3	41,4	-12,9

3.2.6.1.5 IMMERSION IN WATER/ETHANOL BLEND (treatments 6-9)

Table 49 shows the results of wettability evaluation for samples which underwent treatments 6-9 (immersion in ethanol in water at 50%, 70%, 75% and 79%). For all the samples the value of contact angle moderately decreased after each treatment.

A possible correlation between ethanol concentration and contact angle variation may be supposed. Treatment 8 (immersion in 75% EtOH) appears to be the most affecting one, while t7 (immersion in EtOH 70%) and t9 (immersion in EtOH 79%) appear to lead to similar results. Treatment 6, instead, probably due to the higher presence of water, shows different behaviour: Querini silk appears to be the less affected sample, while both white and Finzi silk show a similar contact angle decrease. Also, while pure water leads to more significant variations than those observed with t6, pure alcohol effect is less consistent than diluted alcohol between 70% and 90%.

This observation leads to the conclusion that different alcohol/water concentrations have different effects, and that around 70-75% we can observe a maximization of these effects. Tthis observation matches with Raman results, which show some sign of ethanol/water blend interaction with silk.

Table 49: contact angle variation after treatments 6-9

EtOH50%			
SAMPLE	**α0**	**α24h**	**Δα**
B	53,4	45,7	-7,7
F	53,3	44,6	-8,7
Q	54,3	50,3	-4,1
EtOH 70%			
SAMPLE	**α0**	**α24h**	**Δα**
B	53,4	37,7	-15,7
F	53,3	49,3	-4,0
Q	54,3	45,5	-8,8

EtOH 75%			
SAMPLE	**α0**	**α24h**	**Δα**
B	53,4	34,2	-19,2
F	53,3	41,9	-11,4
Q	54,3	39,9	-14,4
EtOH79%			
SAMPLE	**α0**	**α24h**	**Δα**
B	53,4	39,4	-14,0
F	53,3	48,5	-4,8
Q	54,3	44,0	-10,3

3.2.6.1.6 IMMERSION IN BENZALKONIUM CHLORIDE

Table 50 presents a comparison of contact angle values for silk before and after treatment with benzalkonium chloride. All different types of sample significantly increased their wettability, showing a consistent decrease in the associate contact angle. However, differently from what observed for t2 and t3, the angle is here still measurable despite the decreasing values.

This can be most likely explained by the fact that in the first case the three components of the sanitising solution (water, ethanol and benzalkonium chloride) can perform a synergic action thus altering the wettability of silk sample. In this case, instead, benzalkonium deposited uniformly on samples, thus altering with its presence the contact angle value.

The increase of wettability, however, was almost inversely proportional to the weight gain (after the treatment) due to benzalkonium chloride deposition. In order to better compare the obtained results, table 12 is here reported once again. White silk, the sample with less contact angle variation, is in fact the sample that resulted to increase its weight the most (+376%). Finzi silk, whose weight increase was quite limited ("only" +84%) was subject to a consistent increase in wettability (-35,7^{o}). In the end, Querini silk, whose weight increase was almost as much as white silk one, presented an intermediate wettability increase (-27,4^{o}). It is also interesting to notice that in the case of treatment 3 (immersion in sanitising solution), where the amount of benzalkonium chloride was contained, samples increased so much their wettability after treatments that it was no longer possible to measure the contact angle on their surface. It could be therefore concluded that the increase in wettability is here related to the presence of benzalkonium chloride with an inversely proportional relationship. In order to confirm this hypothesis, further investigations are needed.

Table 50: contact angle variation after treatment 10

SAMPLE	α0	α24h	Δα
B	53,4	31,6	-21,8
F	53,3	17,6	-35,7
Q	54,3	26,9	-27,4

Table12: weight variation for samples immersed in 50% benzaklonium chloride for 24 hours

sample	before treatment	wet 24 hours			dry (24h drying)			dry (1 month drying)		
	weight (g)	weight (g)	Δw (g)	Δw%	weight (g)	Δw (g)	Δw%	weight (g)	Δw (g)	Δw%
B_t10	0,1059	1,3183	1,2124	1145%	0,5038	0,3979	376%	0,4218	0,3159	298%
Q_t10	0,3509	3,3115	2,9606	844%	1,6608	1,3099	373%	0,8980	0,5471	156%
F_t10	0,5238	2,108	1,5842	302%	0,9651	0,4413	84%	1,5318	1,0080	192%

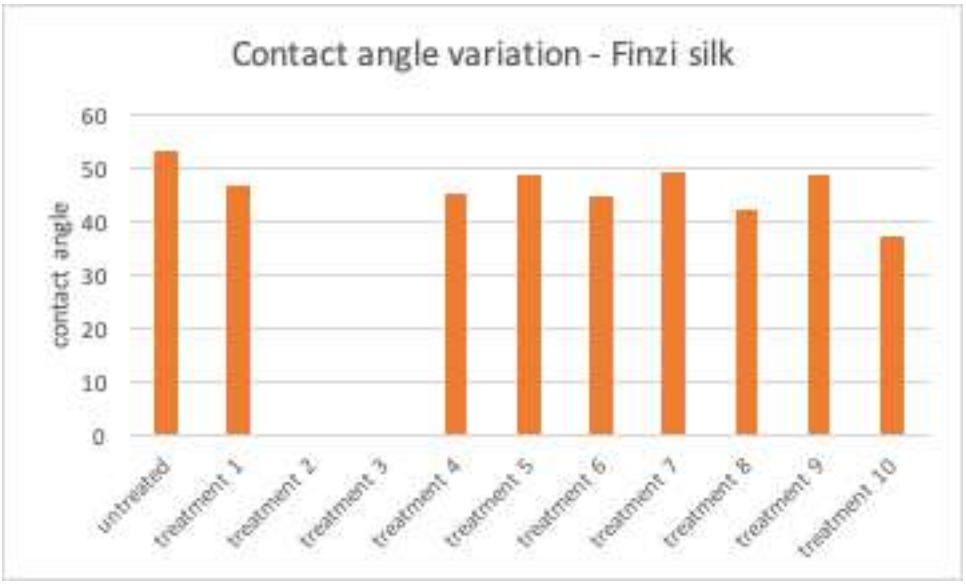

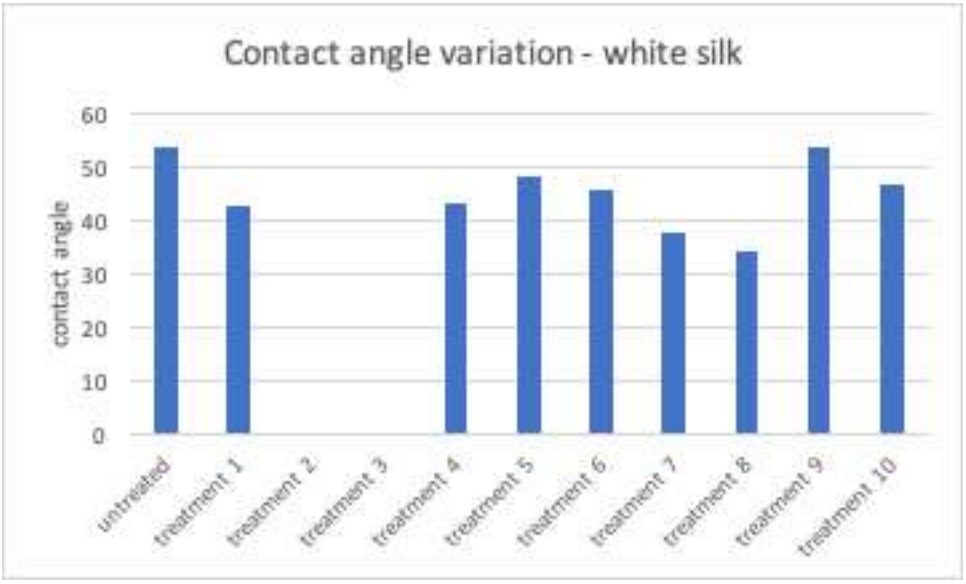

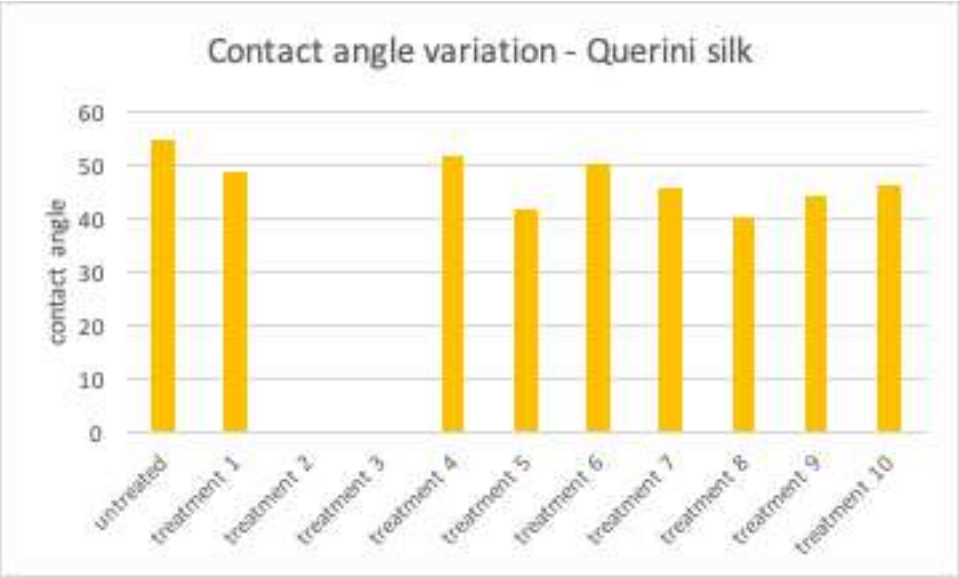

Figure 32: graphical representation of contact angle variation for each treatment

After the above-mentioned results, some conclusions can be drawn, also considering the observations that can be made on figure 32. Moderate wettability increase (contact angle decrease) was detected for all samples treated via vapour exposure or immersion in deionized water or pure ethanol. The effect of ethanol/water blend was, instead, quite significant, greatly increasing the wettability for all samples. Similarly, sanitising solution, also thank to the presence of benzalkonium chloride that acted as surfactant, increased samples' wettability so much that contact angle was no longer measurable after treatment.

In the end, benzalkonium chloride 50% treatment (treatment 10) greatly modified the wettability by depositing on sample surface, as noticed by optical observations.

Concluding, moderate wettability increasing values were detected for all samples treated via vapour exposure or immersion in deionized water or pure ethanol. The effect of ethanol/water blend was, instead, quite significant, greatly increasing the wettability for all samples. Similarly, the sanitising solution, also thank to the presence of benzalkonium chloride that acted as surfactant, increased samples' wettability so much that, after treatment, contact angle was no longer measurable. It can be therefore concluded that benzalkonium chloride presence, especially in a defined concentration range, can affect and probably accelerate silk degradation processed in particular in humid environments.

4. CONCLUSIONS

The present work aimed at studying the possible chemical and visual effects of COVID-19 sanitising treatments on Cultural Heritage artefacts. The focus of the study was put on silk, being this material widely diffused and yet extremely delicate.

Tests have been conducted to simulate possible interactions between sanitising products and silk samples: both vapour exposure and immersion tests were carried out with the aim of reproducing frequently repeated sanitisations' operations. MIBACT – Soprintendenza di Roma recommended sanitising solution (75% ethanol, 20% water, 5% benzalkonium chloride) was tested as reference sanitising product. To verify the effects of each single components, further tests have been conducted on the effects of water, ethanol, ethanol/water blends and benzalkonium chloride alone.

Portable non-invasive analyses have been conducted to investigate chemical, colour and morphological modifications, with the aim of testing a possible procedure to later perform in situ analyses of silk tapestries. These analyses were supported by weight and wettability variation monitoring, together with point analyses performed with SEM and AFM to investigate possible nanometric scale modifications.

Immersion in sanitising solution appeared to be the most impacting treatment, causing benzalkonium chloride to deposit on samples surface, thus modifying silk behaviour (e.g. wettability, water adsorption in humid conditions). Consistent colour fading was observed after immersion treatments in particular for the coloured silks; from the evaluation of single component's effects, it was possible to attribute this modification to the joint effect of ethanol and water.

Besides these observations, however, no significant chemical variations could be observed through spectroscopic analyses. All these things considered, it can be concluded that, from the chemical point of view, the employing of sanitising products does not significantly affect the composition of silk fibres.

Two considerations must, however, be made before considering the use of sanitising products as completely safe for cultural heritage. First, beside chemical investigations, further analyses should be performed to test the variation of mechanical properties after the simulated treatments. This investigation could be performed employing the dynamic mechanical analysis (DMA) technique. DMA

is, in fact, one of the most exploited techniques for mechanical properties evaluation of several materials, including silk [56].

Second, as reported above, consistent colour variations were observed after immersion treatments. This effect should not be underestimated: despite the fact that immersion tests have been performed to verify sanitising solution's effects under *extreme use conditions*, direct interaction between upholsteries and sanitising products is not so unlikely (accidental dripping, accidental spray directly on fabric). Considering the importance of the visual appearance for cultural heritage artefacts, a change in colour - especially if limited to a spot or partial area (e.g. where the solution was spilled or where the spray deposited) – should be considered a detrimental effect. Basing on this consideration, further investigations should also include aging tests (e.g. light) in order to assess how aging could affect the conservation of treated samples.

Therefore, despite the results obtained, it is paramount to perform sanitisations with extreme attention and only if and where they are believed to be necessary, in order to prevent negative consequences for heritage conservation.

5. ACKNOWLEDGMENTS

The present master thesis work was carried out with the support of several Venetian patrons and institutions, united by a common aim: to give their contribution to the present study, helping the development of scientific research on cultural heritage to try to find new solutions to a new problem.

This research, therefore, would not have been realized without the special support of the Fondazione Querini Stampalia (in the person of its Director, Dr Marigusta Lazzari), the Soprintendenza Archeologia Belle Arti e Paesaggio per il Comune di Venezia e Laguna, the renowned textile factories Bevilacqua La Masa and Rubelli (in the person of Dr M.Chiara Klinger Mazzarino), bul also with the fundamental contribution of Dr Sonia Guetta Finzi, Dr Maria Da Villa, Dr Irene Favaretto, Dr Camillo Tonini and P. Rino Sgarbossa. To all of them goes my gratitude, for they gave me suggestions, materials to work on but, most importantly, their time and knowledge, for which I will always be grateful.

My special appreciation and thanks go to all the Conservation Science research group (and to all the "ETA building" researchers), for I felt supported and motivated by their competence and enthusiasm.

I need therefore to express a special thank to my supervisor, Prof. Elisabetta Zendri. Beside the fundamental role she has played along my career as a Conservation Science student, she has always been there to mentor me in my learning and growth path, and it is also thanks to her support if I have become who I am, professionally and personally.

I would also like to sincerely thank my adviser, Dr Eleonora Balliana, from whom I have learnt so much and whose attitude, helpfulness and altruism have inspired me and shaped my way of thinking. Thanks also to Dr Dafne Cimino, for her kindness and for always being there if I needed.

Special thanks go also to Dr Tiziano Finotto and Dr Federica Rigoni, for their fundamental contribution to this research and for having shared their knowledge and time with me.

This project, beside its scientific valence, represents also the conclusion of my master degree. It has been a long and unconventional journey, for which I must thank all the people who accompanied me along my way.

First of all, thanks to my family: my mother Sandra and my father Adriano, who have always been there for me, guiding me with their experience and sensibility.

Thanks then to my long-time friends and, among them, to Federica, Francesco and Veronica. Thank you for supporting me when I needed but also for confronting with me when our opinions were different: sincerity in friendship is priceless. And thanks to Giacomo, for having been there in these

last months, providing me with encouragement and enthusiasm. My special thanks go also to my university colleagues: Federica, Giulia, Martina, Raffaella, Rebecca, Silvia and Servia, for their presence and the time spent together made the last six years happy and memorable.
Last, but not least, I would not have reached this goal without all my CoopCulture colleagues. I must thank all of them for all the things I have learnt in the past three years and for my professional and personal growth. Thank you to Monica, for being there as a lighthouse to guide me in my path, thank you to Cristiana, for always believing in me. Thanks to Adriano, whose silent acknowledgments are the best reward ever. Thanks to Elena, Tiziana and Sara, for being supportive friends: even in the toughest moment you know how to make me smile. Thanks then to all my colleagues: Marina, Monica, Ale, Michela, Irene, Lorenza, Sara, Massimiliano, Alberto and all others (I apologise for not naming you all but I would need too many other pages), I owe you so much. All the things I have learnt and the experiences I have made during these three years are priceless.

I would like this moment to be, rather than the end of a journey, the beginning of a new adventure: I have followed and concluded my educational path, so now it is time to make my way and chase my dreams. I hope all of you will be there to walk with me.

REFERENCES

[1] Opificio delle Pietre Dure, *Misure di contenimento per la prevenzione dal contagio da coronavirus. Verifica della compatibilità di sanificazione degli ambienti con le esigenze di Tutela e Conservazione del Patrimonio Culturale,* Firenze, 2020.

[2] Mibact - ISCR, *Misure di contenimento per il contagio da Coronavirus – Verifica delle compatibilità con le esigenze di tutela e conservazione del patrimonio culturale,* Roma, 2020.

[3] Istituto centrale per la patologia degli archivi e del libro, *Ulteriori delucidazioni su linee guida ICPAL,* 2020.

[4] ICOM , *Museum definition,* Vienna, 2007.

[5] World Health Organization , *Guide to Hygiene and Sanitation in Aviation,* Geneva, 2009.

[6] e. Kampf, "Persistence of coronaviruses on inanimate surfaces and their inactivation with biocidal agents," *Journal of Hospital Infection,* vol. 104, pp. 246-251, 2020.

[7] Regione Emilia Romagna - Istituto per i beni artistici culturali e naturali, *Indicazione operative per la ripresa del prestito bibliotecario.*

[8] World Health Organization, *Cleaning and disinfection of environmental surfaces in the context of COVID-19,* 2020.

[9] e. Rabenau, "Efficacy of various disinfectants against SARS coronavirus," *Journal of Hospital Infection ,* vol. 61, p. 107–111, 2005.

[10] Soprintendenza archeologia, belle arti e paesaggio per il comune di Venezia e la laguna, *Misure di contenimento per il rischio di contagio da coronavirus Covid-19; Utilizzo di prodotti per la sanificazione degli ambienti ecclesiastici; Raccomandazioni e indicazioni operative,* 2020.

[11] Direzione Generale Archeologia, Belle Arti e Paesaggio, Servizio III, MIBACT, *Covid 19 - Segnalazione in merito ai prodotti utilizzati per la sanificazione degli ambienti ecclesiastici,* Roma, 2020.

[12] SOPRINTENDENZA ARCHEOLOGIA BELLE ARTI E PAESAGGIO PER LA CITTÀ METROPOLITANA DI BARI, *EMERGENZA EPIDEMIOLOGICA DA COVID - 19 INTERVENTI DI SANIFICAZIONE IN AREE DI*

INTERESSE CULTURALE, 2020.

[13] SOPRINTENDENZA ARCHEOLOGIA BELLE ARTI E PAESAGGIO PER LE PROVINCE DI CREMONA, LODI E MANTOVA, *Linee guida per la sanificazione di luoghi di culto e della cultura,* Mantova, 2020.

[14] Regione'Ecclesiastica'Lombarda', *Indicazioni per l'igenizzazione e la tutela dei fedeli nei luoghi di culto □ □,* 2020.

[15] Regione Ecclesiastica Puglia, *Apertura dei luoghi di culto - interventi di igienizzazione,* 2020.

[16] Soprintendenza archeologia, belle arti e paesaggio per l'area metropolitana di Roma, la provincia di Viterbo e l'Etruria meridionale, *Emergenza epidemiologica da COVID-19 - disposizioni in merito di interventi di sanificazione in aree di interesse culturale ai sensi del D.Lgs. 42/2004 e ss.mm.ii.,* 2020.

[17] e. Lockner, "Antimicrobial Surfaces," in *Ullmann's Encyclopedia of Industrial Chemistry*, Wiley, 2013.

[18] Antichità Belsito, "benzalconio cloruro," [Online]. Available: http://www.antichitabelsito.it/BENZALCONIO_CLORURO.htm.

[19] Sinopia Restauro, "Scheda di Sicurezza Benzalconio cloruro 50%," [Online]. Available: http://www.sinopiarestauro.it/db_update/allegati/schede_sicurezza_t/1090004.pdf .

[20] W. a. Payne, " The action of three antiseptics/disinfectants against enveloped and non-enveloped viruses," *Journal of Hospital Infection,* vol. 38, pp. 283-295, 1998.

[21] D. Camuffo, Microclimate for Cultural Heritage, Elsevier, 2014.

[22] The Library of Congress (US), *The Impact of Hand Sanitizers on Collection Materials,* 2020.

[23] e. Joachim Klaus, "Disinfection of aircraft Appropriate disinfectants and standard operating procedures for highly infectious diseases," *Bundesgesundheitsbl,* vol. 59, p. 1544–1548, 2916.

[24] e. Koperska, "Degradation markers of fibroin in silk through infrared spectroscopy," *Polymer Degradation and Stability,* vol. 105, no. 105, pp. 185-196, 2014.

[25] Encyclopaedia Britannica, "Silk," [Online]. Available: https://www.britannica.com/topic/silk.

[26] N. Luxford, "Silk Durability and Degradation," in *Understanding and improving the durability of textiles*, Cambridge, Woodhead Publishing Limited, 2012.

[27] e. Aguayo, “A vibrational approach for the study of historical weighted and dyed silks,” *Journal of Molecular Structure ,* vol. 1075, no. 1075, pp. 471-478, 2014.

[28] P. Garside, “The role of fibre identification in textile conservation,” in *Identification of Textile Fibers*, Cambridge, Woodhead publishing, 2009.

[29] e. Garside, “Characterization of Historic Silk by Polarized Attenuated Total Reflectance Fourier Transform Infrared Spectroscopy for Informed Conservation,” *Applied Spectroscopy,* vol. 59, no. 10, pp. 1242-1247, 2005.

[30] e. Koperska, “Evaluating degradation of silk’s fibroin by attenuated total reflectance infrared spectroscopy: Case study of ancient banners from Polish collections,” *Spectrochimica Acta Part A: Molecular and Biomolecular Spectroscopy ,* vol. 135, no. 135, pp. 576-582, 2015.

[31] e. Radzicka, “Rates of Uncatalyzed Peptide Bond Hydrolysis in Neutral Solution and the Transition State Affinities of Proteases,” *Journal of American Chemical Society,* no. 118, pp. 6105-6109, 1996.

[32] S. a. Fugitt, “Catalyzed hydrolysis of amide and peptide bonds in proteins,” *Journal of research of the National Bureau of Standards,* vol. 29, pp. 315-327, 1942.

[33] P. GARSIDE, “Durability of historic textiles,” in *Understanding and improving the durability of textiles*, Cambridge, Woodhead Publishing limited, 2012.

[34] B. a. Vassileva, “Photochemical behaviour of natural silk - II. Mechanism of fibroin photodestruction,” *Polymer degradation and stability,* no. 60, pp. 61-65, 1998.

[35] S. a. Selvakumar, “A study on the effects of ozone treatment on the properties of raw and degummed mulberry silk fabrics,” *Polymer degradation and stability,* no. 91, pp. 2644-2653, 2006.

[36] W. L. Lai, “Consequences of Ultra-Violet Irradiation on the Mechanical Properties of Spider Silk,” *J. Funct. Biomater,* no. 6, pp. 901-916, 2015.

[37] Dwyer and Bradley, “Chemical properties of alcohols and their protein binding sites,” *Cellular and Molecular Life Sciences,* no. 57, pp. 265-275, 2000.

[38] Peeters and Huyskens, “Endothermicity or exothermicity of water/alcohol mixtures,” *Journal of Molecular Structure,* no. 300, pp. 539-550, 1993.

[39] Dwyer, “Molecular Simulation of the Effects of Alcohols on Peptide Structure,” *Biopolymers,* vol. 49, pp. 635-645, 1999.

[40] Compliance Naturally, “WHY 70% ETHANOL IS THE MOST EFFECTIVE DISINFECTANT FOR ANY FOOD OR PHARMA FACILITY,” [Online]. Available: https://www.compliancenaturally.com/blog-page/2018/4/15/why-70-ethanol-is-the-most-effective-disinfectant-for-any-food-or-pharma-facility.

[41] C. f. D. C. a. Prevention, “Chemical Disinfectants,” [Online]. Available: https://www.cdc.gov/infectioncontrol/guidelines/disinfection/disinfection-methods/chemical.html.

[42] CRC PRESS, The handbook of chemistry and physics - 57th edition, 1976-1977.

[43] Johnston-Feller, Color Science in Examination of Museum Objects, The Getty Conservation Institute, 2001.

[44] e. Macchia, “Comparative study of protective coatings for the conservation of Urban Art,” *Journal of Cultural Heritage,* vol. 41, pp. 232-237, 2020.

[45] e. Shao, “Fourier Transform Raman and Fourier Transform Infrared Spectroscopy Studies of Silk Fibroin,” *Journal of Applied Polymer Science,* vol. 96, no. 96, pp. 1999-2004, 2005.

[46] Margariti, “The application of FTIR microspectroscopy in a non-invasive and non-destructive way to the study and conservation of mineralised excavated textiles,” *Heritage Science,* vol. 7, no. 63, 2019.

[47] e. Badillo-Sanchez, “Understanding the structural degradation of South American historical silk: A focal plane Array (fpA) ftiR and multivariate analysis,” *Nature,* vol. 9, no. 17239.

[48] e. Vagnini, “Handheld new technology Raman and portable FT-IR spectrometers as complementary tools for the in situ identification of organic materials in modern art,” *Spectrochimica Acta Part A: Molecular and Biomolecular Spectroscopy,* vol. 176, pp. 174-182, 2017.

[49] e. Milani, “In Situ Noninvasive Study of Artworks: The MOLAB Multitechnique Approach,” *Accounts of Chemical Research,* vol. 3, no. 6, pp. 728-738, 2010.

[50] e. Peets, “Reflectance FT-IR spectroscopy as a viable option for textile fiber identification,” *Heritage Science,* vol. 93, no. 7, 2019.

[51] Mei-Ying-Li, “Study of the degradation mechanism of Chinese historic silk (Bombyx mori) for the purpose of conservation,” *Polymer Degradation and Stability,* vol. 98, pp. 727-735, 2013.

[52] e. Um, “Wet spinning of silk polymer II. Effect of drawing on the structural characteristics and properties of filament,” *International Journal of Biologicam Macromolecules,* vol. 34, pp. 107-119, 2004.

[53] Chomachayi, “Biodegradable Nanocomposites Developed from PLA/PCL Blends and Silk Fibroin Nanoparticles: Study on the Microstructure, Thermal Behavior, Crystallinity and Performance,” *Journal of Polymers and the Environment,* vol. 28, pp. 1252-1264, 2020.

[54] e. Burigo, “Library of FT-Raman spectra of pigments, minerals, pigment media and varnishes, and supplement to existing library of Raman spectra of pigments with visible excitation,” *Spectrochimica Acta Part A,* vol. 57, pp. 1491-1521.

[55] Infrared and Raman Users Group, [Online]. Available: http://www.irug.org/search-spectral-database?reset=Reset.

[56] e. Liu, “Exploring the Structural Transformation Mechanism of Chinese and Thailand Silk Fibroin Fibers and Formic-Acid Fabricated Silk Films,” *Internationa Journal of Molecular Sciences,* vol. 19, no. 3309, 2018.

[57] Victoria and Albert Museum, “Cleaning Textiles,” Victoria and Albert Museum, 2016. [Online]. Available: http://www.vam.ac.uk/content/articles/c/cleaning-textiles/. [Accessed 1st June 2020].

[58] e. Carr, “Surface chemical investigation into the cleaning procedures of ancient tapestry materials Part 1,” *Journal of Material Science,* vol. 39, pp. 7317-7325, 2004.

[59] e. a. Jaramillo-Quiceno, “Structural and thermal properties of silk fibroin films obtained from cocoon and waste silk fibers as raw materials,” no. 200, pp. 384-388, 2017.

[60] e. Zhang, “Using FTIR spectroscopy to detect sericin on historic silk,” *Science China - Chemistry,* vol. 53, no. 3, pp. 626-631, 2010.